Rochester Institute of Technology
RIT Digital Institutional Repository

Theses

1987

A Multipurpose Test Mask for Exposure Tool Characterization

Brian Benamati

Follow this and additional works at: https://repository.rit.edu/theses

Recommended Citation
Benamati, Brian, "A Multipurpose Test Mask for Exposure Tool Characterization" (1987). Thesis. Rochester Institute of Technology. Accessed from

This Thesis is brought to you for free and open access by the RIT Libraries. For more information, please contact repository@rit.edu.

A MULTIPURPOSE TEST MASK
FOR
EXPOSURE TOOL CHARACTERIZATION

by

Brian L. Benamati

A Thesis Submitted

in

Partial Fulfillment

of the

Requirements for the Degree of

MASTER OF SCIENCE

in

Electrical Engineering

Approved By:

Prof. Dr. Lynn Fuller (Thesis Advisor)

Prof. Dr. Renan Turkman (Committee)

Prof. Dr. George Brown (Committee)

Prof. Rob Pearson (Committee)

DEPARTMENT OF ELECTRICAL ENGINEERING

COLLEGE OF ENGINEERING

ROCHESTER INSTITUTE OF TECHNOLOGY

ROCHESTER, NEW YORK

DECEMBER, 1987

930120

PREFACE

Photolithographers, especially those responsible for exposure tools, will learn that the following work is of significance in both informational and functional form. The design offered herein presents a unique combination of patterns which can be employed in the characterization, optimization and monitoring of exposure tools. The wide variety of both optical and electrical test structures as well as alignment targets available allow this design to be truely multipurpose. The procedures defined are complete and proven, providing the novice with adequate knowledge to examine an exposure tool's capabilities.

The concept of this design evolved from an existing design which has proven itself worthy with many years of constant use. Necessary modifications and additions were made to improve the design's usefulness and understanding in its intended application. Full credit is given here to Dr. Edward T. Nelson for the design of the Process Development Mask Set, the original design on which the following work is based.

A MULTIPURPOSE TEST MASK FOR EXPOSURE TOOL CHARACTERIZATION

by

Brian L. Benamati

Electronic Research Laboratory, Eastman Kodak Company

Rochester, New York

ABSTRACT

Of the many facets of integrated circuit fabrication, photolithography may very well be the most important due to the number of levels required for the fabrication of sophisticated devices. Therefore it is imperative to understand the performance capabilities of an exposure tool and identify its inherent limitations. Many methods have been developed which concentrate specifically on evaluating resolution, critical dimensions or registration. Often test patterns exist which vary widely for applications with respect to steppers, 1X scanning projection aligners and other 1X exposure equipment.

The following work is focused on the requirements of evaluating and optimizing all aspects of performance for various exposure tools with one basic design. The structures available allow this design to be compatible with all existing exposure equipment at the RIT Center for Microelectronics as well as additional tools which are likely to be available in the near future. This provides a consistent manner by which the characterization of each tool may be done as well as the ability to compare various tools directly.

TABLE OF CONTENTS

		Page
	LIST OF FIGURES	v-viii
I.	INTRODUCTION	1,2
II.	LITERATURE SEARCH	3-6
III.	MASK DESCRIPTION	7-11
IV.	PROCEDURES	12-29
V.	RESULTS AND ANALYSIS	30-44
VI.	CONCLUSIONS	45
	ACKNOWLEDGEMENTS	46
	REFERENCES	47-50
	BIBLIOGRAPHY	51-53
	APPENDIX A: STATISTICAL ANALYSIS	54
	APPENDIX B: OPTICAL VERNIER INTERPRETATION	55
	APPENDIX C: LINEWIDTH STRUCTURE THEORY	56
	APPENDIX D: ALIGNMENT STRUCTURE THEORY	57
	APPENDIX E: CELL DESCRIPTIONS AND ILLUSTRATIONS	58-101
	APPENDIX F: CHARACTERIZATION REPORT	102-117
	APPENDIX G: SEM MICROGRAPHS	118-129

LIST OF FIGURES

		Page
1.	ETM-1 Wafer Map for 1X 4"x4" Mask	7
2.	ETM-1 Wafer Map for 1X 5"x5" Mask	8
3.	ETM-1S Layout for 10X 5"x5" Reticle	9
4.	ETM-1 Cell Layout	11
5.	3" Wafer Map	16
6.	Critical Dimension Histogram	16
7.	100 mm Wafer Map	17
8.	Critical Dimension Histogram	17
9.	3" Wafer Map	23
10.	Overlay Histograms	23
11.	100 mm Wafer Map	24
12.	Overlay Histograms	24
13.	Design Layout Errors	31
14.	E-beam Tape Conversion Errors	32
15.	Alignment Test Device Chrome Zapping	33
16.	Mask C.D. Map (1X 5"x5")	34
17.	Mask C.D. Histogram (1X 5"x5").........................	35
18.	Wafer Linewidth vs. Mask Linewidth	36
19.	Line Within a Field of Lines vs. Isolated Line	37
20.	Linewidth After Etch vs. Linewidth Before Etch	38
21.	Electrical Linewidth vs. Optical Linewidth	39
22.	Example of Overlay with Acceptable Alignment	40
23.	Example of Overlay with Translation Error	41
24.	Example of Overlay with Rotation Error	42
25.	Electrical vs. Optical Alignment Evaluation (X-Axis) ..	43

Page

A1. Normal Curve 54

A2. Optical Vernier 55

A3. Electrical Linewidth Test Structure 56

A4. Electrical Alignment Test Structure 57

A5. Cell A 58

A6. Cell C 59

A7. Cell AC 60

A8. Cell B (Block Diagram) 61

A9. Cell B (Detail) 62

A10. Cell D (Block Diagram) 63

A11. Cell D (Detail) 64

A12. Cell DB (Block Diagram) 65

A13. Cell DB (Detail) 66

A14. Lines/Spaces (0.6-0.8 microns) 67

A15. Lines/Spaces (1.0-1.6 microns) 68

A16. Lines/Spaces (1.8-2.4 microns) 69

A17. Lines/Spaces (2.6-4.0 microns)....................... 70

A18. Lines/Spaces (5.0-10.0 microns) 71

A19. Contact Geometries 72

A20. Island Geometries 73

A21. Checkerboard Patterns 74

A22. Clear Field Focus Star 75

A23. Dark Field Focus Star 76

A24. Clear Field 45 Degree Resolution Charts 77

A25. Dark Field 45 Degree Resolution Charts 78

LIST OF FIGURES (CONT'D)

Page

A26. Clear Field Resolution Chart 79

A27. Dark Field Resolution Chart 80

A28. Clear Field Murray Daggers 81

A29. Dark Field Murray Daggers 82

A30. Clear Field Resolution Chart 83

A31. Dark Field Resolution Chart 84

A32. Electrical Linewidth Structure for 2 Micron Lines 85

A33. Electrical Linewidth Structure for 2 Micron Spaces 86

A34. Electrical Linewidth Structure for 3 Micron Lines 87

A35. Electrical Linewidth Structure for 3 Micron Spaces 88

A36. Electrical Linewidth Structure for 5 Micron Lines 89

A37. Electrical Linewidth Structure for 5 Micron Spaces 90

A38. Manual Alignment Cross 91

A39. GCA Alignment Cross 92

A40. Perkin-Elmer 200/300 Series AFA CF-CF Target 93

A41. Perkin-Elmer 200/300 Series AFA CF-DF Target 94

A42. Perkin-Elmer 500/600 Series AFA CF-CF Target 95

A43. Perkin-Elmer 500/600 Series AFA CF-DF Target 96

A44. Optical Verniers (+/- 1 micron range) 97

A45. Optical Verniers (+/- 3 micron range) 98

A46. Electrical Alignment Test Structure (CF-CF) 99

A47. Electrical Alignment Test Structure (CF-DF) 100

A48. GCA Street Target 101

A49. C.D. Uniformity Map (Line Within a Field of Lines) 103

A50. C.D. Histogram (Line Within a Field of Lines) 104

LIST OF FIGURES (CONT'D)

Page

A51. C.D. Uniformity Map (Isolated Line) 105

A52. C.D. Histogram (Isolated Line) 106

A53. Linewidth vs. Exposure (2 Micron Line) 107

A54. Linewidth vs. Exposure (3 Micron Line) 108

A55. Linewidth vs. Exposure (5 Micron Line) 109

A56. Optical Spacewidth vs. Exposure Setting 110

A57. Resolution Capabilities 111

A58. Alignment Histogram 112

A59. Overlay Wafer Map (Acceptable Alignment) 113

A60. Overlay Wafer Map (Translational Error) 114

A61. Overlay Wafer Map (Rotational Error) 115

A62. Optical Alignment Evaluation 116

A63. Electrical Alignment Evaluation 117

A64. ETM-1 Cell D Aligned to Cell A (SEM) 118

A65. Line/Space Elements (SEM) 119

A66. Contact Array (SEM) 120

A67. Island Array (SEM) 121

A68. Checkerboard Array (SEM) 122

A69. Focus Star (SEM) 123

A70. 45 Degree Resolution Charts (SEM) 124

A71. 1-5 Micron Resolution Chart (SEM) 125

A72. Murray Daggers (SEM) 126

A73. 6-10 Micron Resolution Chart (SEM) 127

A74. Resist Imaging Over Topography (SEM) 128

A75. Electrical Alignment Structures (SEM) 129

I. INTRODUCTION

The Multipurpose Test Mask for Exposure Tool Characterization (subsequently referred to as ETM-1 for Exposure Test Mask, Revision 1) is a versatile design which addresses almost all aspects of photolithography. The design is based on use with a positive photoresist scheme, although it could be used with negative acting resists. If necessary, masks could certainly be fabricated with reversed tones.

The design contains numerous optical and electrical structures which are used to evaluate the performance of an exposure tool with respect to resolution and overlay. In many instances both dark and clear field patterns are included for comparison. The structures, which have been chosen due to their popularity in industry, are clearly labeled for easy recognition.

The mask can be used for single level exposures to evaluate resolution capability, exposure dose uniformity and photoresist profiles. Various other conditions of photoresist processing such as the effects of postbake temperaures and development conditions can be evaluated as well.

When used for bi-level experiments, the mask is offset and aligned to a patterned first level wafer. This procedure allows for numerous tests with respect to the exposure tool's alignment capability, distortion and mix and match capability. The analysis of resist imaging over the topographies introduced by the first level can also be performed.

The advantage of this design concept is that only one mask is required for bi-level tests. This completely eliminates mask registration errors as a contributor to the total overlay error and concentrates on the exposure tool itself. Also since the design is identical for all categories of exposure tools, direct comparisons can be performed on the the same structures.

Descriptions are provided for the masks and the device itself including all of the individual components. This is supported by plots from the design files for illustration purposes. When necessary, the theory and test procedures for certain structures are included.

Numerous procedures are presented with many variations possible. The basic procedures intended for use are outlined in detailed process sheets as well as the recommended evaluation procedures for results. Many of these tests can be combined simultaneously in process for maximum efficiency.

A complete characterization was performed on a Perkin-Elmer 200 series scanner to test the design and is included in the results and analysis section. All results are presented and the advantages and disadvantages of the design are discussed. Recommendations for possible improvements are entertained.

Wise use of this test mask in a variety of situations will certainly provide the information necessary to establish design rules compatible with a particular exposure tool and likely provide a means for optimizing its performance. It will become readily apparent that this design is self-sufficient.

II. LITERATURE SEARCH

The semiconductor industry has been striving for the reduction of geometries to improve device performance and reduce cost. This need has stressed the capabilities of the photolithographic process, specifically the exposure tools. Exposure equipment has evolved from early contact and proximity tools to projection scanners and steppers, with each in use today depending on the demands. Non-optical approaches such as E-beam and x-ray lithography have challenged the more traditional techniques, but by no means overcome them (1).

Inherent problems with contact and proximity aligners such as mask damage and registration error brought about the introduction of 1X projection scanners in the early 1970's (2). This was considered by many the most significant step taken in meeting the demands of the VLSI industry (3). The subsequent introduction of steppers pushed the exposure tool's performance beyond that of its scanner counterpart. However, recent advances in scanner technology (4), such as MID UV exposure (5) and magnification compensation (6) have become established. Projection scanning systems are now challenging the perceived edge held by steppers and maintain a strong market share (7).

The performance of an exposure tool consists of its ability to transfer a mask image to a wafer, reproducing the pattern's dimension and location (8). This involves characteristics such as resolution, critical dimension variation, and overlay (9). These items are directly impacted by machine parameters such as light source uniformity, focus determination and alignment techniques (10).

Often optical techniques have been used to evaluate feature definition and dimensions. Such techniques include scanning slit systems and the interpretation of diffraction grating patterns (11). An industry proven optical pattern used for linewidth determination is the Murray Dagger (12), which involves a graduated series of lines.

In the last decade electrical measurement techniques have been investigated for the evaluation of linewidths. As early as 1958, van der Pauw introduced the concept of measuring the resistivity of an arbitrary conductive disc (14). This has been implemented effectively in a basic cross bridge linewidth structure that is widely accepted (14). Advanced variations of this structure such as split cross bridge structures have been used successfully for evaluation in the submicron range (15). Extensive use of these patterns can determine the latitude of a photoresist process (16). Inaccuracies of the cross bridge test device are reported to be as high as 15%, due to various error components such as self-heating (17).

Most recently emphasis has been placed on registration rather than linewidth (18). Optical patterns such as verniers, have long been the predominant method of evaluation. Mask superposition errors have since been determined electrically at rates of up to 200X faster than optical vernier interpretation (19). The data output from these electrical tests can be formatted into histograms, vector maps, contour maps and X-Y plots (20).

Various stuctures have been used with wide ranges of accuracy reported. The earliest electrical alignment potentiometers yielded accuracies of 0.1 microns (21). Double cross bridge structures have shown more consistent

results in the region of 0.06 microns (22). The most accurate results of 0.01 microns have reportedly been achieved with a split "stickman" pattern (23).

The tremendous amount of data available has permitted a higher degree of analysis and conjecture over the components contributing to overlay errors. Mathematical models divide the error components into systematic and random categories (24). Each category can be broken down further into its linear and nonlinear components. In fact, stepper experts have identified systematic errors such as lens abberations and random errors such as stage movements (25). Meanwhile, scanner experts have defined systematic errors such as mirror irregularites and the random component of carriage scan precision (26).

The overlay components have also been broken down with respect to their physical appearance on the wafer. The widely accepted categories with this approach are translation, rotation and expansion or contraction (27). This analysis has been used to a large extent for the evaluation of projection scanners and in the attempt to match overlay signatures from one machine to another (28). As a result of this effort, an overlay error component of up to 2 microns per 100 mm due to wafer size distortion from thermal processing has been discovered (29).

Finally, equipment personnel have evaluated the overlay errors as a function of the tooling involved in the masking operation. The major components for projection scanners have been reported to be: alignment 40%, machine distortion 37%, mask expansion 15%, wafer distortion 5% and mask registration error 3% (30). With the use of a test mask these components can be segregated, characterized and optimized individually to provide the highest degree of

exposure tool performance possible.

One such test mask has been developed for process characterization and has been used extensively for a number of years, primarily for monitoring photo-lithographic processes (31). The original designer was Dr. Edward T. Nelson and full credit is given here because the design concept for the Exposure Test Mask was a derivative of his original work. The original two mask set was reduced to one using an alignment offset concept and structures more appropriate for the intended needs were implemented.

III. MASK DESCRIPTION

Three photomasks have been fabricated which are specifically designed for use with the existing exposure tools at RIT. The Kasper and Cobilt Contact Aligners will use the 1X 4"x4" mask while the Perkin-Elmer 100/200 Scanners will use the 1X 5"x5" mask. The GCA Stepper utilizes the 10X 5"x5" reticle.

The ETM-1 1X 4"x4" mask is fabricated on a 4"x4"x.090" low expansion (LE) glass plate with antireflective (AR) chrome and is written with a 0.2 micron E-beam spot size. The array is stepped with forty-five (45) die that are 7.80 mm by 7.80 mm in size as shown in Figure 1.

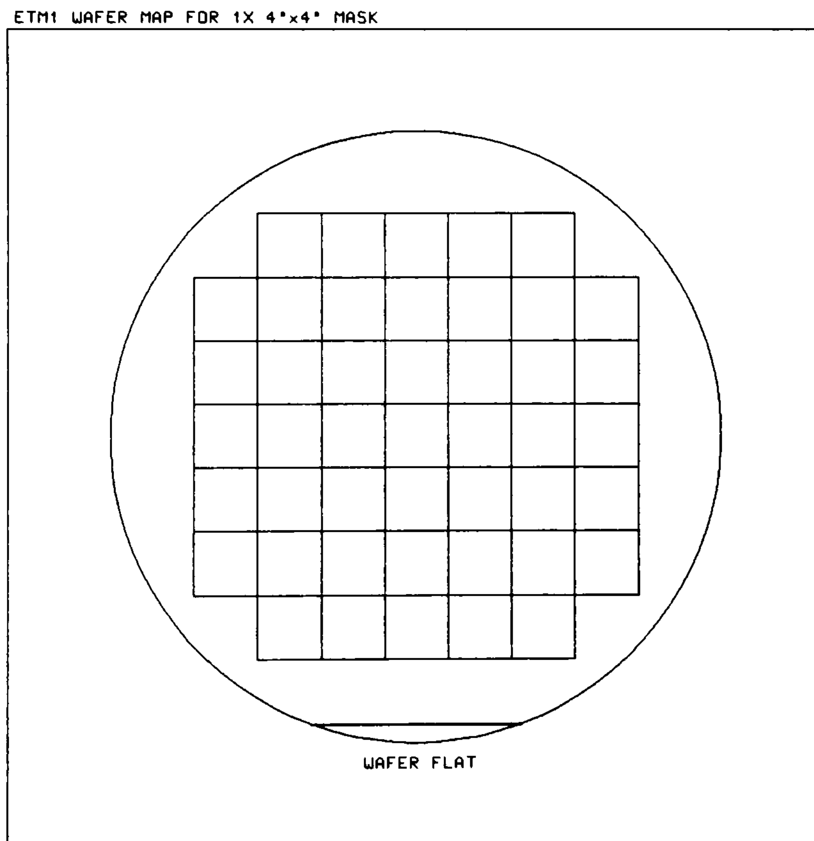

Figure 1: ETM-1 wafer map for 1X 4"x4" mask.

The ETM-1 1X 5"x5" mask is fabricated on a 5"x5"x.090" low expansion (LE) glass plate with antireflective (AR) chrome and is written with a 0.2 micron E-beam spot size. The array is stepped such that seventy-seven (77) die are centered within the boundries of a 100 mm wafer as shown in Figure 2. The die size is 7.80 mm by 7.80 mm.

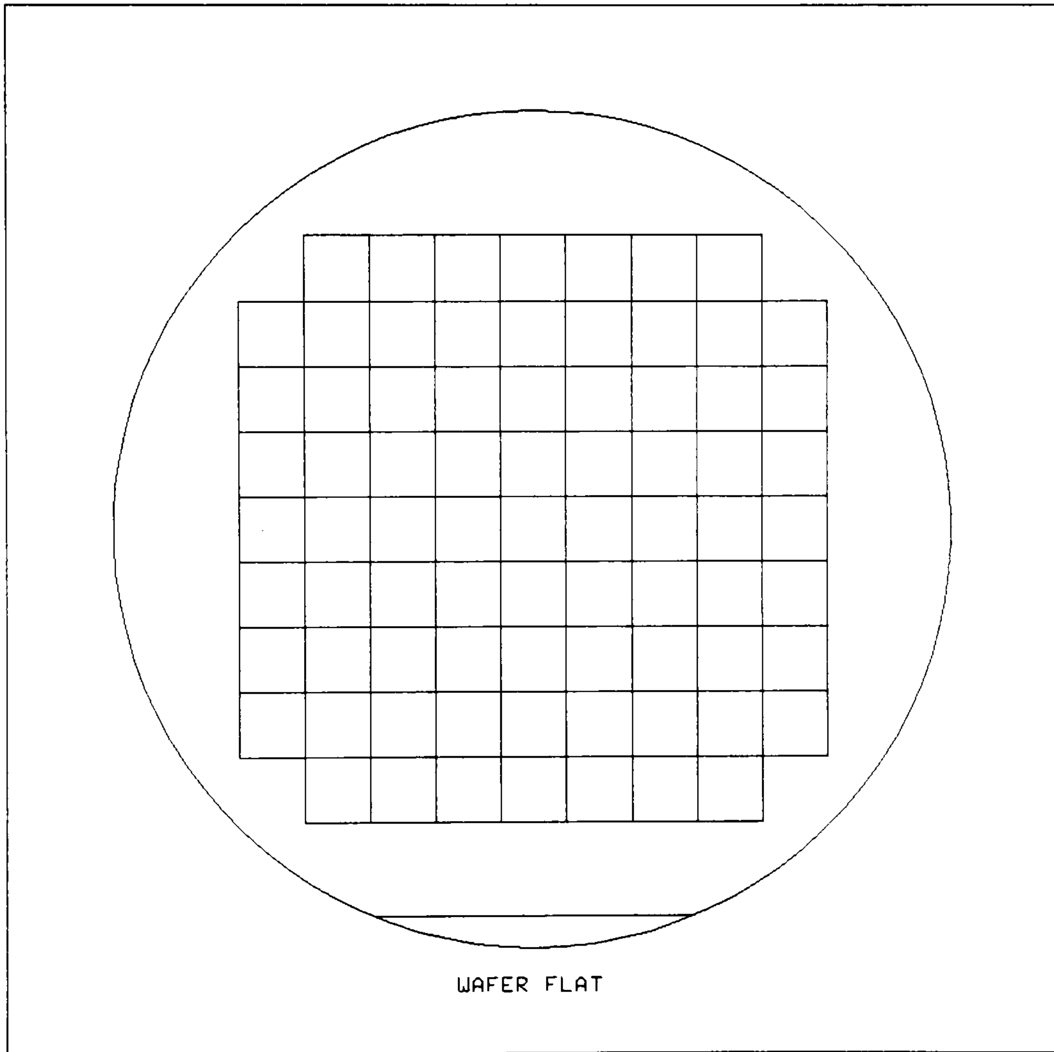

Figure 2: ETM-1 wafer map for 1X 5"x5" mask.

The ETM-1S 10X 5"x5" reticle is fabricated on a 5"x5"x.090" low expansion (LE) glass plate with antireflective (AR) chrome and is written with a 1.0 micron E-beam spot size. The 7.90 mm x 7.90 mm die is centered on the reticle as shown in Figure 3. The 10X reticle border is designed 100 micron wide to include GCA street targets. Stepping distance should be maintained at 7.80 mm x 7.80 mm so that the borders overlap on each field resulting in a final border width of 100 microns.

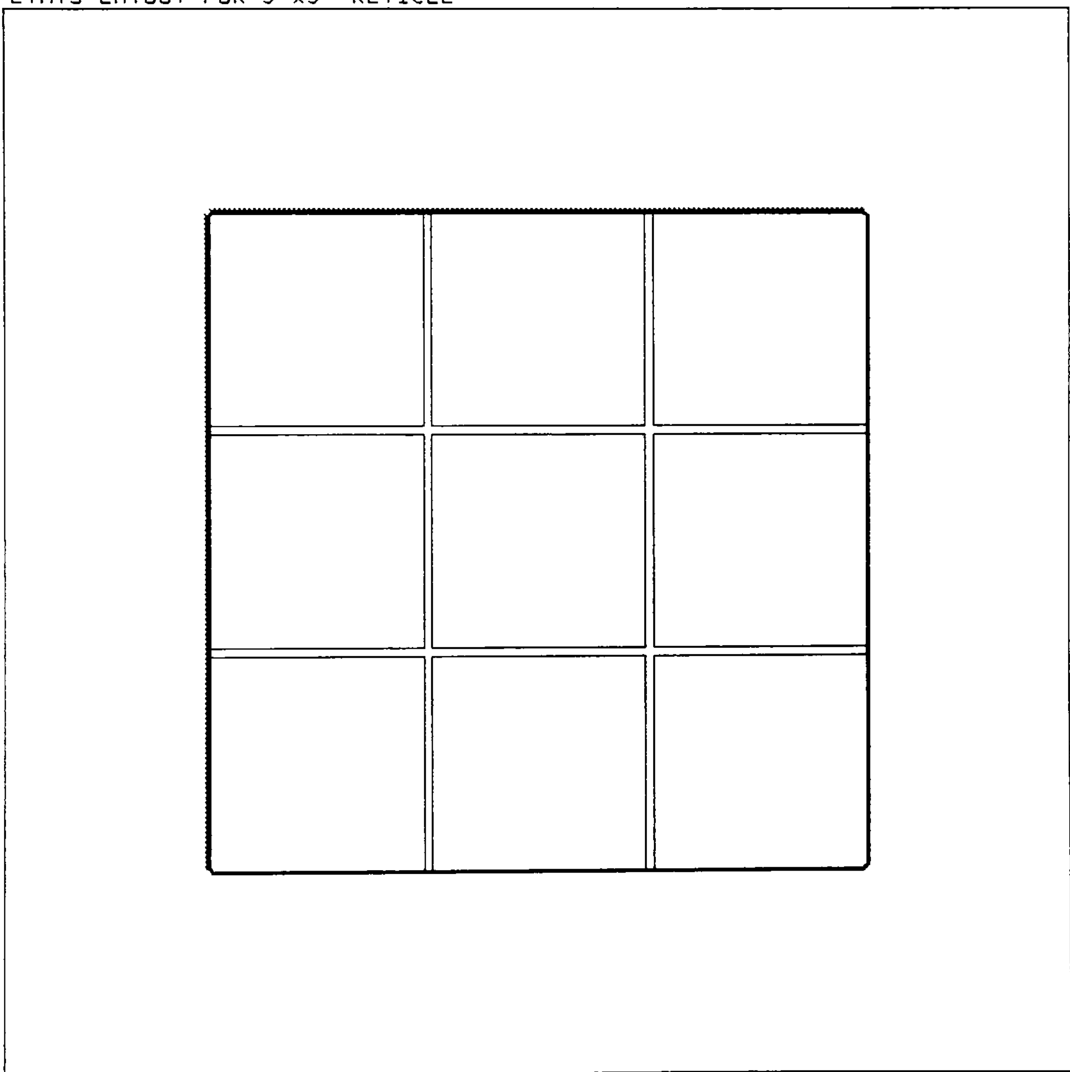

Figure 3: ETM-1S layout for 10X 5"x5" reticle.

The ETM-1 device is divided into nine cells which are 1.25 mm x 1.25 mm in size (see Figure 4). Internal borders dividing the cells are clear and 100 microns wide. Final perimeter borders are 100 microns wide and opaque. This scheme provides allowances for alignment offsets to be performed for bi-level experiments. This is accomplished by offsetting the mask with respect to the wafer by one third of the device or one cell (see section IV for details).

All figures are presented as the cells would appear with the wafer flat down during inspection, which allows the data to "read" correctly. The mask should be installed in the exposure tool to provide this condition. Coordinates are oriented and labeled according to the convention used during viewing a wafer during alignment in a Perkin-Elmer 200/300 series scanner.

Cells A and C are located on top of each other on both the left and right sides of the die. These cells contain line/space elements which are vertical in one cell and horizontal in the other. When an alignment offset is made during a bi-level test, these elements will cross each other orthogonally, providing a topographical study.

Cell B is on top of cell D in the center column of the die. These cells contain all of the optical and electrical test structures as well as alignment targets. For bi-level tests Cell B has all of the first level information and cell D has all of the second level information. A complete description and illustration of each cell component is included in Appendix E.

The general cell layout of the ETM-1 device is illustrated below.

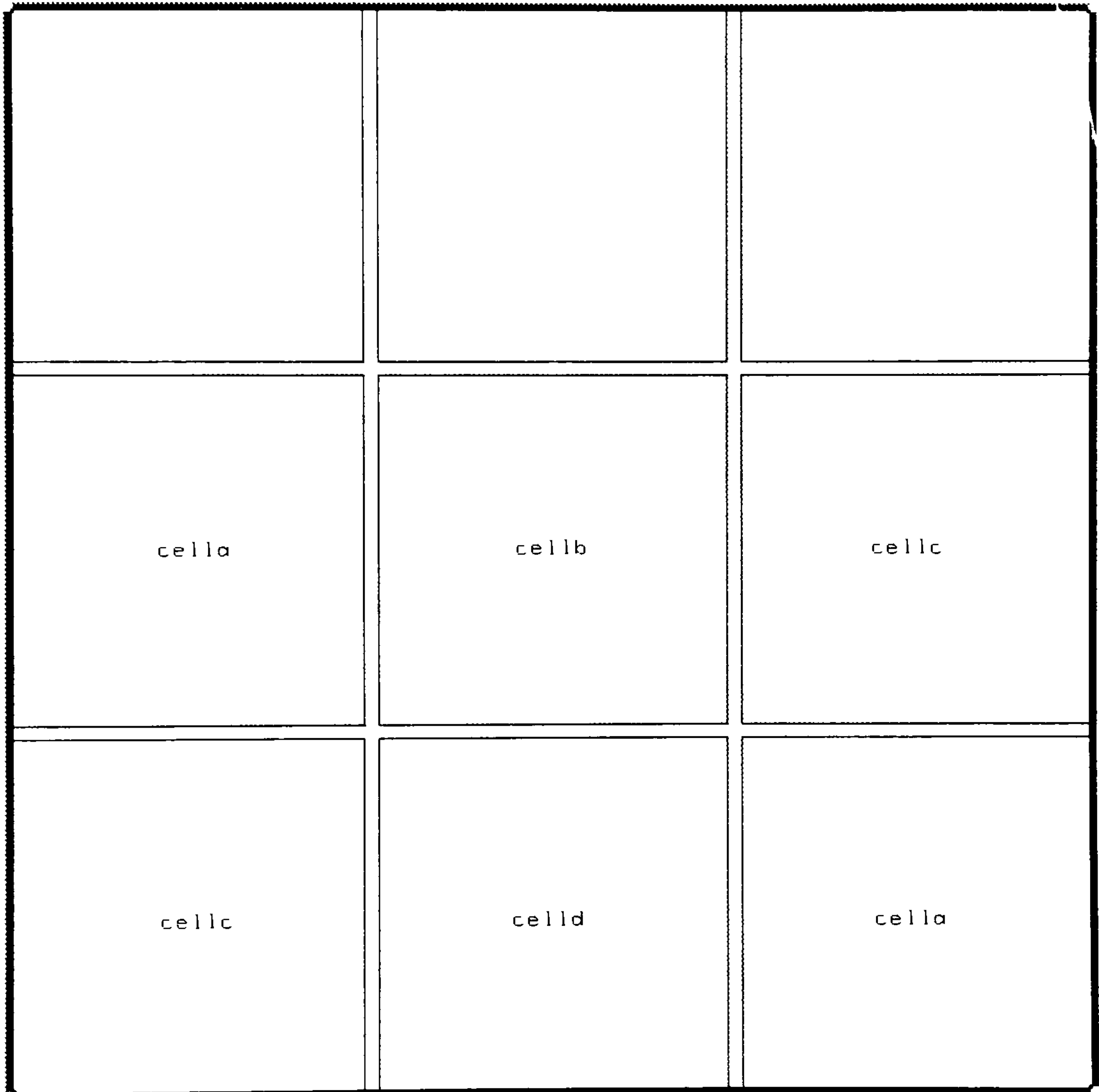

Figure 4: ETM-1 cell layout.

IV. TEST PROCEDURES

The versatility of ETM-1 allows a wide variety of tests to be performed, with many variations possible. Evaluations are comprised of optically inspecting exposed wafers, scanning electron microscopy analysis and the probing of electrical test structures. Direct comparison of different exposure tools can be performed by reviewing the results of these tests. The procedures are broken down into the cataegories of single level and bi-level, which are described below.

Single level tests evaluate the exposure tool's resolution capability as well as exposure dose control and resist processing conditions. All experiments are accomplished by coating wafers with photoresist, exposing, developing and inspecting. Wafers should satisfy flatness requirements of less than three microns overall. Electrical test procedures require additional processing and wafers of the opposite type than the intended diffusion (if any). Procedures for single level tests are outlined in the sections that follow.

Bi-level tests evaluate the exposure tools's capability with respect to various overlay components such as alignment, magnification and distortion as well as the ability to pattern features over topography. The bi-level tests are accomplished by offsetting the mask with respect to a previously patterned wafer in the direction shown by an offset arrow and aligning the appropriate targets. Procedures for bi-level tests are outlined in the sections that follow. Patterned first level wafer preparation is discused below.

It is convenient to prepare a set of first level wafers which can have the photoresist stripped and be reused continuously for the bi-level experiments. This procedure is outlined below. The electrical structures require different processing which is described in those particular sections.

1. Scibe wafers for identification (quantity of 25).
2. Scrub wafers.
3. Clean wafers for furnace operation.
4. Grow 4000-8000 A of oxide.
5. Coat the wafers with 1.2 microns of photoresist and prebake.
6. Install the appropriate ETM-1 mask in a 1X contact aligner or a "standard scanner" which is known to have negligible distortion.
7. Expose the wafers with a dose appropriate for 2 to 3 micron lines.
8. Develop and postbake the wafers.
9. Etch the oxide until the wafer backsides dewet.
10. Strip the photoresist.
11. Scrub the wafers.

The procedures for each test are detailed on the following sheets along with corresponding data sheets. These procedures can be used in conjunction with the standard process steps for a specific laboratory, with minor changes made as required. Care must be taken during certain deposition and diffusion steps that adequate masking oxide is present on the wafers front surfaces.

1. LINEWIDTH VS. EXPOSURE DOSE

Description: This procedure determines the process latitude of an exposure tool with respect to exposure dose variations and is used to select the proper dose required for 1:1 image transfer from the mask.

Evaluation: Critical dimensions (CD) will be evaluated.

Test Points: Five wafers (one for each exposure) will be evaluated at three positions on the line/space elements (typically 2 micron lines) of cell A.

Procedure:

1. Coat the wafers with 1.2 microns of photoresist and prebake.
2. Select five exposure doses within a range which may result in images which are slightly scummed to those slightly overexposed.
3. Expose the wafers on the exposure tool, using one wafer for each dose.
4. Develop and postbake the wafers.
5. Evaluate the CD at the positions determined and record.
6. Plot the mean CD of each wafer as a function of exposure dose.

Further Investigation: Wafers with different materials such as oxide, nitride, polysilicon and aluminum can be evaluated to determine their effects on exposure dose requirements.

2. CRITICAL DIMENSION UNIFORMITY

Description: This procedure evaluates the exposure tool's capability to transfer images from the mask onto the wafer. The major error components will be intensity non-uniformity, mask CD integrity and focal plane deviation.

Evaluation: Critical dimensions will be evaluated.

Test Points: One wafer where the line/space elements of cell A will be measured on all die within the wafer. Typically the 2 micron lines are the feature chosen for this evaluation.

Procedure:

1. Coat the wafers with 1.2 microns of photoresist and prebake.
2. Select an exposure dose which will provide a 1:1 transfer of the 2 micron lines from the mask to the wafer.
3. Expose the wafer on the exposure tool using the selected dose.
4. Develop and postbake the wafer.
5. Evaluate the CD at all positions and record on the corresponding C.D. Data Sheet for the exposure tool used (see pages 16 and 17).
6. Plot a histogram of the data on the C.D. Data Sheet provided.
7. Calculate the mean and standard deviation of the data population (see Appendix A).

**************** CRITICAL DIMENSION DATA SHEET FOR 3" WAFERS ****************

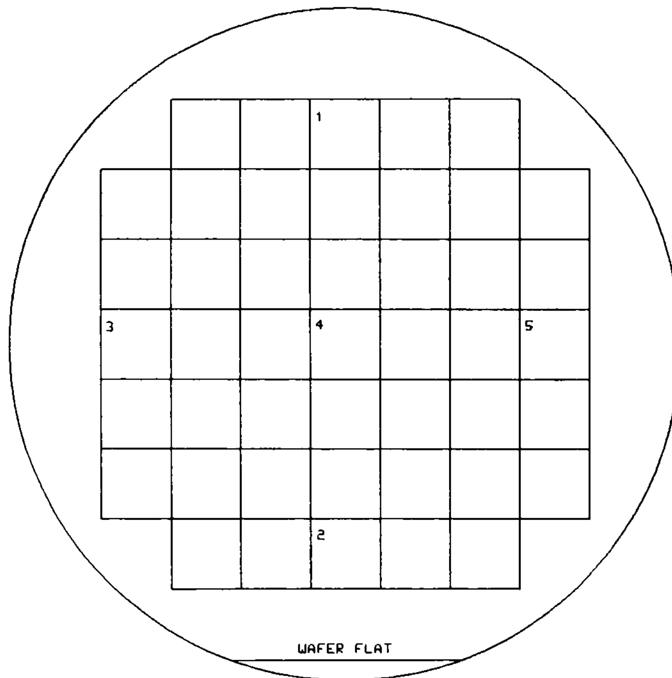

FIGURE 5: 3" WAFER MAP

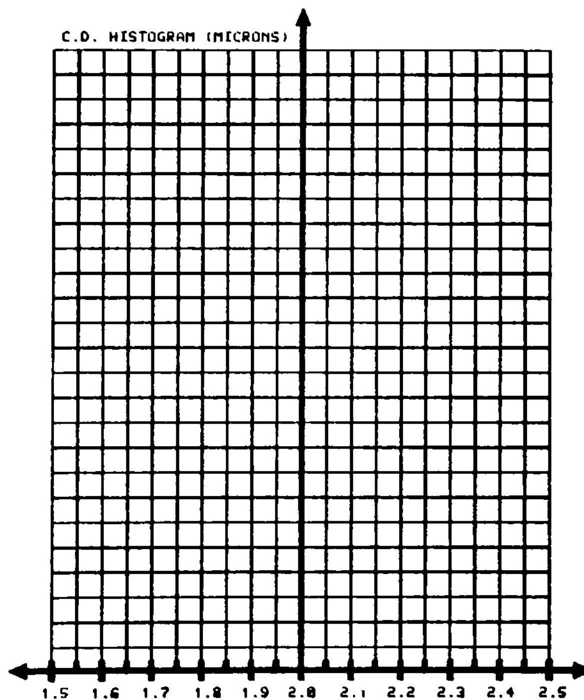

FIGURE 6: CRITICAL DIMENSION HISTOGRAM

X AVE =   SIGMA =   3 SIGMA =

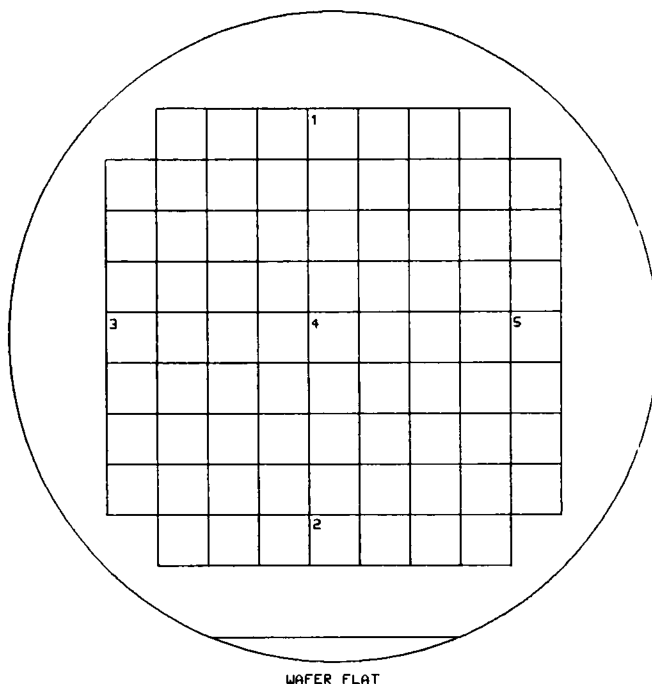

FIGURE 7: 100 MM WAFER MAP

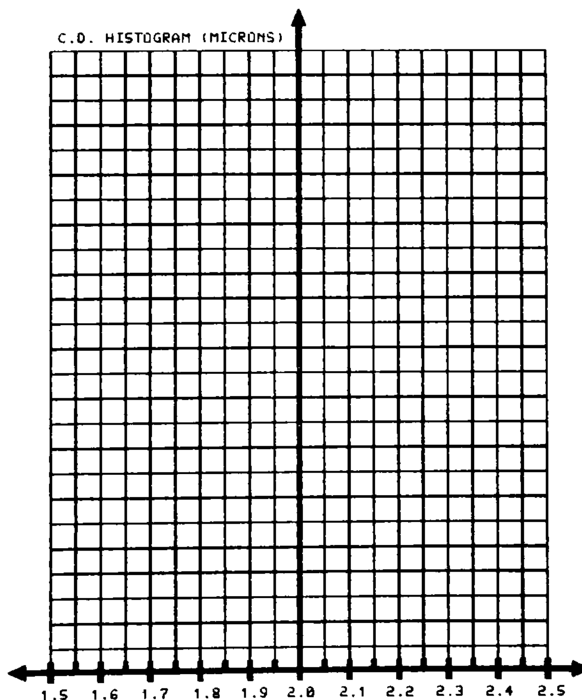

FIGURE 8: CRITICAL DIMENSION HISTOGRAM

X AVE = SIGMA = 3 SIGMA =

3. RESOLUTION

Description: Optical Inspection of the various resolution patterns will be performed to determine the exposure tool's limitions for the geometries presented. Scanning Electron Microscopy analysis can be used to ultimately document this evaluation.

Evaluation: Optical inspection at high magnification (such as 600X or 800X) as well as Scanning Electron Microscopy analysis.

Test Points: One wafer, three to five positions on the wafer should be identified which provide a reasonable sample of the wafer. SEM micrographs will be taken of the worst case positions on the wafer.

Procedure: The wafer used for procedure 2 can be used for this evaluation.

1. Coat the wafers with 1.2 microns of photoresist and prebake.
2. Select an exposure dose which will provide a 1:1 transfer of the 2 micron lines from the mask to the wafer.
3. Expose the wafer on the exposure tool using the selected dose.
4. Develop and postbake the wafer.
5. Optically inspect the line/space elements as well as both clear and dark field patterns and record the results.
7. Take SEM micrographs of the features at the threshold of "failure".

4. ELECTRICAL LINEWIDTH EVALUATION

Description: Van der Pauw linewidth structures are fabricated and probed to determine the average electrical linewidth. Two devices for each particular dimension reside in each 12 pad structure. One has the feature alone by itself and the other has the feature within a field of other features.

Evaluation: Electrical probing as defined in Appendix C.

Test Points: One wafer, all die locations on the wafer should be probed.

Procedure:

1. Grow 600-1000 A oxide.
2. Deposit 3.3-4.0 KA of polysilicon.
3. Phosphorus dope for 15-30 ohms/square sheet resistance and deglaze.
4. Coat the wafers with 1.2 microns of photoresist and prebake.
5. Expose the wafer on the exposure tool with the appropriate dose.
6. Develop and postbake the wafer.
7. Evaluate the CD at all positions and record on the C.D. Data Sheet.
8. Etch the polysilicon.
9. Strip the photoresist.
10. Probe the wafer for linewidth and record on the C.D. Data Sheet.
11. Plot a histogram of the data on the C.D. Data Sheet.
12. Calculate the mean and standard deviation of the data population (see Appendix A).
13. Compare the CD data evaluated on the resist to that evaluated electrically after the etch.

5. ELECTRICAL SPACEWIDTH EVALUATION

Description: Van der Pauw spacewidth structures are fabricated and probed to determine the average electrical spacewidth. Two devices for a particular dimension reside in each 12 pad test structure. One has the feature alone by itself and the other has the feature within a field of other features.

Evaluation: Electrical probing as defined in Appendix C.

Test Points: One wafer, all die locations on the wafer should be probed.

Procedure:

1. Grow 4000-10000 A oxide.
2. Coat the wafers with 1.2 microns of photoresist and prebake.
3. Expose the wafer on the exposure tool with the appropriate dose.
4. Develop and postbake the wafer.
5. Evaluate the CD (space) at all positions and record on the corresponding C.D. Data Sheet.
6. Etch the oxide and ensure the wafer backsides dewet.
7. Strip the photoresist.
8. Phosphorus dope for 15-30 ohms/square sheet resistance and HF deglaze.
9. Probe the wafer for spacewidth and record on the C.D. Data Sheet.
10. Plot a histogram of the data on the C.D. Data Sheet.
11. Calculate the mean and standard deviation of the data population (see Appendix A).
12. Compare the CD data evaluated on the resist to that evaluated electrically after the etch.

6. PHOTORESIST PROCESS CONDITIONS

Description: This procedure can be used to obtain optimized processing conditions with respect to the photoresist and developer under constant exposure tool conditions.

Evaluation: Optical inspection at high magnification (such as 600X or 800X) as well as Scanning Electron Microscopy analysis.

Test Points: The number of wafers and sample positions depends on the nature of the test involved. SEM micrographs will be taken of the worst sites.

Procedure:

1. Coat the wafers with photoresist. The variables possible include: photoresist material (speed, viscosity) and coat thickness.
2. Prebake the wafers. The variables possible include: time interval, temperature and oven configuration (convection vs. hot plate).
3. Expose the wafer on the exposure tool using a constant exposure dose.
4. Develop the wafer. The variables include: developer strength, mode of application (batch, dunk, puddle, spray) and time interval.
5. Postbake the wafer. The possible variables include: time interval, temperature and oven configuration (convection vs. hot plate).
6. Optically inspect the line/space elements.
7. Take SEM micrographs of the edge profiles for the varied conditions.

7. ALIGNMENT ACCURACY

Description: This procedure is used to determine the alignment capability of an exposure tool. Second level alignment and exposures will be performed on patterned first level wafers. Optical verniers will be reviewed and alignment data populations will be analyzed.

Evaluation: Optical verniers with 0.2 micron resolution.

Test Points: Ten wafers at positions 1 and 2 on the Overlay Data Sheet (see pages 23 and 24).

Procedure:

1. Coat the patterned wafers with 1.2 microns of photoresist and prebake.
2. Offset the mask with respect to wafer in the direction of the arrow.
3. Align the wafer to the mask target which is appropriate for that tool.
4. Expose the wafer with a dose appropriate for 2 to 3 micron lines..
5. Develop and postbake the wafer.
6. Evaluate the optical verniers in both X and Y directions as defined in Appendix B.
7. Record the data in the spaces provided on the Overlay Data Sheet.
8. Plot histograms of the data for both X and Y alignment on the Overlay Data Sheet.
9. Calculate the mean and standard deviation of the data populations (see Appendix A).

********************** OVERLAY DATA SHEET FOR 3" WAFERS **********************

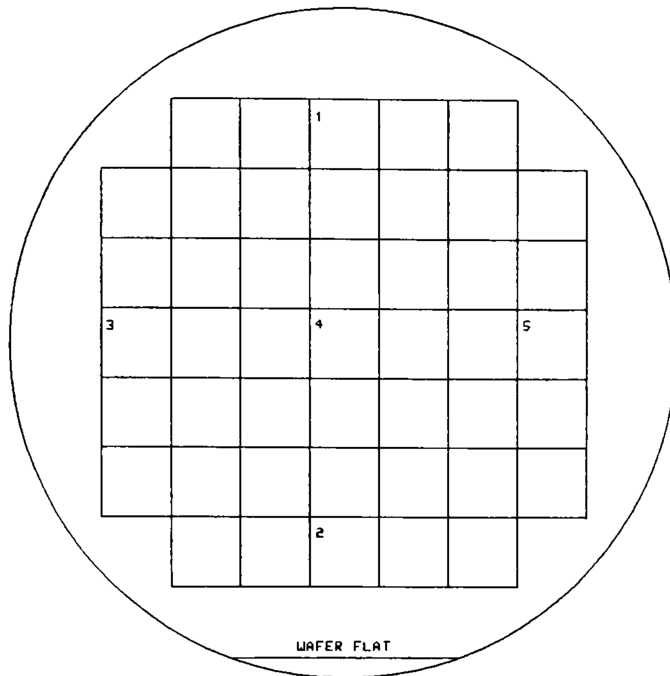

FIGURE 9: 3" WAFER MAP

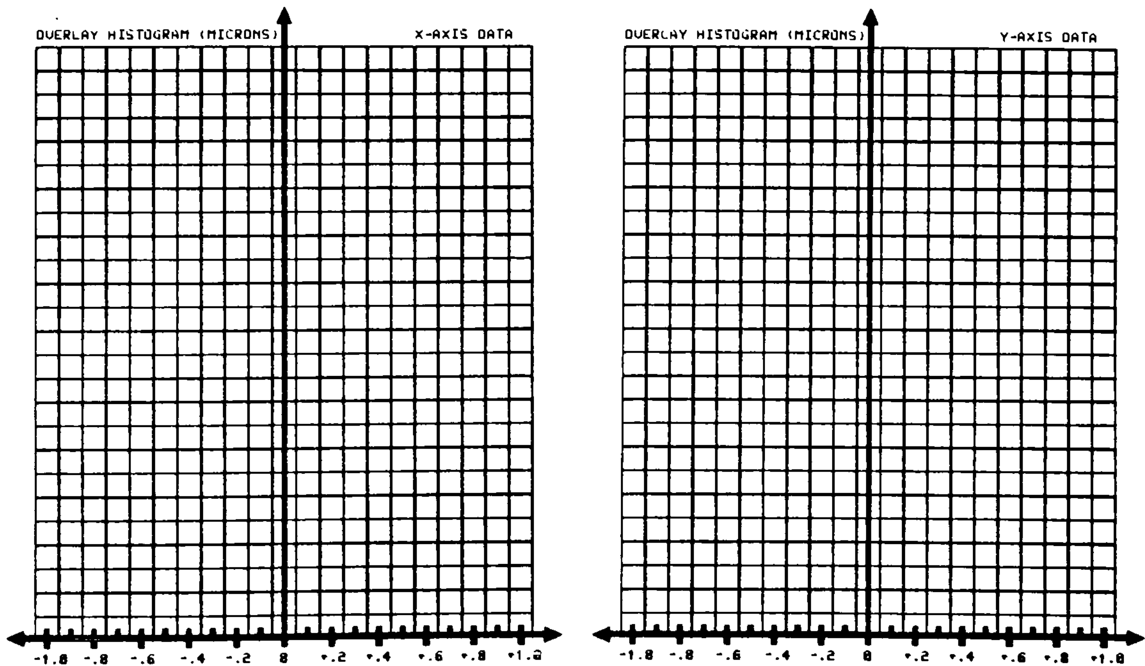

FIGURE 10: OVERLAY HISTOGRAMS

X AVE =

Y AVE =

X SIGMA =

Y SIGMA =

3*X SIGMA =

3*Y SIGMA =

******************* OVERLAY DATA SHEET FOR 100 MM WAFERS ********************

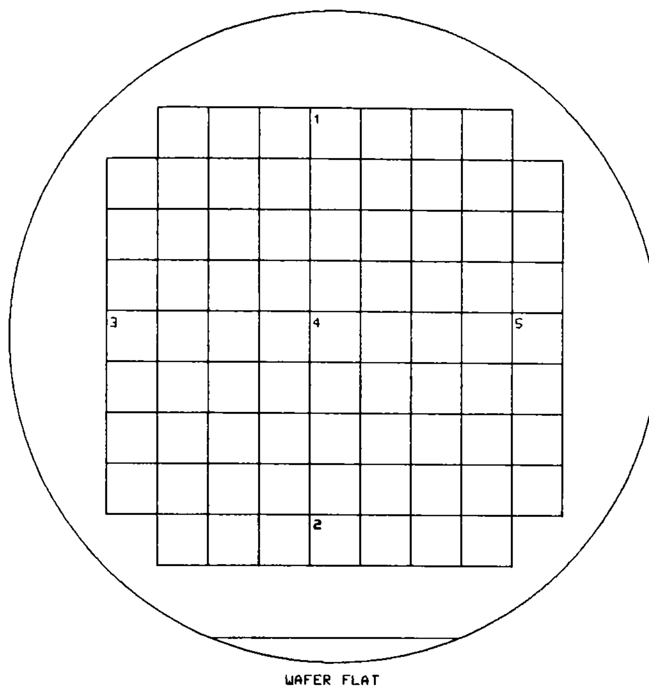

FIGURE 11: 100 MM WAFER MAP

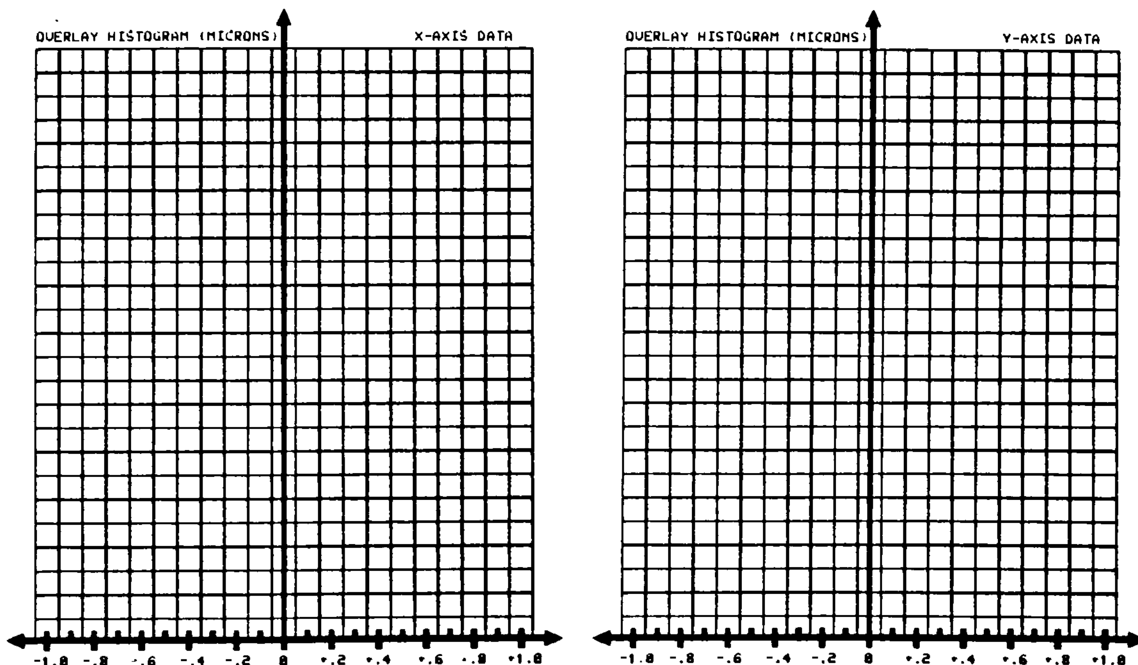

FIGURE 12: OVERLAY HISTOGRAMS

X AVE =

Y AVE =

X SIGMA =

Y SIGMA =

3*X SIGMA =

3*Y SIGMA =

8. DISTORTION / MAGNIFICATION

Description: This procedure determines the amount of overlay error introduced due to distortion and magnification problems. Second level exposures will be done on patterned first level wafers. Optical verniers are reviewed and various distortion / magnification values calculated.

Evaluation: Optical verniers with 0.2 micron resolution.

Test Points: One wafer at positions 1 through 5 on the Overlay Data Sheet.

Procedure: Wafers used for for procedure 7 can be used for this evaluaton.

1. Coat the wafers with 1.2 microns of photoresist and prebake.
2. Offset the mask with respect to wafer in the direction of the arrow.
3. Align the wafer to the mask target which is appropriate for that tool.
4. Expose the wafer with a dose appropriate for 2 to 3 micron lines.
5. Develop and postbake the wafer.
6. Evaluate the optical verniers for both X and Y (see Appendix B).
7. Record the data on the corresponding Overlay Data Sheet.
8. Calculate the values X mag, Y mag and Theta Skew from the formulas.

$$X\ mag = X2 - X1, \quad Y\ mag = Y3 - Y5, \quad Theta\ Skew = X3 - X5 + Y2 - Y1$$

Note: These parameter definitions are particular only to ETM-1 and are not necessaily interchangeable with those defined by specific equipment manufacturers.

9. RESIST IMAGING OVER TOPOGRAPHY

Description: Due to stray reflections off of certain surfaces and edges, resist notching can occur when patterns are imaged over other features below them. This test provides a series of line/space elements which cross each other providing the situation which can be evaluated.

Evaluation: Optical inspection at high magnification (such as 600X or 800X) as well as Scanning Electron Microscopy analysis.

Test Points: One wafer at three to five positions on the wafer. SEM micrographs will be taken of the worst case positions on the wafer.

Procedure: Wafers used for for procedure 7 can be used for this evaluaton.

1. Coat the wafers with 1.2 microns of photoresist and prebake.
2. Offset the mask with respect to wafer in the direction of the arrow.
3. Align the wafer to the mask target which is appropriate for that tool.
4. Expose the wafer with a dose appropriate for 2 to 3 micron lines.
5. Develop and postbake the wafer.
6. Optically inspect the line/space elements at their intersections.
7. Take SEM micrographs of the features at their intersections.
8. Compare the limitations to those from a wafer with no topography.

Further Evaluation: The use of dyed resists can substantially improve the situation experienced over topography and could be evaluated.

10. MIX AND MATCH CAPABILITY

Description: This procedure can be used to determine the feasibility of exposing a first level on one exposure tool and the second on another. First level wafers will be patterned on one machine in 4000 to 8000 A of oxide and subsequently aligned and exposed on another tool.

Evaluation: Optical verniers with 0.2 micron resolution,

Test Points: One wafer at positions 1 through 5 on the Overlay Data Sheet.

Procedure:

1. Coat the wafers with 1.2 microns of photoresist and prebake.
2. Expose the wafer on tool 1 with a dose for 2 to 3 micron lines.
3. Develop and postbake the wafer.
4. Etch the oxide until the wafer backsides dewet.
5. Strip the photoresist.
6. Coat the wafers with 1.2 microns of photoresist and prebake.
7. Offset in the direction of the arrow and align the wafer to the mask.
8. Expose the wafer with a dose appropriate for 2 to 3 micron lines.
9. Develop and postbake the wafer.
10. Evaluate the optical verniers for both X and Y (see Appendix B).
11. Record the data in the spaces provided on the Overlay Data Sheet.
12. Calulate the distortion / magnification values given below.

X mag = X2 - X1, Y mag = Y3 - Y5, Theta Skew = X3 - X5 + Y2 - Y1

11. ELECTRICAL ALIGNMENT EVALUATION (CLEARFIELD TO CLEARFIELD STRUCTURE)

Description: Alignment and processing is performed to bare p-type wafers which results in a resistor bridge structure that can be evaluated electrically for both X and Y alignment data.

Evaluation: Electrical probing as defined in Appendix D.

Test Points: One wafer at all die locations on the wafer should be probed.

Procedure:

1. Grow 600-1000 A oxide.
2. Deposit 3.3-4.0 KA of polysilicon.
3. Coat the wafers with 1.2 microns of photoresist and prebake.
4. Expose the wafer with a dose appropriate for 2 to 3 micron lines.
5. Develop and postbake the wafer.
6. Etch the polysilicon and strip photoresist.
7. Clean wafers, grow 2000 A oxide (or deposit 5000 A LTO).
8. Coat the wafers with 1.2 microns of photoresist and prebake.
9. Offset, align and expose wafers with dose for 2 to 3 micron lines.
10. Develop and postbake the wafer.
11. Etch the the oxide or LTO.
12. Phosphorus dope for 15-30 ohms/square sheet resistance and HF deglaze.
13. Probe the wafer for alignment and record on the Overlay Data Sheet.
14. Plot a histogram of the data on the Overlay Data Sheet.
15. Calculate the mean and standard deviation of the data population (see Appendix A).

12. ELECTRICAL ALIGNMENT EVALUATION (CLEARFIELD TO DARKFIELD STRUCTURE)

Description: Alignment and processing is performed to bare p-type wafers which result in a resistor bridge structure that can be evaluated electrically for both X and Y alignment data.

Evaluation: Electrical probing as defined in Appendix D.

Test Points: One wafer at all die locations on the wafer should be probed.

Procedure:

1. Grow 8000 A oxide.
2. Coat the wafers with 1.2 microns of photoresist and prebake.
3. Expose the wafer with a dose appropriate for 2 to 3 micron lines.
4. Develop and postbake the wafer.
5. Etch the oxide until wafer bakesides dewet and strip photoresist.
6. Clean the wafers and grow 4000 A oxide.
7. Coat the wafers with 1.2 microns of photoresist and prebake.
8. Offset, align and expose wafers with a dose for 2 to 3 micron lines.
9. Develop and postbake the wafer.
10. Etch the oxide, ensure wafer backsides dewet and strip photoresist.
11. Phosphorus dope for 15-30 ohms/square sheet resistance and HF deglaze.
12. Probe the wafer for alignment and record on the Overlay Data Sheet.
13. Plot a histogram of the data on the Overlay Data Sheet.
14. Calculate the mean and standard deviation of the data population (see Appendix A).

V. RESULTS AND ANALYSIS

The primary objective of this work was the design, fabrication and documentation of the Exposure Test Mask and the corresponding procedures. Complete functionality of the mask has been demonstrated by the characterization of a Perkin-Elmer Micralign 241 Scanner. The procedures defined in section IV were performed and the results are included in Appendix F. It is not the intent here to discuss the actual performance of the exposure tool, but rather the mask itself.

Certain problems associated with the first masks received are discussed below. These were corrected by subsequent revisions and therefore may or may not be present, depending on which revision is used. Minor layout errors resulted in the absence of label characters on two structures. Also, data conversion errors during the E-beam tape generation resulted in significant loss of data in the contact, island and checkerboard arrays. Finally, design oversights rendered the alignment 12 pads useless, until the masks were repaired.

The results concluding this section pertain to the accuracy which can be expected from the use of this design. In all cases the data presented pertains to the 1X 5"x5" mask as it was used during the previously mentioned characterization. Special attention should be given to the C.D. integrity of the mask (see Figures 16, 17) and the associated test results illustrated in Figures 18 and 19. Correlation of electrical and optical test devices is presented for linewidth studies in Figures 20 and 21 and alignment studies in Figure 25. Examples of the major overlay components are shown in Figures 22-24. SEM micrographs of the optical structures are included in Appendix G.

Unknown difficulties with the data conversion of certain geometries completely "colored in" characters which had been designed as spaces in a dark field as shown in the figure below.

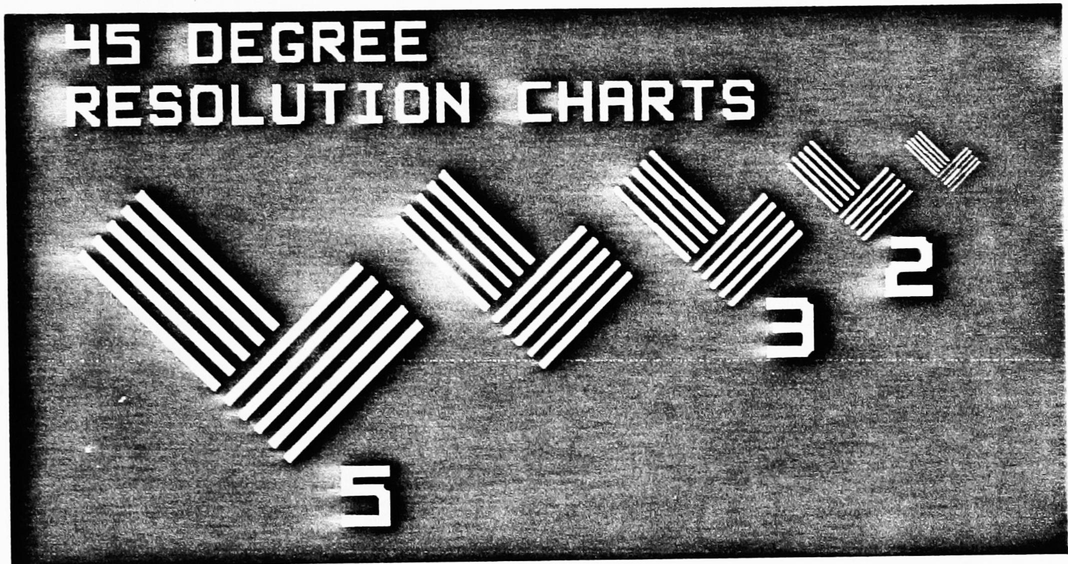

Figure 13: Design Layout Errors.

Major problems between the generation of E-beam tapes and their legibility at the mask manufacturer caused entire arrays of contacts, islands and checkerboards to be severed as shown in the SEM micrographs below.

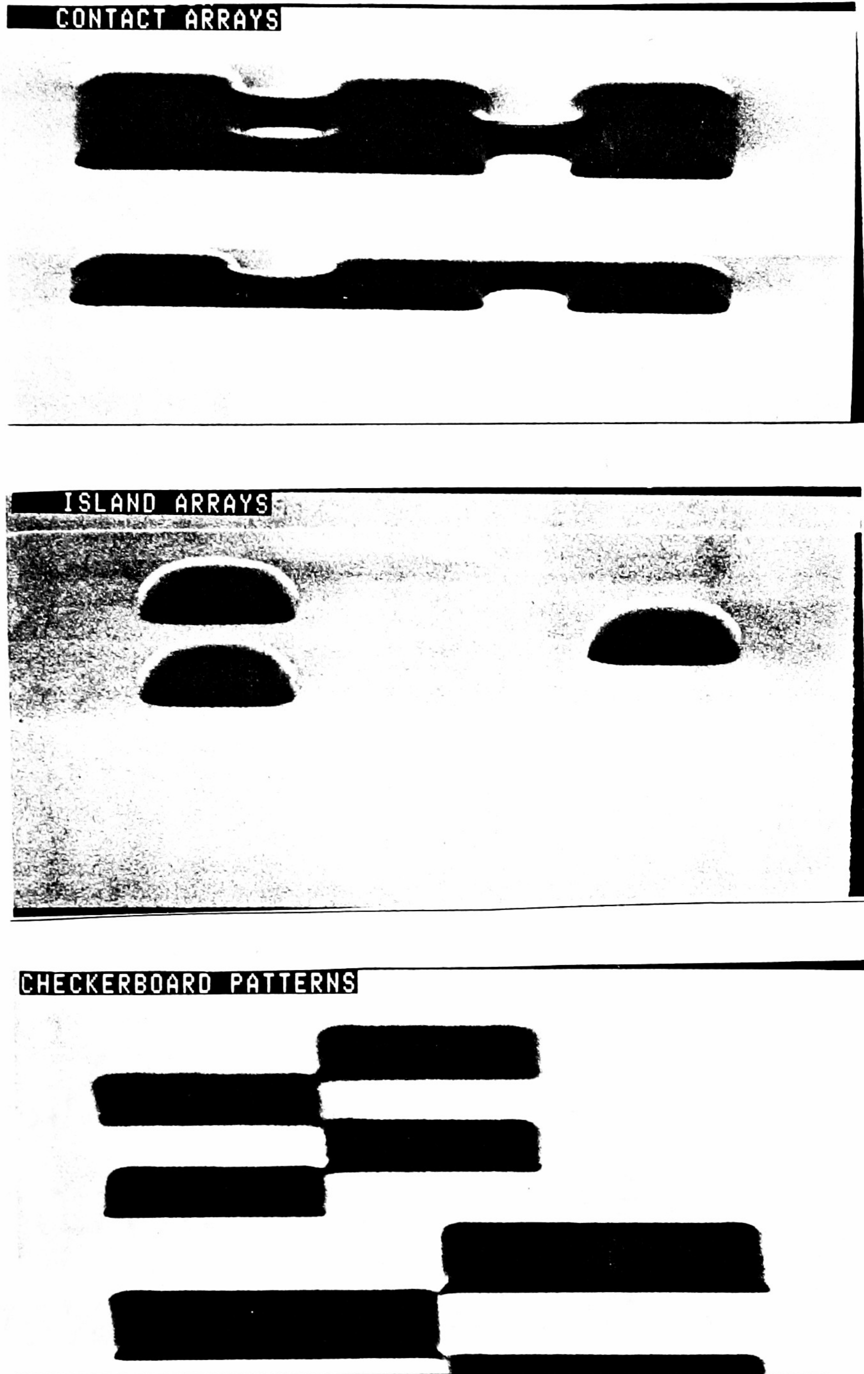

Figure 14: E-beam Tape Conversion Errors.

An artifact of the alignment test device cell resulted in unwanted chrome on the 1X mask and 10X reticle. This cell was revised for new mask orders and physically repaired on the plates which had been received. The SEM micrographs below show the region before and after the chrome was removed with a laser.

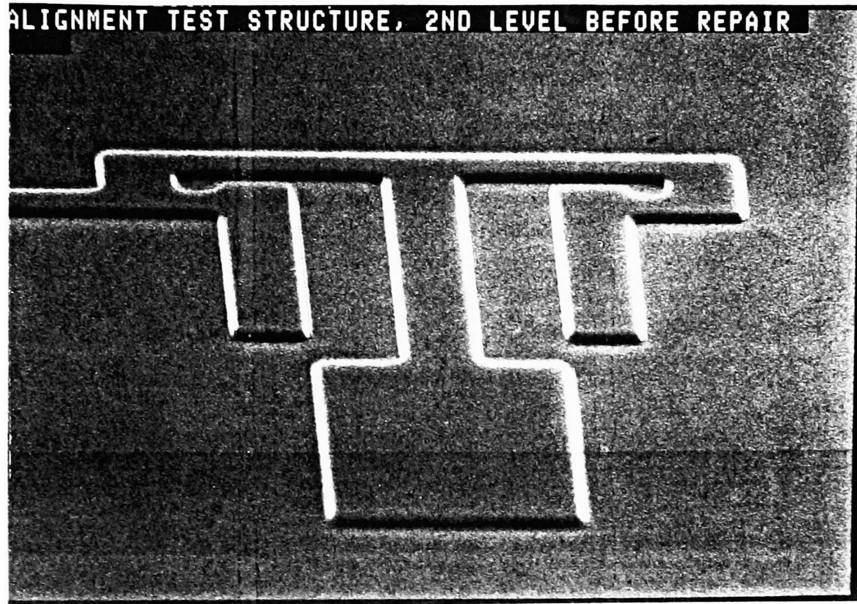

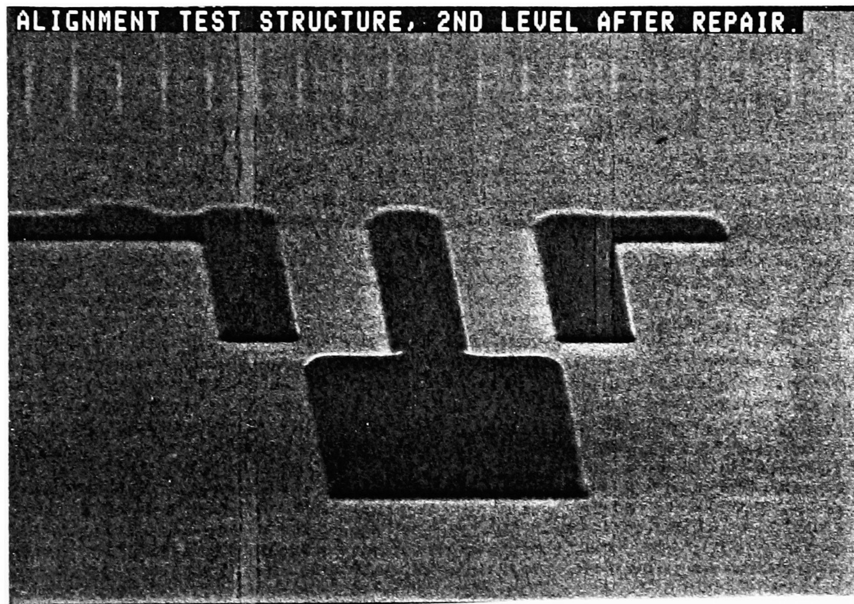

Figure 15: Alignment Test Device Chrome Zapping.

These masks were ordered with a dimensional tolerance of +/- .15 microns. The chrome images on the mask were optically measured with a Leitz microscope equipped with the C.D. scanning slit package and are given below. The mask data is presented as if it were mapped directly to a wafer, and is compared to that of an exposed wafer in Figure 18.

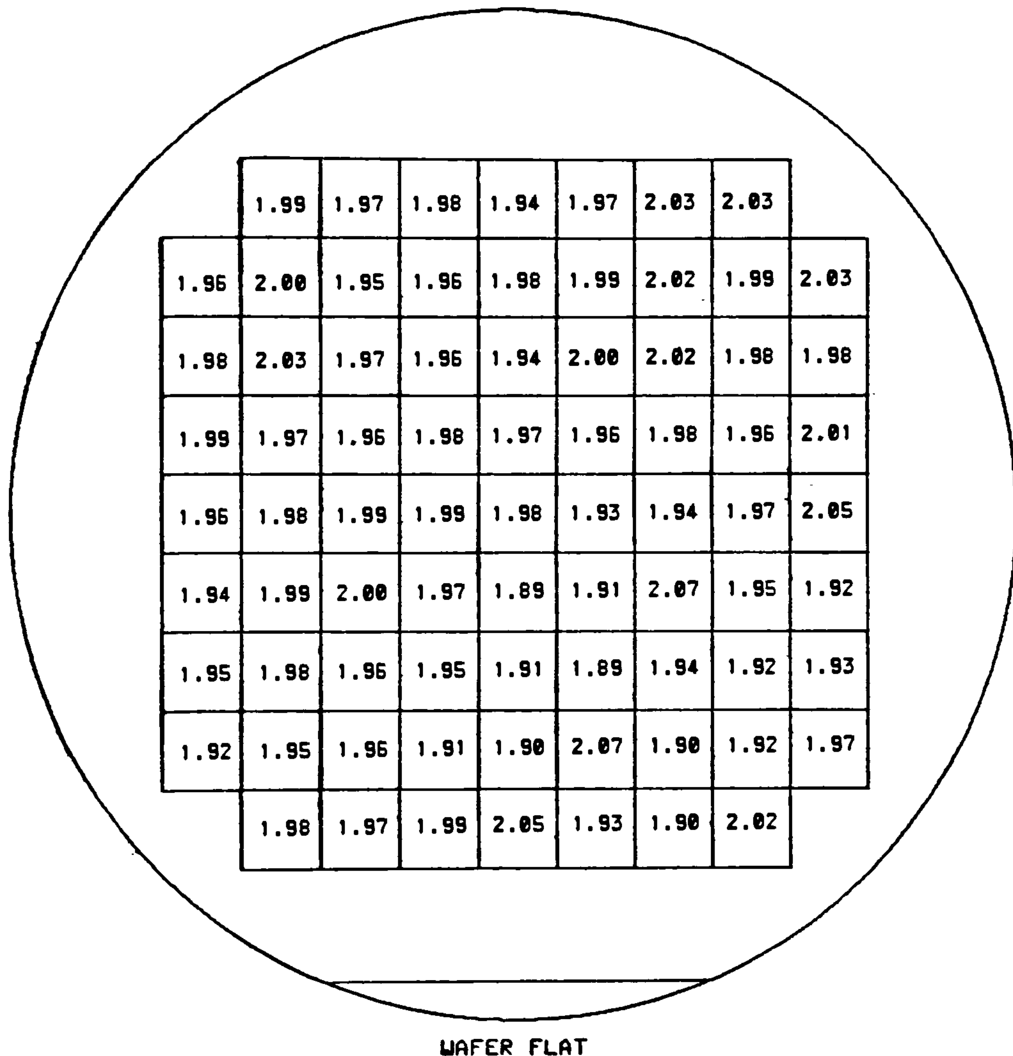

Figure 16: Mask C.D. Map (1X 5"x5")

Statistical representation of the mask C.D. data population is illustrated below in the form of a histogram. The slight offset from a nominal dimension of 2 microns is almost negligible and the dimensional population is considered to be very acceptable. This can be compared to those on an exposed wafer as shown in Figures A50 and A52.

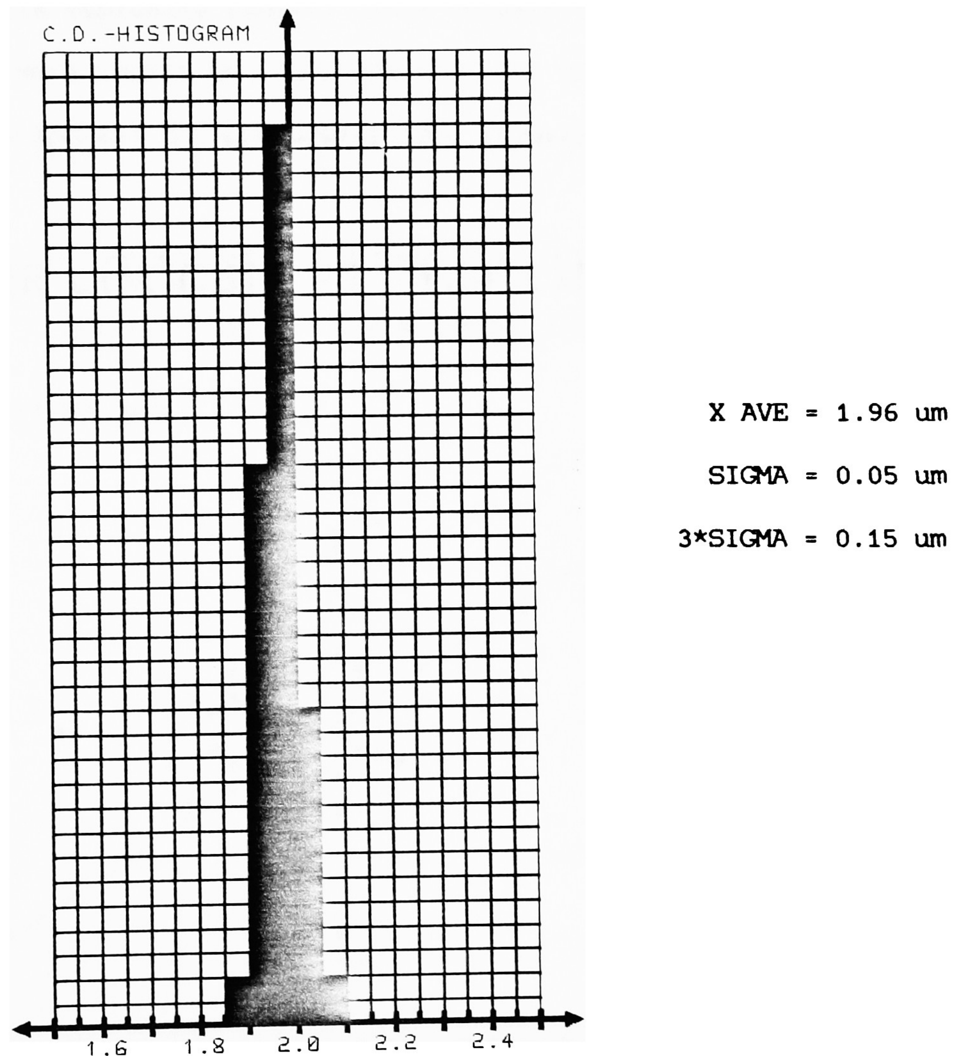

Figure 17: Mask C.D. Histogram (1X 5"x5").

The correlation plot below was achieved with a 1:1 mapping of the die-to-die C.D. measurements taken on the mask and an exposed wafer. The plot defines the exposure tool's ability to transfer the mask image to the wafer. As is evident, the variation in the wafer linewidth is not primarily due to the mask line dimension. In fact, a close study revealed that these variations corresponded directly to position along the exposure slit of the Perkin-Elmer 241 scanner. Maximum increase in wafer linewidth occurred at both ends of the slit where the intensity is typically lowest. This reveals that other processing conditions can have more impact on linewidth than the mask dimension itself. Refer to Figures A49 and A51 for the actual data in wafer maps.

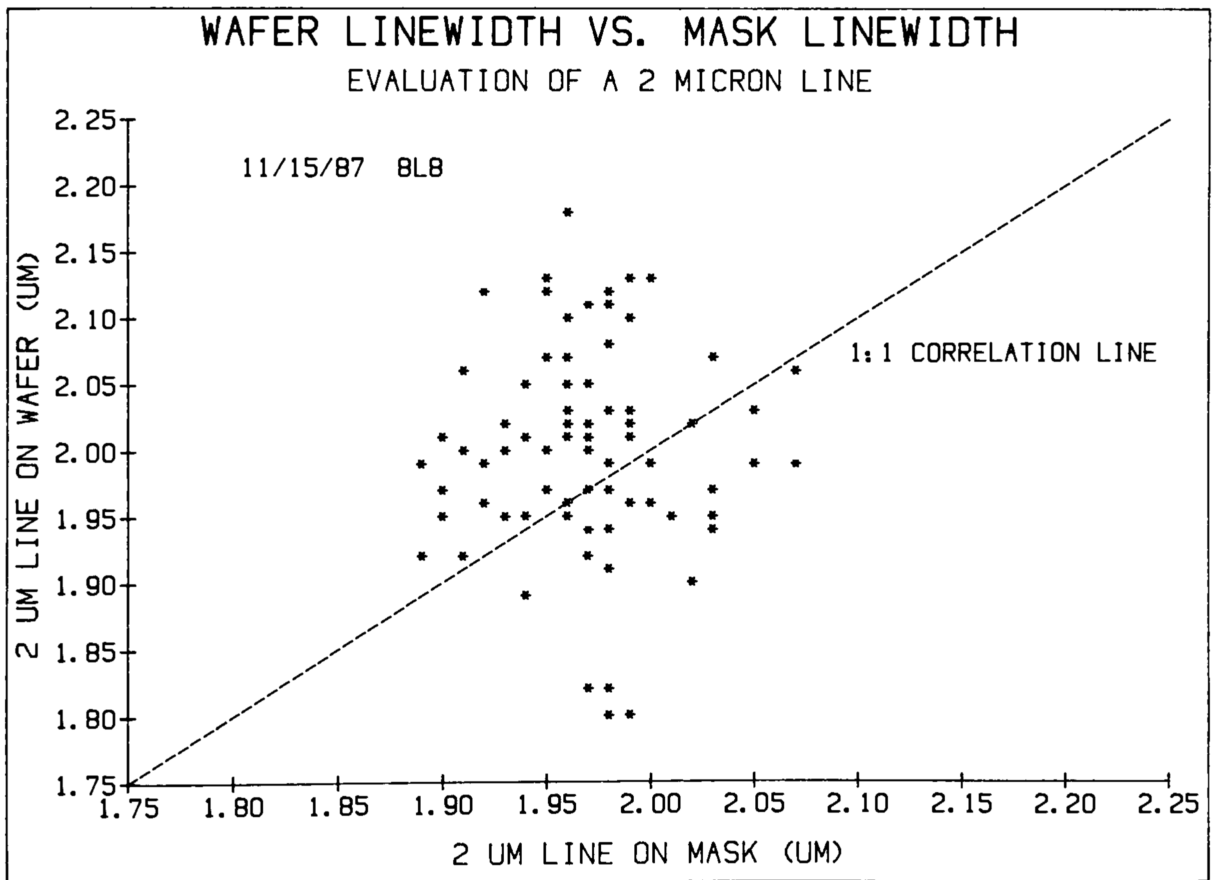

Figure 18: Wafer Linewidth vs. Mask Linewidth.

The correlation plot below reveals a 0.05 micron decrease in the dimension of a 2 micron line which resides in a field of other lines. This is actually opposite of the expected result, which by intuition suggests that isolated lines would be narrower due to improved development reaction conditions. This inconsistency is best explained by differences observed in the background light and focus conditions used during the optical measurement procedure. Confirmation of this with SEM analysis was inconclusive due to the inability to detect linewidth variations that small. Refer to Figures A49 through A52 for the actual data.

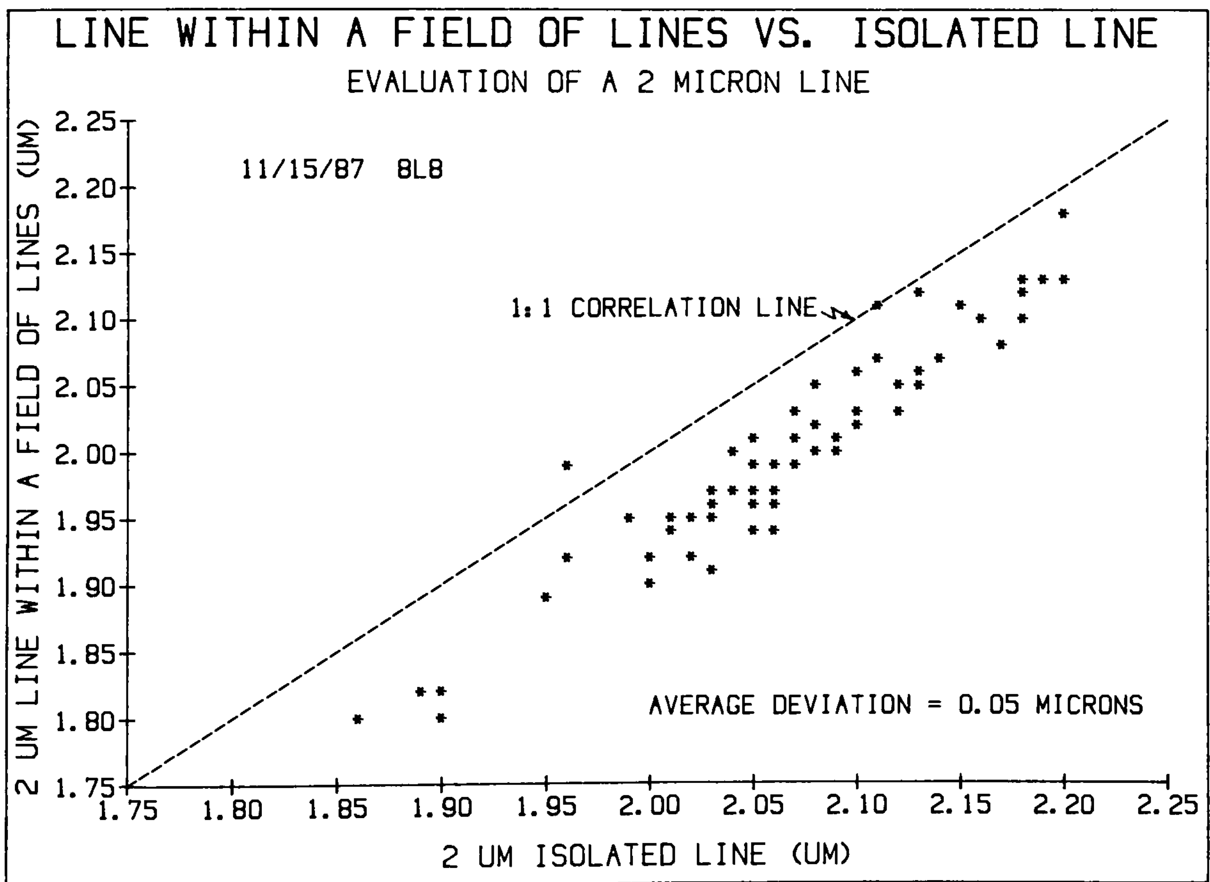

Figure 19: Line Within a Field of Lines vs. Isolated Line

The correlation plot below depicts the linewidth loss incurred during a polysilicon etch using a typical plasma etch process. Both the photoresist (before etch) and polysilicon (after etch and strip) images were evaluated optically for various wafers from an exposure series. It is evident that the linewidth loss is 0.4 microns, or 0.2 microns per side. Refer to Figures A53 through A55 for the actual data.

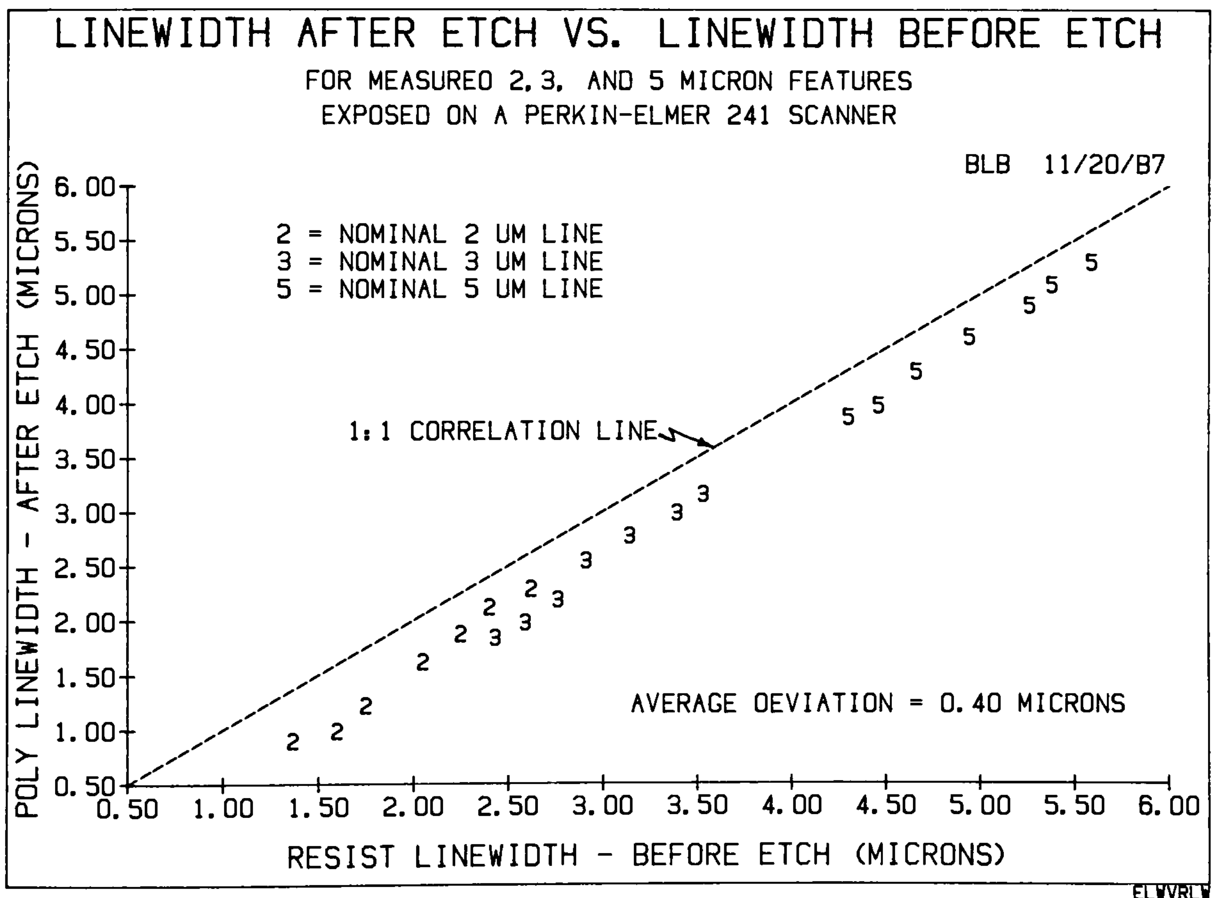

Figure 20: Linewidth After Etch vs. Linewidth Before Etch

Missing Page

A normal alignment was performed on a wafer when the bi-level experiments were done. The wafer map below plots vectors indicating the direction of mis-registration of the wafer with respect to the mask, as determined by optical vernier interpretation. The vectors are very small in this case because the alignment is quite good. Figure A59 has all of the actual measured data in another wafer map.

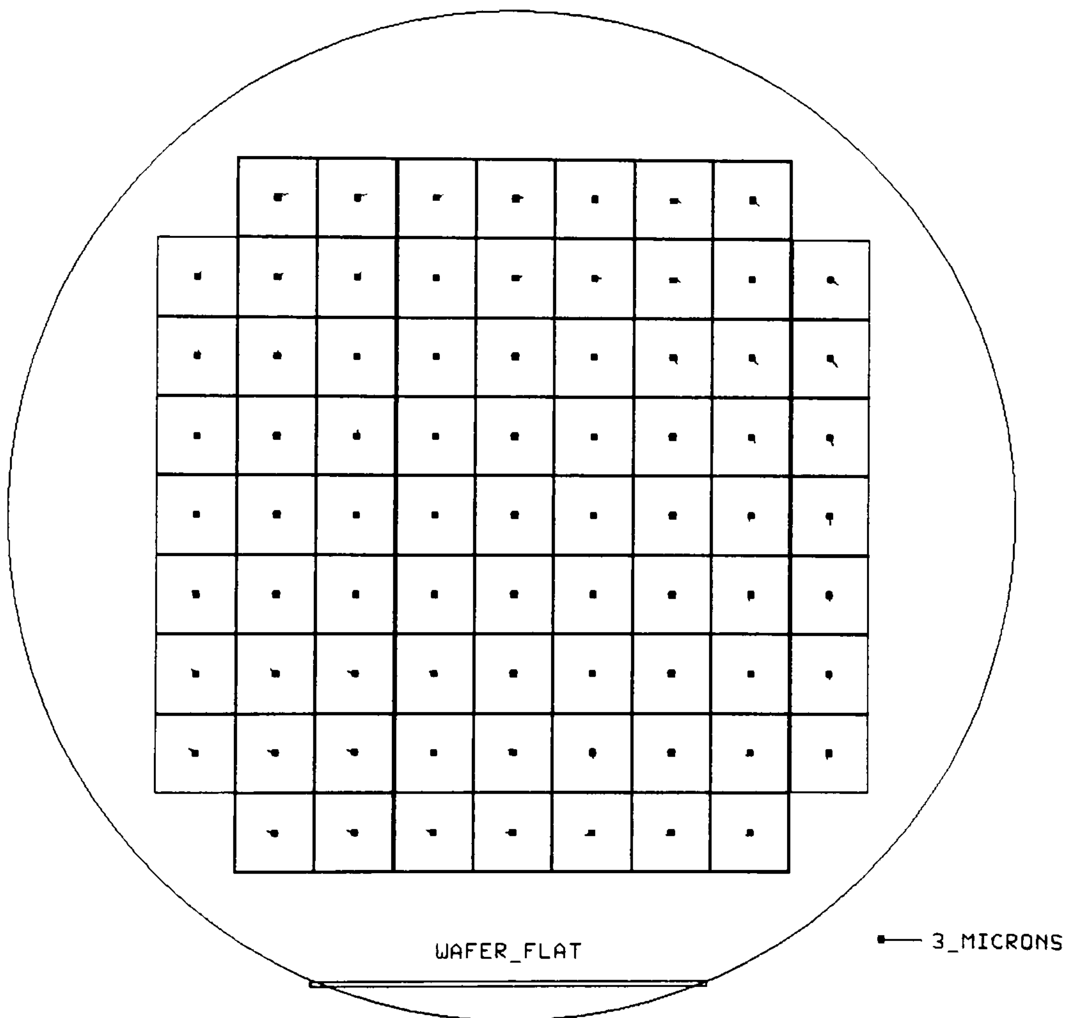

Figure 22: Example of Overlay with Acceptable Alignment.

A large translational (X-Y) error was deliberately introduced during the alignment of one wafer when the bi-level experiments were performed. The resulting overlay wafer map from the optical vernier evaluation is shown below with vectors indicating the direction of misregistration of the wafer with respect to the mask. Figure A60 tabulates the actual measured data in another wafer map.

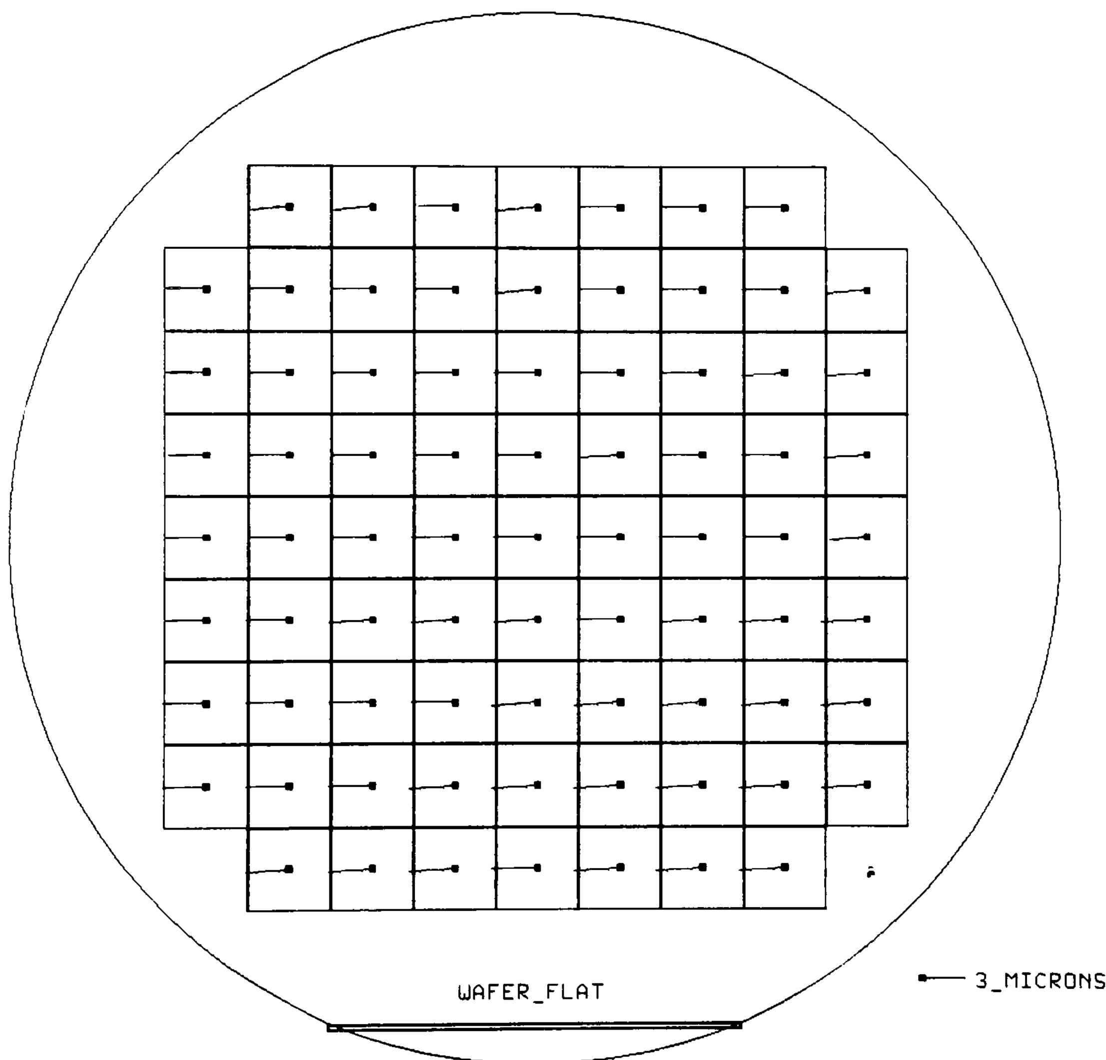

Figure 23: Example of Overlay with Translation Error.

A large rotational (theta) error was deliberately introduced during the alignment of one wafer when the bi-level experiments were performed. The overlay wafer map from optical vernier evaluation is shown below with vectors indicating the direction of misregistration of the wafer with respect to the mask. Figure A61 includes the actual measurements in a wafer map.

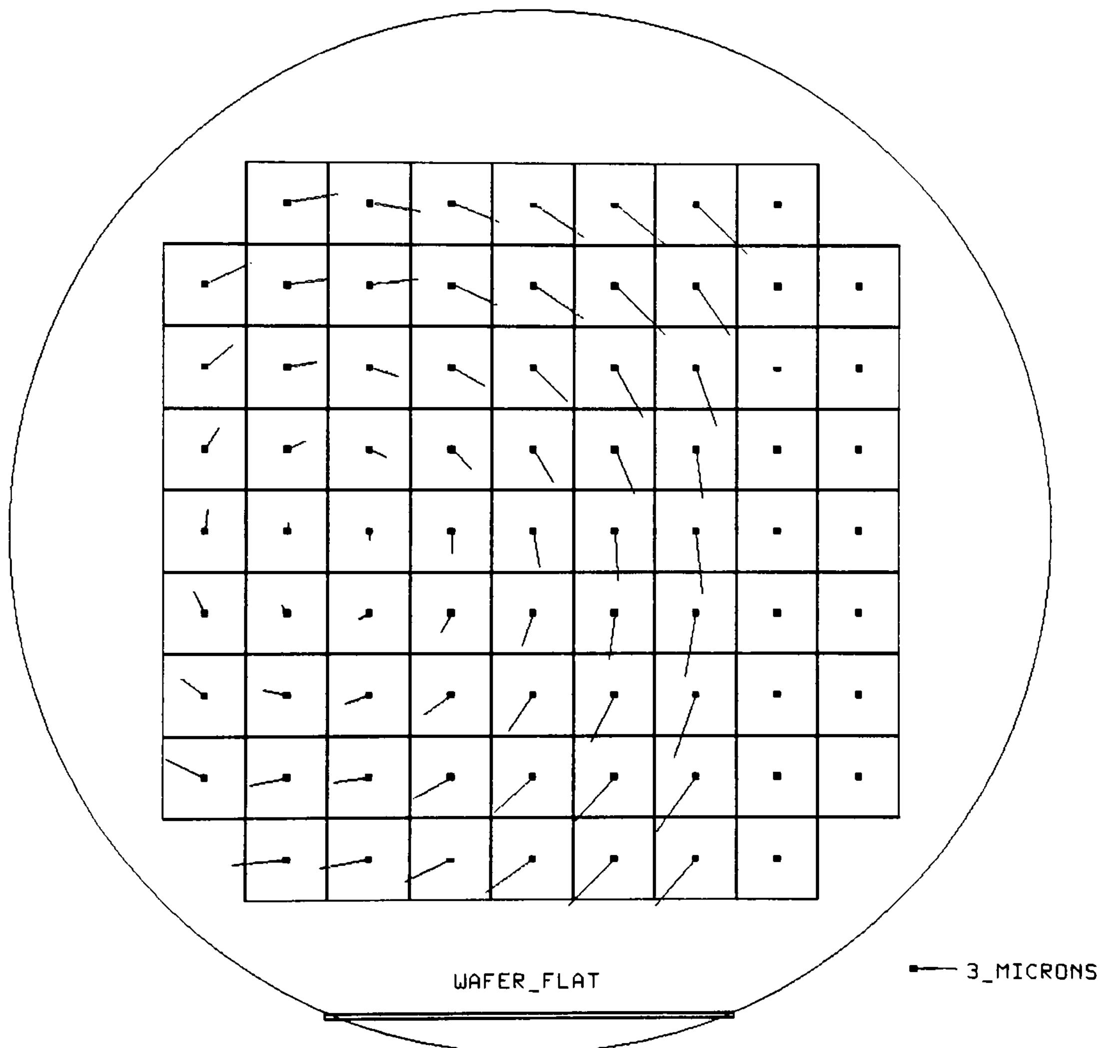

Figure 24: Example of Overlay with Rotation Error.

The electrical alignment test structures are created by a resistor bridge resulting from two superimposed patterns. Wafers were made with rotational errors which provided many different data points. The correlation plot below reveals the comparison between the electrical results and optical verniers. The device should be insensitive to all processing conditions, however errors in this case can be attributed to mask problems resulting from the laser zapping discussed on page 33.

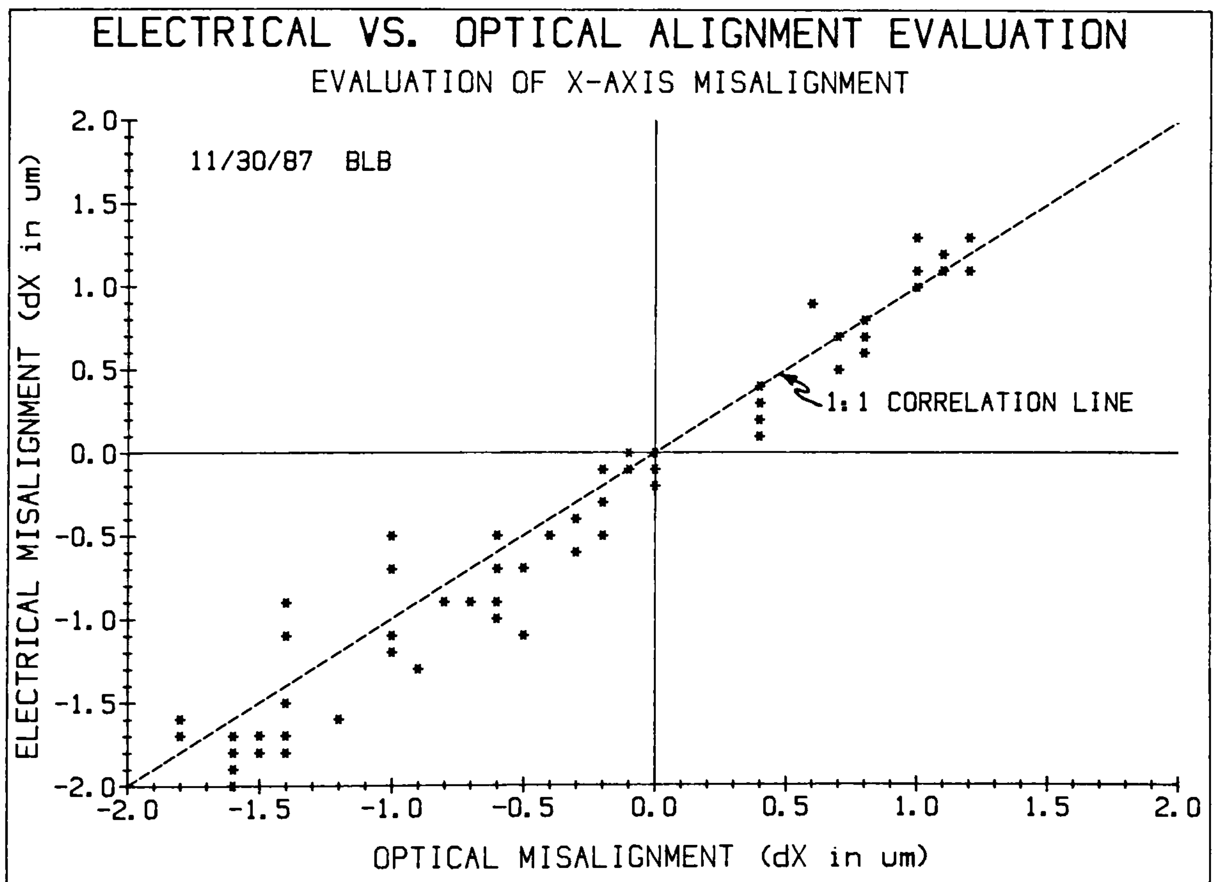

Figure 25: Electrical vs. Optical Alignment Evaluation (X-Axis).

Difficulties arose during the testing of electrical structures which were created from phosphorus diffusions directly into the silicon, such as the electrical spacewidth structures. It was expected that the results would be influenced by the oxide etch and phosphorus lateral diffusion, but unacceptable errors were obtained during the probing. These were most likely due to a number of different reasons, which are discussed below.

Potential problems were observed during the wafer probing. First of all, extremely high contact resistances were measured for the diffused structures as compared to the polysilicon devices. Secondly, large ranges in sheet resistance values were measured, and appeared to be dependent on the geometry. This was not the case during the evaluation of the polysilicon devices. Finally, very large supply voltages were required to force the desired test current.

Devices of this nature are usually tested on product wafers with metal lines routed from the test device to metal bond pads. Under the constraints of this design, all of this had to be done with the diffusion itself. Changes may be possible in the process sequence which could improve the testability of the spacewidth devices.

A boron diffusion into n-type wafers and the use of mercury probes could greatly reduce the effects of high contact resistance, as would an HF acid dip immediately prior to probing. Also, a more sophisticated LOCOS process, which leaves nitride to mask the field oxide growth in the active area, would help isolate the sidewalls of the diffusion and alleviate any problems arising from surface leakage currents. These improvements could be investigated in the future if deemed necessary.

VI. CONCLUSIONS

The Multipurpose Test Mask for Exposure Tool Characterization is indeed a versatile design which can be used to completely evaluate the performance of an exposure tool. The cell design exceeds user requirements and minimal effort is needed to establish its use. The procedures offered were proven in a demonstration of an actual characterization. Future investigations can be performed which will compare the performance of a variety of tools.

All single level procedures were completed with results which were beyond expectations. The optical resolution patterns served as very good indicators. Correlation between the optical and electrical linewidth structures was acceptable for the polysilicon structures. Further development work is required for acceptable correlation of the diffused (darkfield / space) structures.

The bi-level experiments also proved to be very informational. Confidence in the electrical alignment structures can be gained with future investigations and improvements in the automated probing procedures. Also, another structure which has a clear field first level and dark field second level would be beneficial in the processing of polysilicon alignment test structures.

It is believed that with a moderate amount of experience, this mask can be used to optimize all of the exposure tools for which it was intended for and subsequently be used on a routine basis for monitoring their performance. The design meets all expectations and should be recognized as a powerful tool for photolithography and its impact on integrated circuit fabrication.

ACKNOWLEDGEMENTS

This project was made possible by the efforts extended from my colleagues at Eastman Kodak Company. Mike Guidash is appreciated for his offerings with CAD layout procedures and file information. Norm Discher, Herb Earhardt and Ed Nelson offered basic cells which ultimately were used and added great strength that the design would have otherwise lacked. Ken Brawn offered relentless support with final file editing and E-beam tape generation, not to mention the Focus Star design. Finally, John Conner established the testing programs and technical support for the electrical test structures.

REFERENCES

(1) R. K. Watts, J.H. Bruning, "A Review of Fine-Line Lithographic Techniques: Present and Future," Solid State Technology, pp. 99-105, May 1981.

(2) J. Bossung, "Projection Mask Alignment," Kodak Microelectronics Seminar: Interface '72, pp. 9-14, 1972.

(3) B. Allsop, "Projection Aligners in Production A Whole New Ballgame," Kodak Microelectronics Seminar: Interface '76, pp. 20-27, 1976.

(4) J. D. Buckley, "Expanding the Horizons of Optical Projection Lithography," Solid State Technology, pp. 77-82, May 1982.

(5) J. P. Robic, S. E. Knight, W. A. Straub, "Mid-UV Lithography with Positive Resist - A Multifunctional Tool and Process Evaluation," Solid State Technology, pp. 147-150, May 1983.

(6) J. J. Greed, Jr., D. A. Markle, "Variable Magnification in a 1:1 Projection Lithography System," SPIE Vol. 334: Optical Microlithography - Technology for the mid-1980s, pp. 2-9, 1982.

(7) H. O. Madsen, R. O. Rice, G. Southers, "Is a Stepper Really Better Than a Scanner? A 1:1 Comparison," Kodak Microelectronics Seminar: Interface, 1984.

(8) H. R. Rottmann, "Improving Registration in Photolithography," SPIE Vol. 342 Integrated Circuit Metrology, pp. 54-59, 1982.

(9) J. W. Bossung, E. S. Muraski, "Advances in Projection Microlithography," Solid State Technology, pp. 109-112, August 1979.

(10) A. Minvielle, R. Rice, "Spectral Output Variations in Perkin-Elmer Micralligns," Kodak Microelectronics Seminar: Interface '79, pp. 60-65, 1979.

(11) W. A. Bosenberg, H.P. Kleinknecht, "Linewidth Measurement on IC Wafers by Diffraction from Grating Test Patterns," Solid State Technology, pp. 79-85 July 1983.

(12) K. Murray, "Measuring Dimensions Using Murray Daggers," Semiconductor International, pp. 69-73, December 1982.

(13) L. J. van der Pauw, "A Method of Measuring Specific Resistivity and Hall Effect of Discs of Arbitrary Shape," Philips Research Reports Vol. 13, pp.1-9, February 1958.

(14) M. G. Buehler, S. D. Grant, W. R. Thurber, "Bridge and van der Pauw Sheet Resistors for Characterizing the Line Width of Conducting Layers," Journal of the Electrochemical Society, Vol. 125, pp. 650-654, April 1978.

(15) M. G. Buehler, "Measuring Conductor Widths and Spacings Electrically," NASA Technical Briefs, pp. 22-23, July/August 1987.

(16) J. A. Littlehale, "Determining Process Latitude with Electrically Measurable Test Structures," Kodak Microelectronics Seminar: Interface '84, 1984.

(17) M. A. Mitchell, V. Nagaswami, "Monitoring Wafer Stepper Performance with Electrical Test Structures," SPIE Vol. 342 Integrated Circuit Metrology, pp. 82-86, 1982.

(18) C. Murray, "Measurement Tools for Overlay Registration," Semiconductor International, pp. 62-68, February 1987.

(19) T. J. Russell, T. F. Leedy, R. L. Mattis, "A Comparison of Electrical and Visual Alignment Test Structures for Evaluating Photomask Alignment in Integrated Circuit Manufacturing," Technical Digest, International Electron Devices Meeting, pp. 7a-7f, 1977.

(20) D. A. Perloff, "A Four-Point Electrical Measurement Technique for Characterizing Mask Superposition Errors on Semiconductor Wafers," IEEE Journalnal of Solid-State Circuits, Vol. SC-13, No. 4, pp. 436-444, August 1978.

(21) T. J. Russell, D. A. Maxwell, "A Production Compatible Microelectronic Test Pattern for Evaluating Photomask Misalignment," Semiconductor Measurement Technology, National Bureau of Standards Special Publication 400-51, 1979.

(22) D. Yen, "Electrical Test Methods for Evaluating Lithographic Processes and Equipment, "SPIE Vol. 342 Integrated Circuit Metrology, pp. 73-81, 1982.

(23) C. P. Ausschnitt, T. A. Brunner, S. C. Yang, "Overlay Characterization of Projection Aligners Using Electrical Probe Techniques," SPIE Vol. 342 Integrated Circuit Metrology, pp. 65-72, 1982.

(24) D. S. Perloff, D. H. Hwang, T. F. Hasan, J. Frey, "Microelectronic Test Structures for Characterizing Fine-Line Lithography," Solid State Technology, pp. 136-140, May 1981.

(25) C. Van Peski, "Method of Characterizing Wafer Steppers," SPIE Vol. 342 Integrated Circuit Metrology, pp. 60-64, 1982.

(26) D. W. T. Yau, "Overlay Signature Analysis and Matching for 1:1 Projection Mask Aligner," Kodak Microelectronics Seminar: Interface '81, pp. 88-90, 1981.

(27) T. F. Hasan, S. U. Katzman, D. S. Perloff, "Automated Electrical Measurements of Registration Errors in Step-and-Repeat Optical Lithography Systems," IEEE Transactions on Electron Devices, Vol. ED-27, No.12, pp. 2304-2312, 1980.

(28) R. Hershel, D. Hackleman, C. Lage, S. Shevenock, B. Tillman, "Registration Monitor for 1:1 Aligners," Kodak Microelectronics Seminar: Interface '80, pp. 88-92, 1980.

(29) D. H. Leebrick, D. W. Kisker, "An Electrical Alignment Test Device and its Use in Investigating Processing Parameters," Kodak Microelectronics Seminar: Interface '77, pp. 66-83, 1977.

(30) M. Makita, N. Moriuchi, K. Kadota, "Analysis of Registration Errors in 1:1 Projection Mask Aligners," Kodak Microelectronic Seminar: Interface '81, pp. 104-108, 1981.

(31) E. T. Nelson, "Z7 Process Development Mask Set," Kodak Technical Report, Nov. 1983.

(32) "Quality Productivity Workshop," U.S. Apparatus Division, Eastman Kodak Company, 1984.

(33) E. T. Nelson, "Z7 Process Development Mask Set," Kodak Technical Report, Nov. 1983.

BIBLIOGRAPHY

B. Allsop, "Projection Aligners in Production A Whole New Ballgame," Kodak Microelectronics Seminar: Interface '76, pp. 20-27, 1976.

C. P. Ausschnitt, T. A. Brunner, S. C. Yang, "Overlay Characterization of Projection Aligners Using Electrical Probe Techniques," SPIE Vol. 342 Inte-egrated Circuit Metrology, pp. 65-72, 1982.

J. W. Bossung, E. S. Muraski, "Advances in Projection Microlithography," Solid State Technology, pp. 109-112, August 1979.

J. Bossung, "Projection Mask Alignment," Kodak Microelectronics Seminar: Interface '72, pp. 9-14, 1972.

J. D. Buckley, "Expanding the Horizons of Optical Projection Lithography," Solid State Technology, pp. 77-82, May 1982.

W. A. Bosenberg, H. P. Kleinknecht, "Linewidth Measurement on IC Wafers by Diffraction from Grating Test Patterns," Solid State Technology, pp. 79-85, July 1983.

M. G. Buehler, S. D. Grant, W. R. Thurber, "Bridge and van der Pauw Sheet Resistors for Characterizing the Line Width of Conducting Layers," Journal of the Electrochemical Society, Vol. 125, pp. 650-654, April 1978.

M. G. Buehler, "Measuring Conductor Widths and Spacings Electrically," NASA Technical Briefs, pp. 22-23, July/August 1987.

J. J. Greed, Jr., D. A. Markle, "Variable Magnification in a 1:1 Projection Lithography System," SPIE Vol. 334: Optical Microlithography - Technology for the mid-1980s, pp. 2-9, 1982.

T. F. Hasan, S. U. Katzman, D. S. Perloff, "Automated Electrical Measurements of Registration Errors in Step-and-Repeat Optical Lithography Systems," IEEE Transactions on Electron Devices, Vol. ED-27, No.12, pp. 2304-2312, 1980.

R. Hershel, D. Hackleman, C. Lage, S. Shevenock, B. Tillman, "Registration Monitor for 1:1 Aligners," Kodak Microelectronics Seminar: Interface '80, pp. 88-92, 1980.

K. Ishikawa, "Guide to Quality Control," White Plains, N.Y., Kraus International Publications, 1971.

D. H. Leebrick, D. W. Kisker, "An Electrical Alignment Test Device and its Use in Investigating Processing Parameters," Kodak Microelectronics Seminar: Interface '77, pp. 66-83, 1977.

J. A. Littlehale, "Determining Process Latitude with Electrically Measurable Test Structures," Kodak Microelectronics Seminar: Interface '84,

H. O. Madsen, R. O. Rice, G. Southers, "Is a Stepper Really Better Than a Scanner? A 1:1 Comparison," Kodak Microelectronics Seminar: Interface, 1984.

M. Makita, N. Moriuchi, K. Kadota, "Analysis of Registration Errors in 1:1 Projection Mask Aligners," Kodak Microelectronic Seminar: Interface '81, pp. 104-108, 1981.

A. Minvielle, R. Rice, "Spectral Output Variations in Perkin-Elmer Micraligns," Kodak Microelectronics Seminar: Interface '79, pp. 60-65, 1979.

M. A. Mitchell, V. Nagaswami, "Monitoring Wafer Stepper Performance with Electrical Test Structures," SPIE Vol. 342 Integrated Circuit Metrology, pp. 82-86, 1982.

C. Murray, "Measurement Tools for Overlay Registration," Semiconductor International, pp. 62-68, February 1987.

K. Murray, "Measuring Dimensions Using Murray Daggers," Semiconductor International, pp. 69-73, December 1982.

E. T. Nelson, "Z7 Process Development Mask Set," Kodak Technical Report, Nov. 1983.

D. A. Perloff, "A Four-Point Electrical Measurement Technique for Characterizing Mask Superposition Errors on Semiconductor Wafers," IEEE Journal of Solid-State Circuits, Vol. SC-13, No. 4, pp. 436-444, August 1978.

D. S. Perloff, D. H. Hwang, T. F. Hasan, J. Frey, "Microelectronic Test Structures for Characterizing Fine-Line Lithography," Solid State Technology, pp. 136-140, May 1981.

J. P. Robic, S. E. Knight, W. A. Straub, "Mid-UV Lithography with Positive Resist - A Multifunctional Tool and Process Evaluation," Solid State Technology, pp. 147-150, May 1983.

H. R. Rottmann, "Improving Registration in Photolithography," SPIE Vol. 342 Integrated Circuit Metrology, pp. 54-59, 1982.

T. J. Russell, T. F. Leedy, R. L. Mattis, "A Comparison of Electrical and Visual Alignment Test Structures for Evaluating Photomask Alignment in Integrated Circuit Manufacturing," Technical Digest, International Electron Devices Meeting, pp. 7a-7f, 1977.

T. J. Russell, D. A.Maxwell, "A Production Compatible Microelectronic Test Pattern for Evaluating Photomask Misalignment," Semiconductor Measurement Technology, National Bureau of Standards Special Publication 400-51, 1979.

L. J. van der Pauw, "A Method of Measuring Specific Resistivity and Hall Effect of Discs of Arbitrary Shape," Philips Research Reports Vol. 13, pp. 1-9, February 1958.

C. Van Peski, "Method of Characterizing Wafer Steppers," SPIE Vol. 342 Integrated Circuit Metrology, pp. 60-64, 1982.

R. K. Watts, J. H. Bruning, "A Review of Fine-Line Lithographic Techniques: Present and Future," Solid State Technology, pp. 99-105, May 1981.

D. W. T. Yau, "Overlay Signature Analysis and Matching for 1:1 Projection Mask Aligner," Kodak Microelectronics Seminar: Interface '81, pp. 88-90, 1981.

D. Yen, "Electrical Test Methods for Evaluating Lithographic Processes and Equipment, "SPIE Vol. 342 Integrated Circuit Metrology, pp. 73-81, 1984.

APPENDIX A: STATISTICAL ANALYSIS

A statistical approach to data populations can be very advantageous for process evaluation (32). The information below is provided as background on the subject. Many computers and calculators have statistical functions which can perform the required calculations.

$$\bar{X} = u = \frac{\sum X}{n}$$

where: $\bar{X}$ = u = X ave = mean

X = individual data point

n = population size

$$\sigma = \sqrt{\frac{\sum (Xi - \bar{X})^2}{n}}$$

σ = sigma = standard deviation

Xi = the (i)th observation

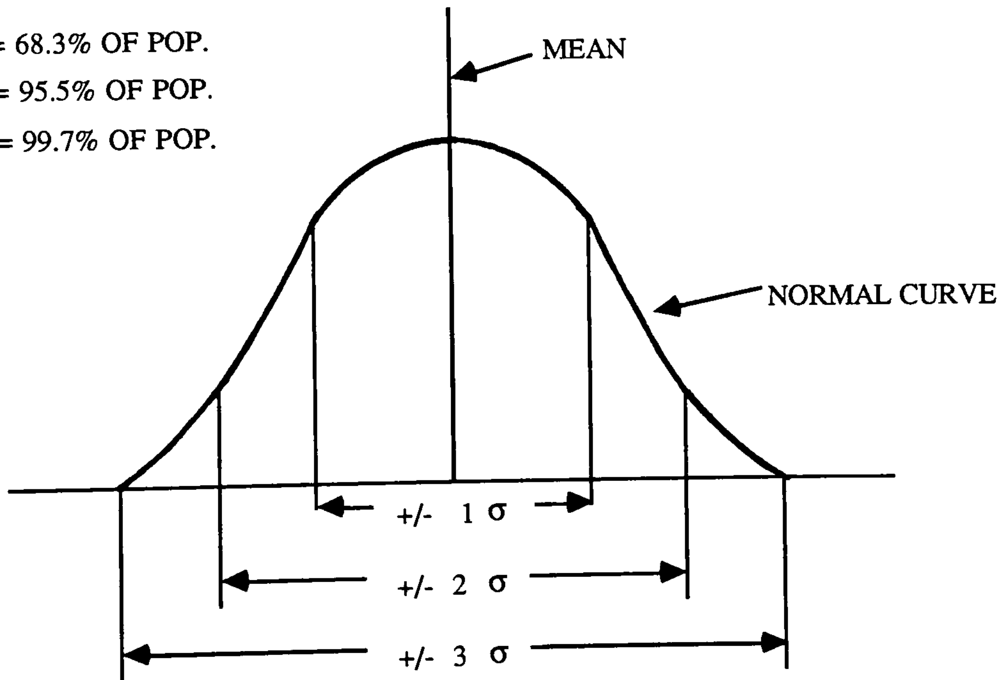

Figure A1: Normal Curve

APPENDIX B: OPTICAL VERNIER INTERPRETATION

A vernier is a pattern which can be visually interpreted to determine the misregistration from one photolithographic level to another. It consists of a series of "hash marks" which are defined on both levels. The pitch these marks is slighty different for the first level (wafer) than it is for the second level (mask or resist). The resolution of the verniers on ETM-1 is 0.2 microns, however interpolation permits 0.1 micron readings.

Misregistration is determined by visually inspecting the vernier and locating the region where the hash marks are best aligned. The vernier will indicate misalignment of the wafer with respect to the mask. Movement of the wafer in the opposite direction will correct the situation. Figure A2 illustrates a "Y" misalignment of -0.7 microns. A wafer movement of 0.7 microns in the positive direction would correct the situation.

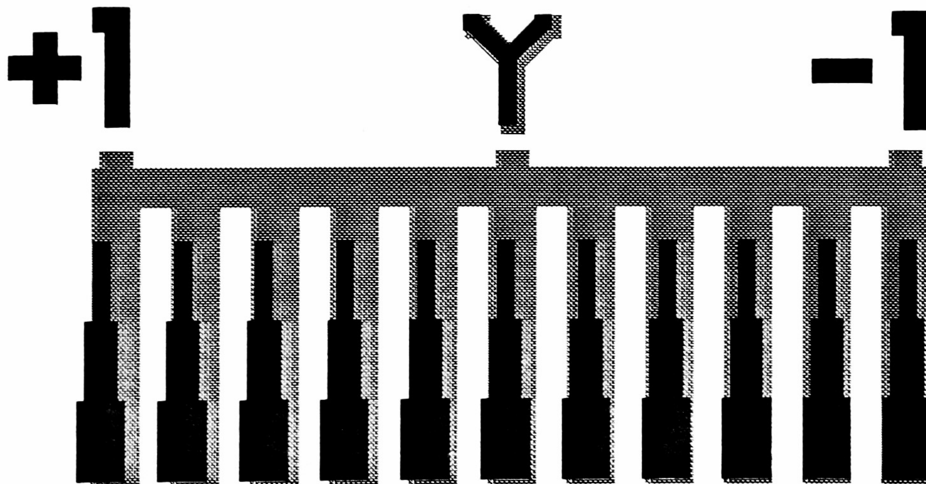

Figure A2: Optical Vernier

APPENDIX C: LINEWIDTH STRUCTURE THEORY

Two electrical linewidth devices reside in each 12 pad structure. One has a feature within a field of other features and the other one has a feature which is all alone (see Fig. A3). The structure is used to determine the sheet resistance (Rs) of the conductor and the average electrical linewidth (W). This is accomplished with electrical probing and using the relationships below.

Sheet resisistance is determined by forcing a current through pads 3 (9) and 4 (10) and measuring the voltage drop between pads 5 (11) and 6 (12) with the chuck grounded. Linewidth is then determined by forcing a current through pads 1 (7) and 5 (11) and measuring the voltage drop between pads 3 (9) and 4 (10). "L" is the drawn length between pads 3 (9) and 4 (10) which is 100 microns on the 2 and 3 micron devices, and 140 microns for the 5 micron device.

$$Rs = \frac{\pi}{\ln 2} * \frac{V(5-6)}{I(3-4)} , \quad W = Rs * L * \frac{I(1-5)}{V(3-4)}$$

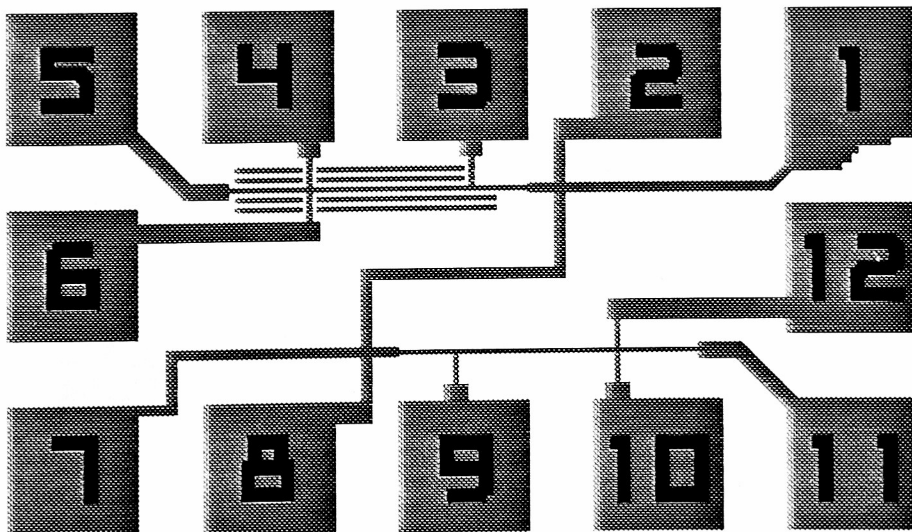

Figure A3: Electrical Linewidth Test Structure

APPENDIX D: ALIGNMENT STRUCTURE THEORY

Two electrical alignment devices reside in each 12 pad structure (33). One is oriented to be sensitive to "X" alignment and the other is oriented to to be sensitive to "Y" alignment (see Figure A4). Electrical probing of the device determines the misalignment and is accomplished by grounding the chuck and pad 8 (9) and applying a dc voltage to pad 4 (12). The voltage difference between pad 3 (10) and pad 6 (2) is then measured. Calculation of the misalignment uses the relationships below, where "W" is the drawn nominal width of the resistors. The value of "W" for this design is 4 microns.

$$dX = \frac{V2 - V10}{V12} * W \quad , \qquad dY = \frac{V3 - V6}{V4} * W$$

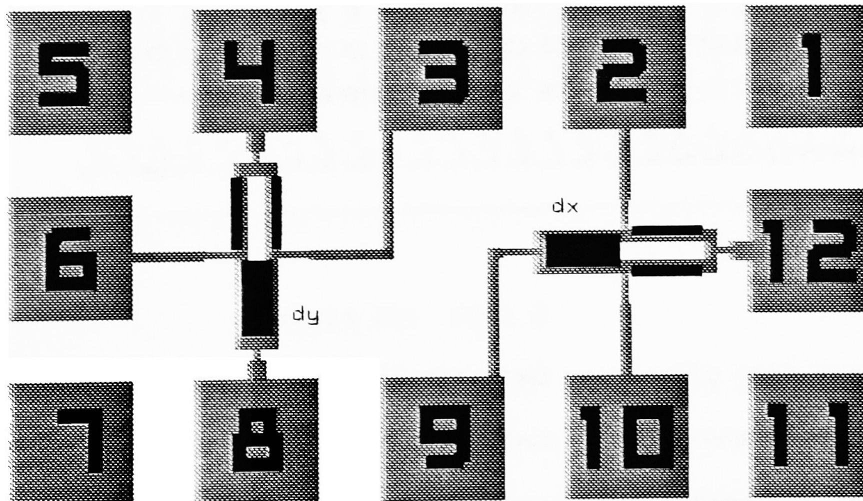

Figure A4: Electrical Alignment Test Structure

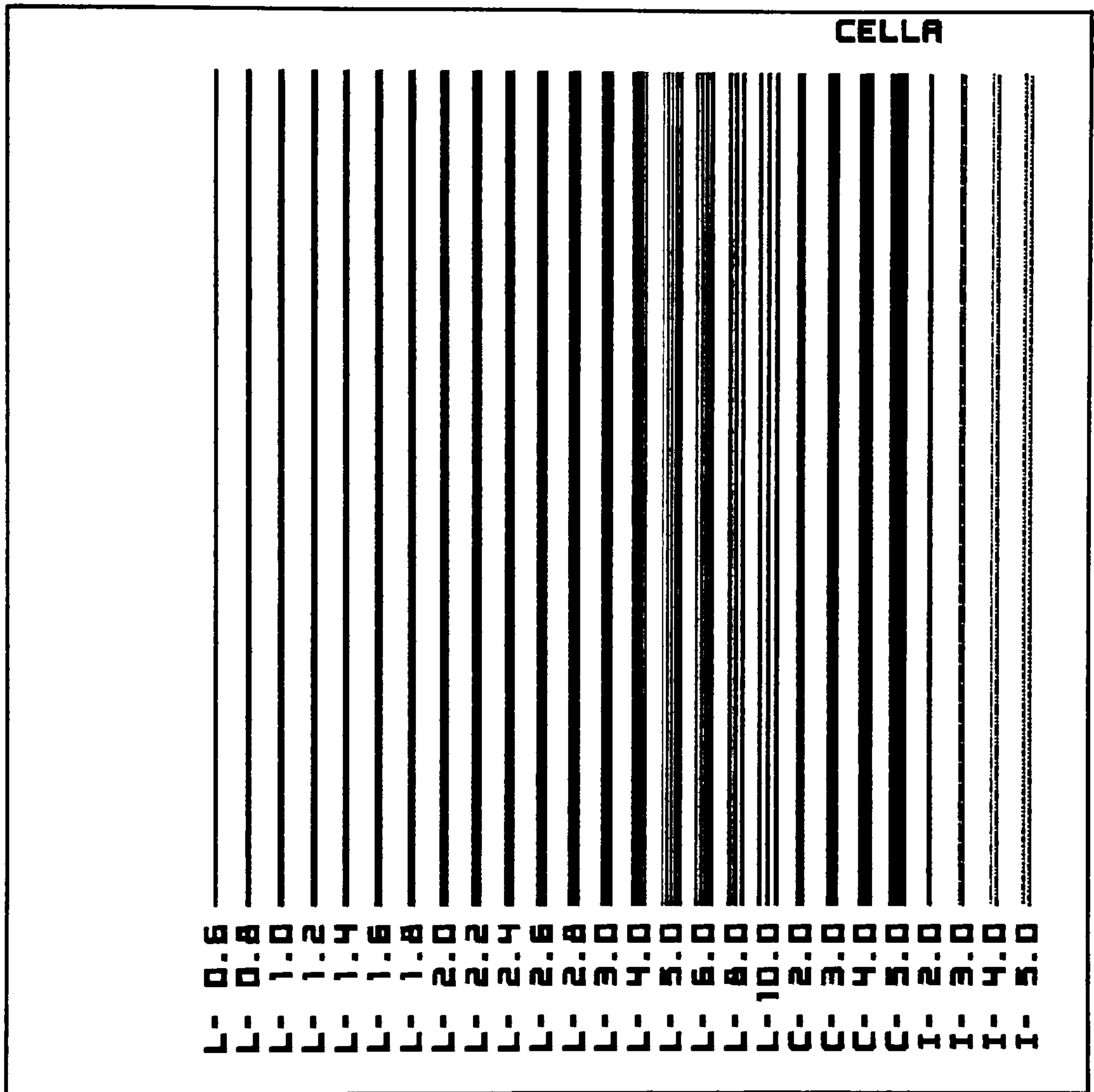

Figure A5: Cell A

This cell features line/space elements oriented vertically with respect to the wafer flat, along with a variety of contact and island geometries. The purpose of these elements is to evaluate the resolution capabilities for features perpendicular to wafer flat.

APPENDIX E: CELL DESCRIPTION AND ILLUSTRATIONS

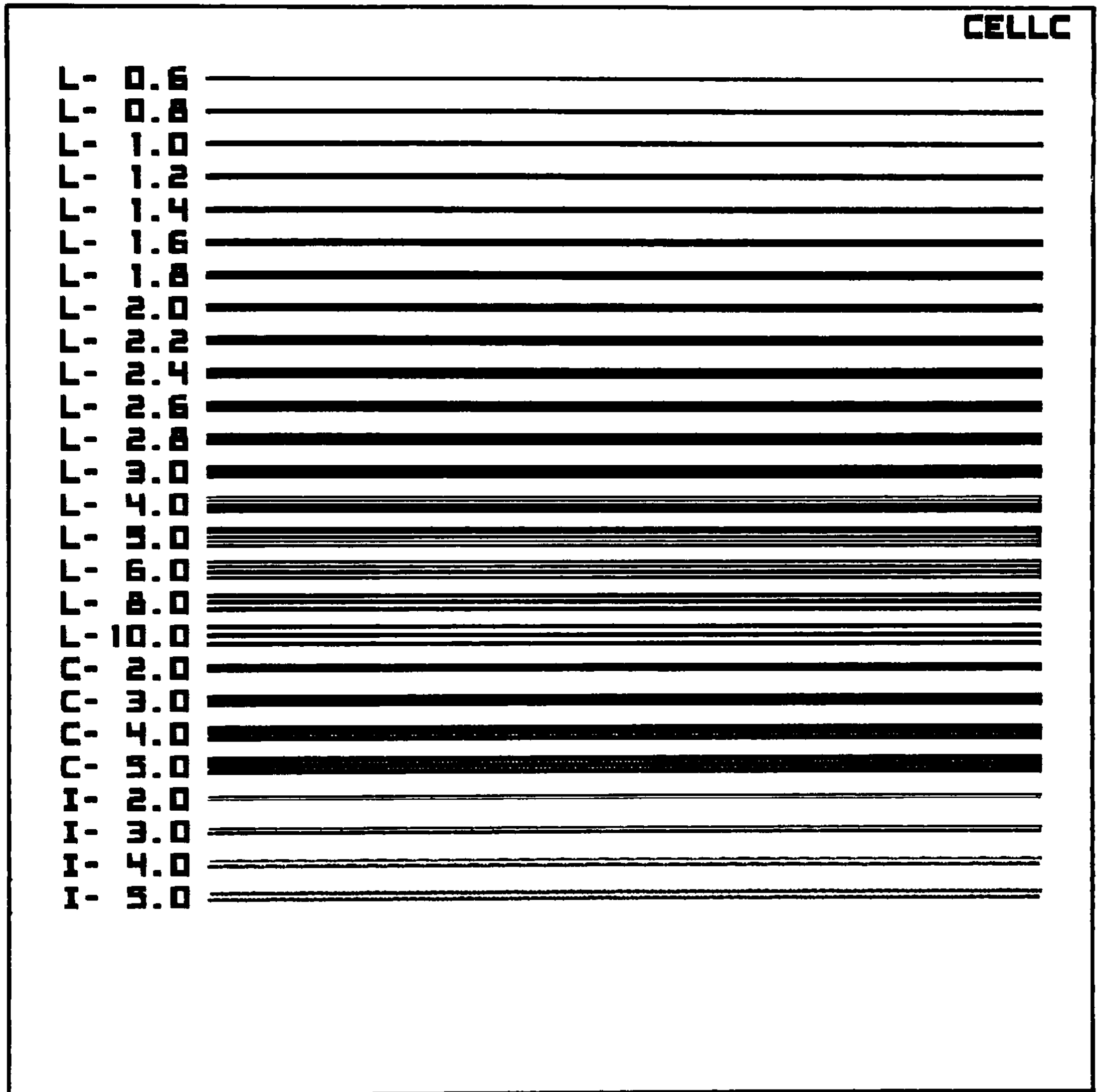

Figure A6: Cell C

This cell features line/space elements oriented horizontally with respect to the wafer flat, along with contact and island geometries. A comparison of the exposure tool's capability to resolve features which are orthogonal in relationship to one another can be accomplished.

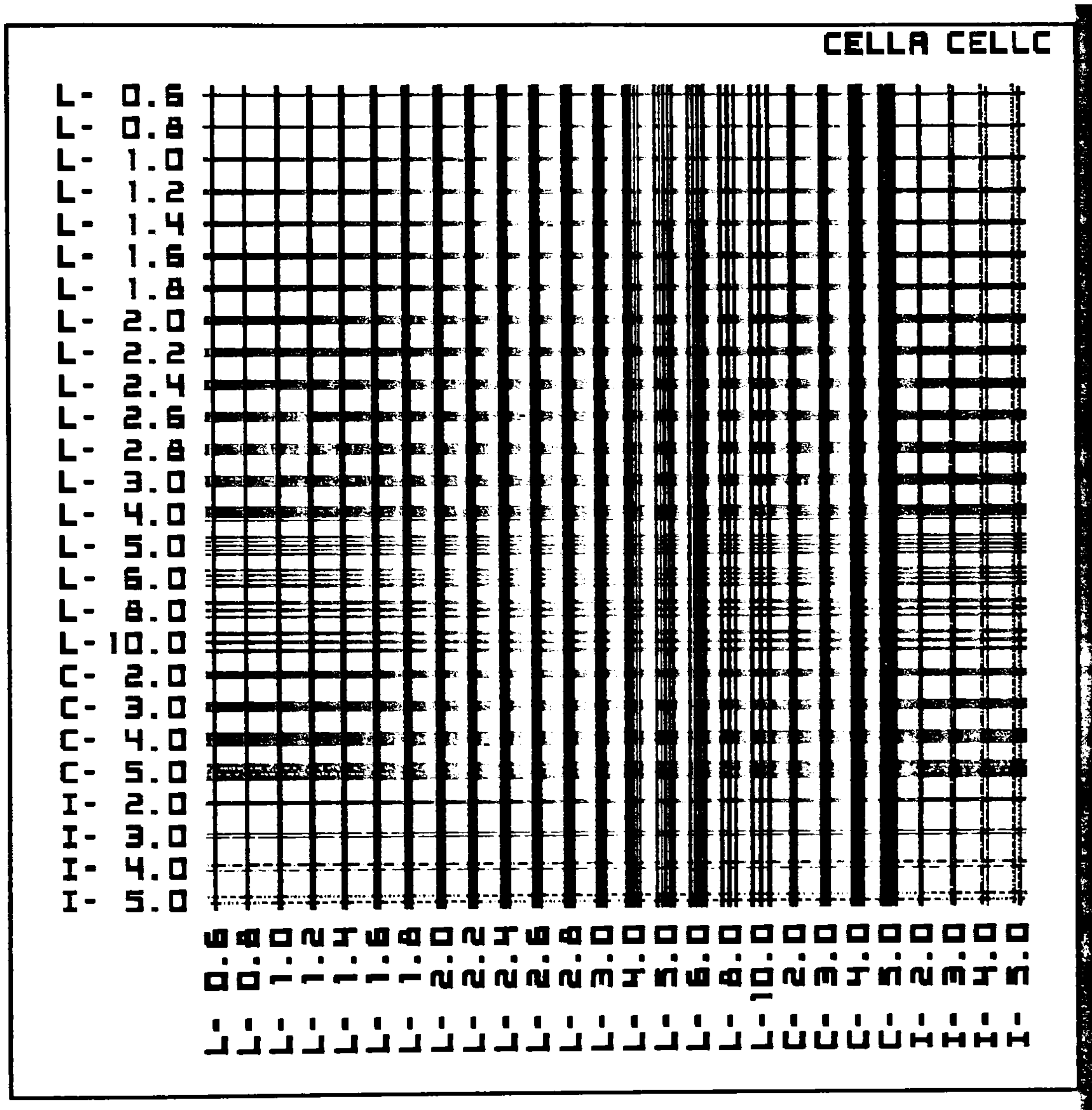

Figure A7: Cell AC

This cell is shown for illustration purposes only. It represents the appearance of cell A being offset and aligned to cell B in a bi-level experiment. This demonstrates the exposure tool's capability to resolve features which cross over orthoganal topographies below them.

APPENDIX E: CELL DESCRIPTION AND ILLUSTRATIONS

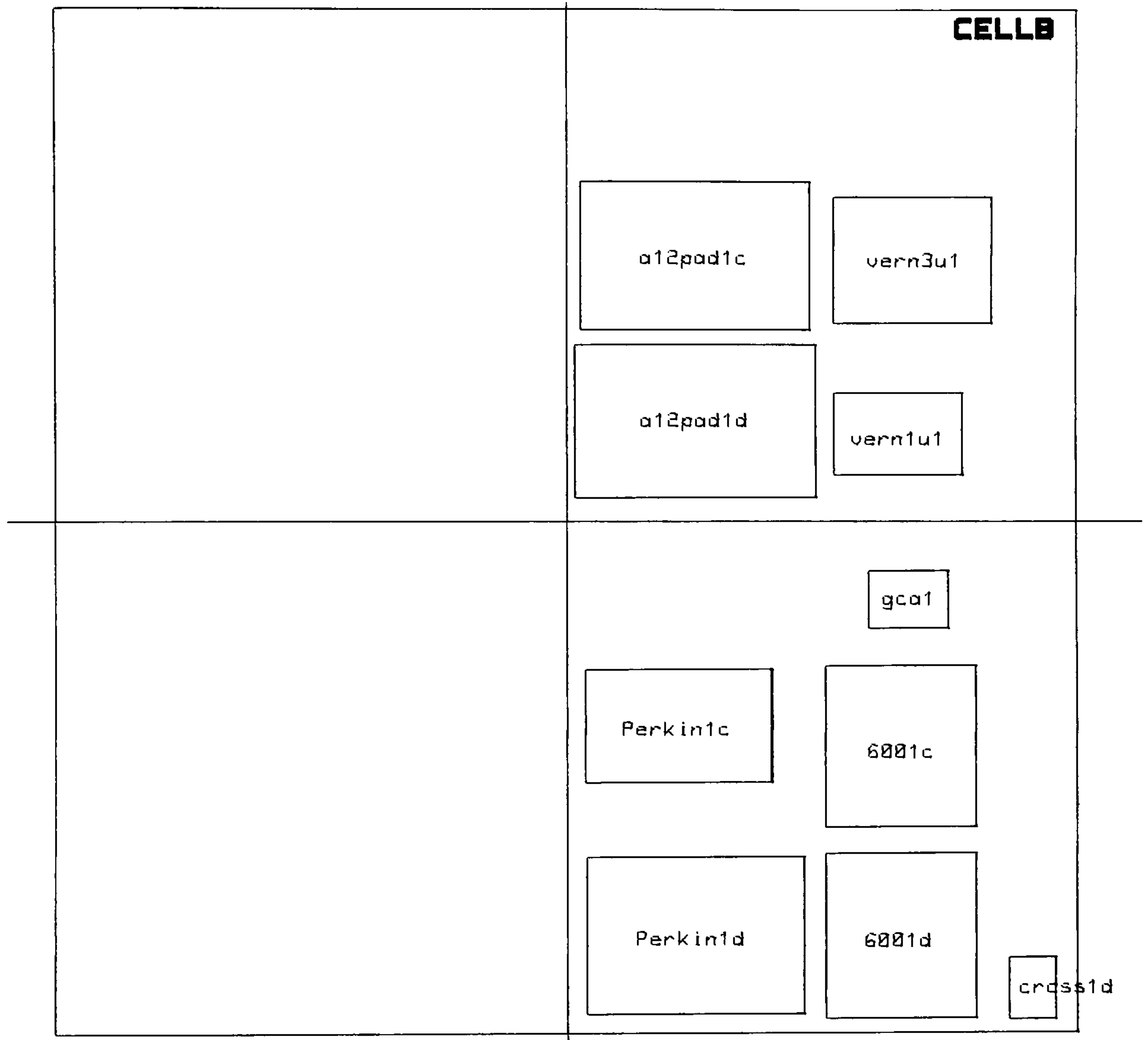

Figure A8: Cell B (Block Diagram)

The first level patterns for all bi-level structures are located in this cell. Relative positions are illustrated in the block diagram above. The clear left hand side of cell B provides a site for the resolution patterns of cell D to occupy after an offset and alignment is peformed in a bi-level test.

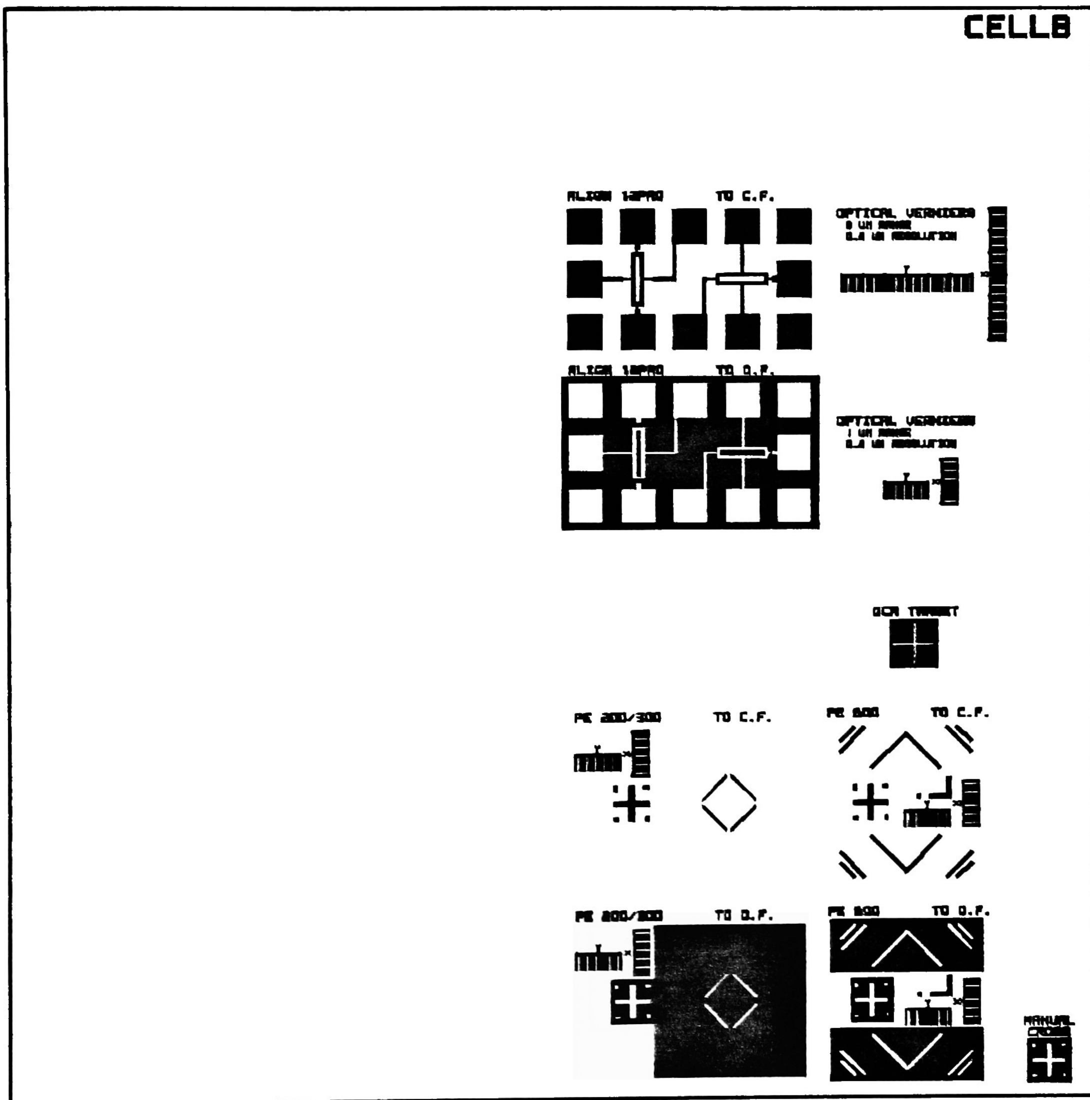

Figure A9: Cell B (Detail)

The first level patterns for all bi-level structures are located in this cell. The complete detailed illustration is shown above. The clear left hand side of cell B provides a site for the resolution patterns of cell D to occupy after an offset and alignment is peformed in a bi-level test.

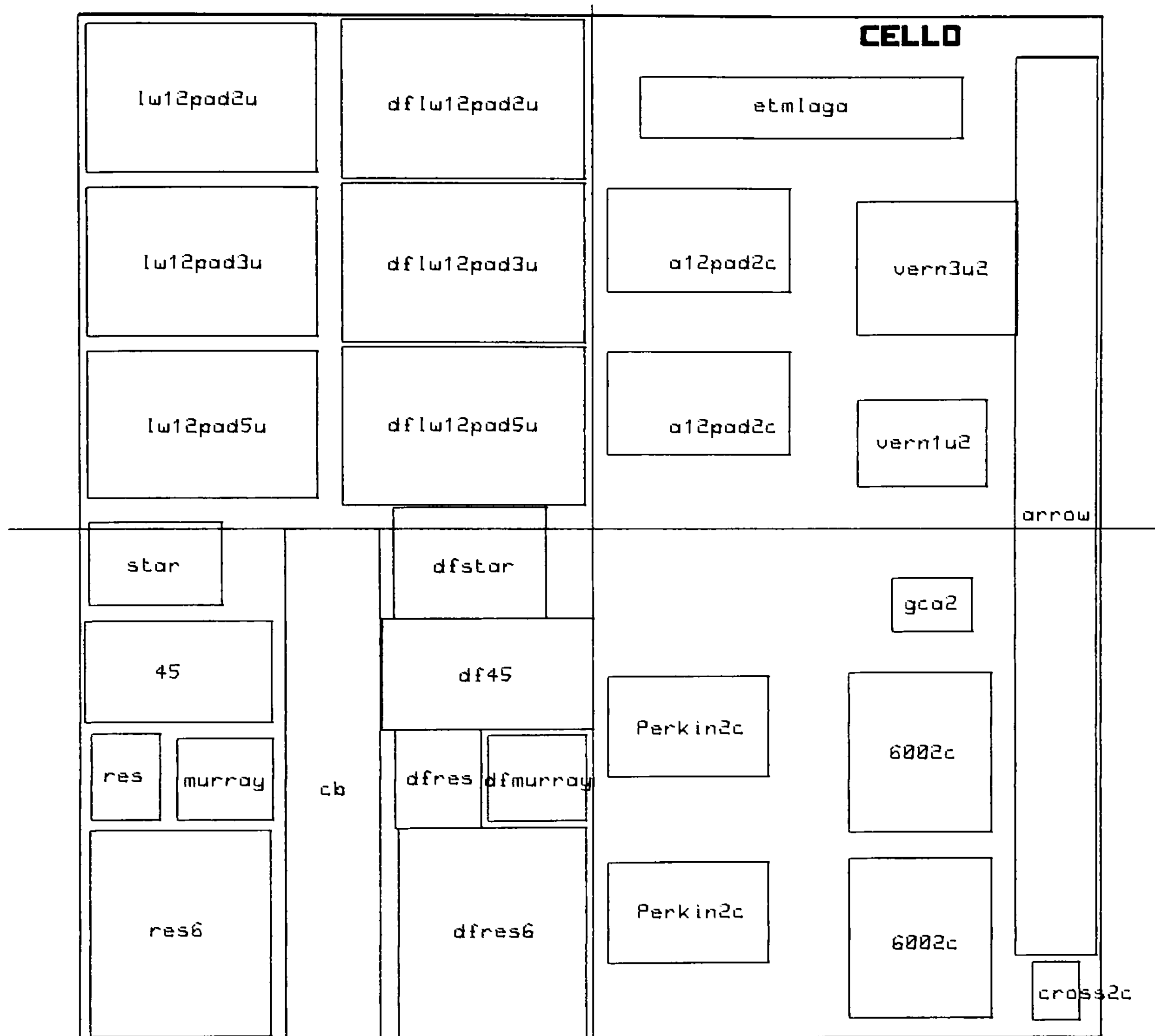

Figure A10: Cell D (Block Diagram)

The majority of structures are located in this cell. Their relative positions are illustrated in the block diagram above. The primary function of this cell is to compare numerous optical and electrical test patterns, as well as provide second level alignment targets for bi-level experiments.

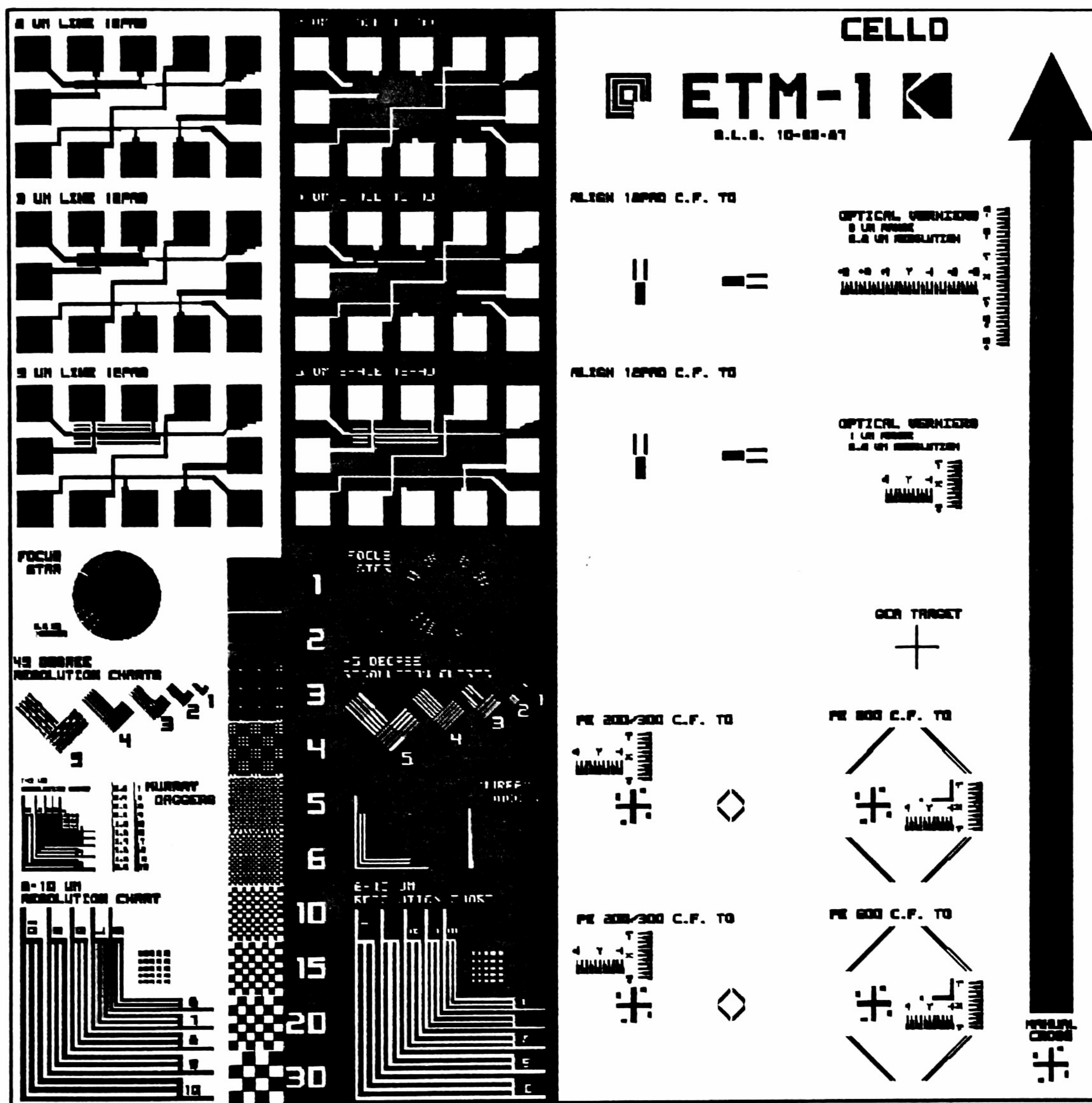

Figure A11: Cell D (Detail)

The majority of structures are located in this cell. The complete detailed illustration is shown above. The primary function of this cell is to compare optical and electrical test patterns, as well as provide second level alignment targets for bi-level experiments.

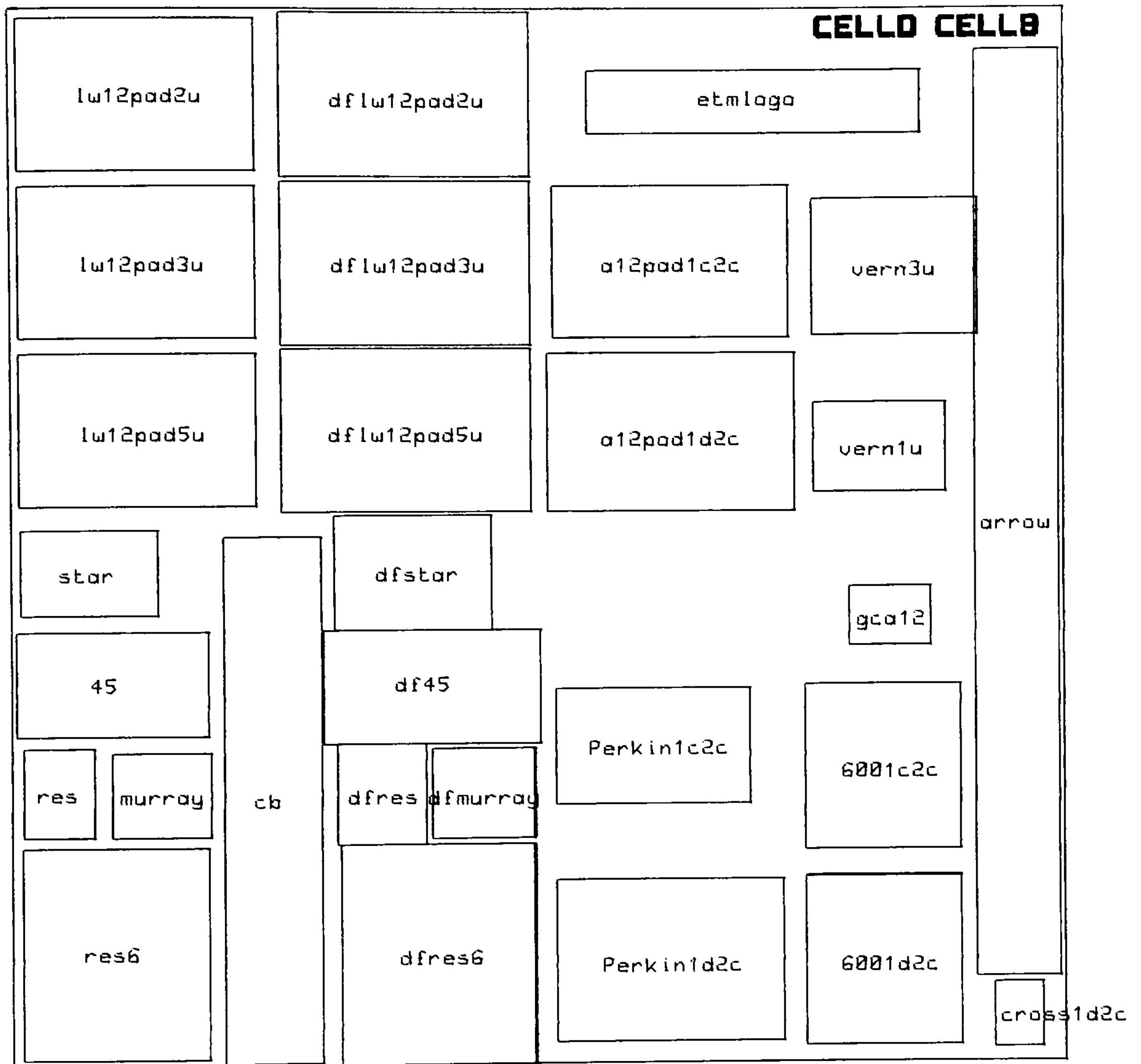

Figure A12: Cell DB (Block Diagram)

This cell is shown for illustration purposes only. It represents the appearance of cell D being offset and aligned to cell B in a bi-level experiment. The relative positions of the component blocks are illustrated above.

APPENDIX E: CELL DESCRIPTION AND ILLUSTRATIONS

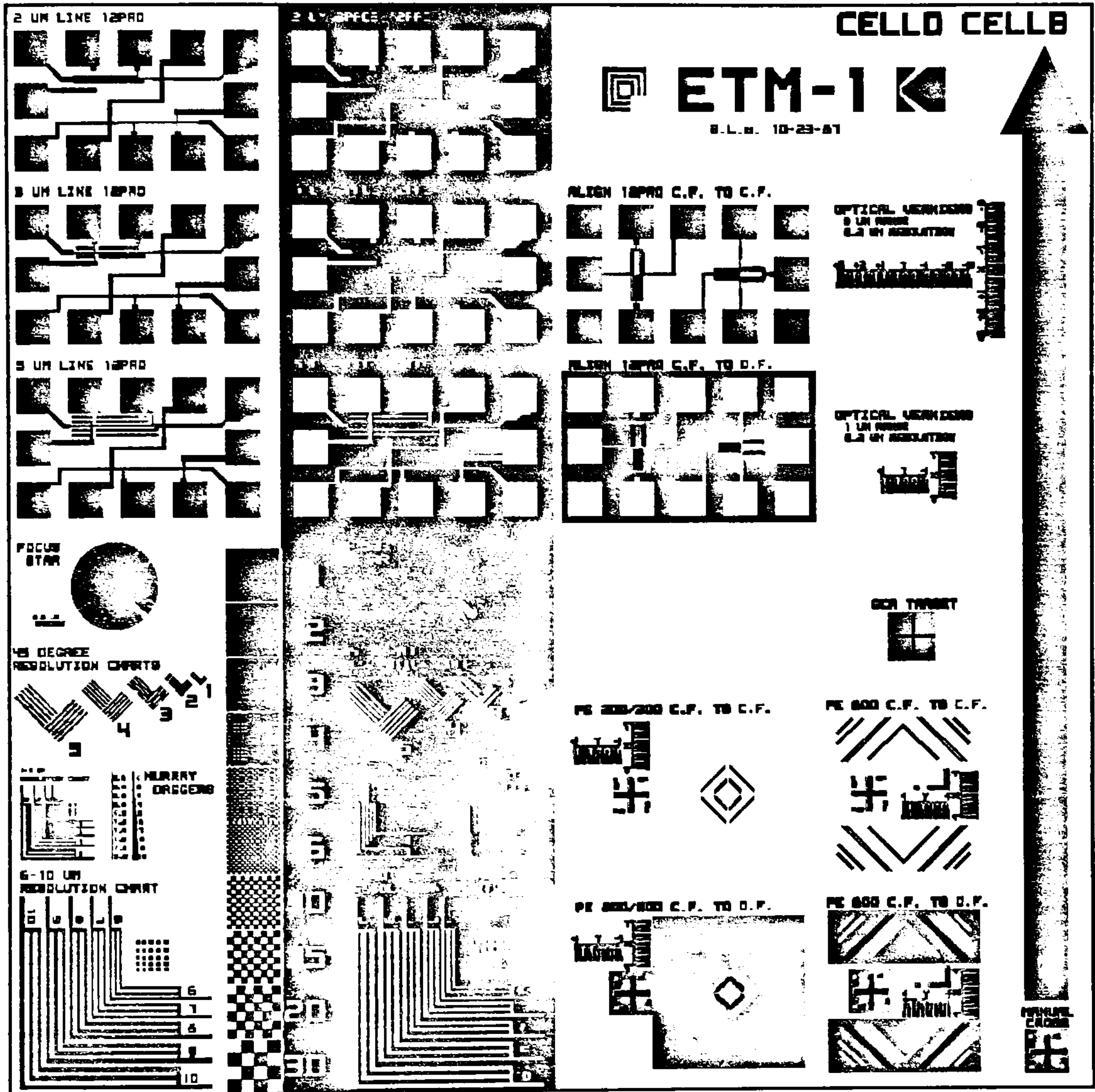

Figure A13: Cell DB (Detail)

This cell is shown for illustration purposes only. It represents the appearance of cell D being offset and aligned to cell B in a bi-level experiment. The complete detailed illustration is shown above.

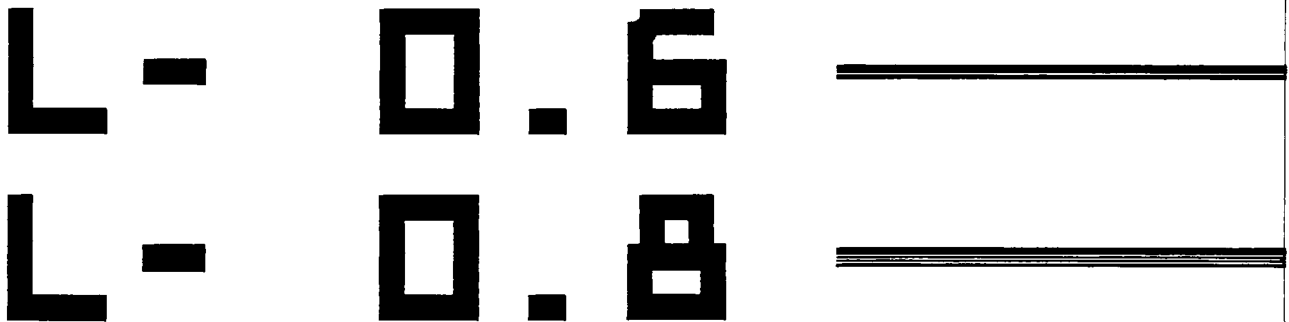

Figure A14: Lines/Spaces (0.6-0.8 microns)

Equal bars of lines and spaces are provided for dimensions 0.6 and 0.8 microns. The bars are approximately 1 millimeter long which eases the task of fracturing the wafer for edge profile analysis on a SEM.

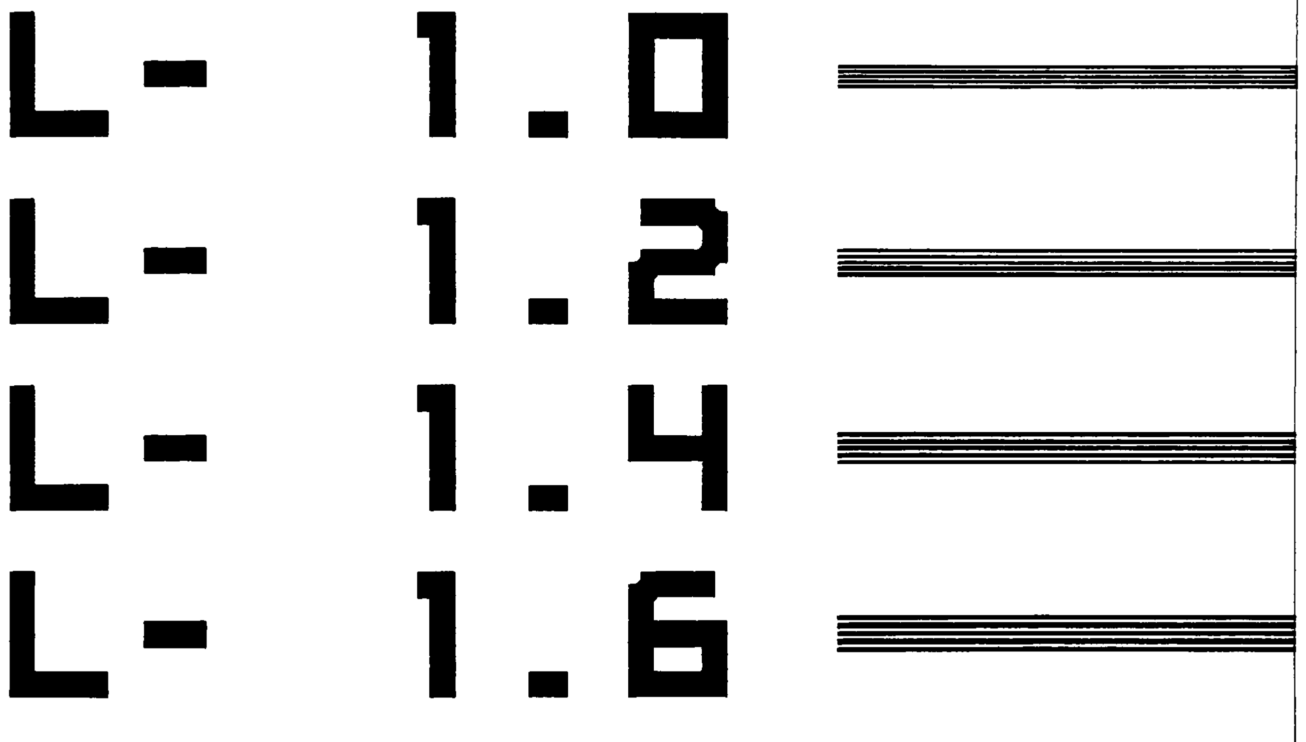

Figure A15: Lines/Spaces (1.0-1.6 microns)

Equal bars of lines and spaces are provided for dimensions 1.0, 1.2, 1.4, and 1.6 microns. The bars are approximately 1 millimeter long which eases the task of fracturing the wafer for edge profile analysis on a SEM.

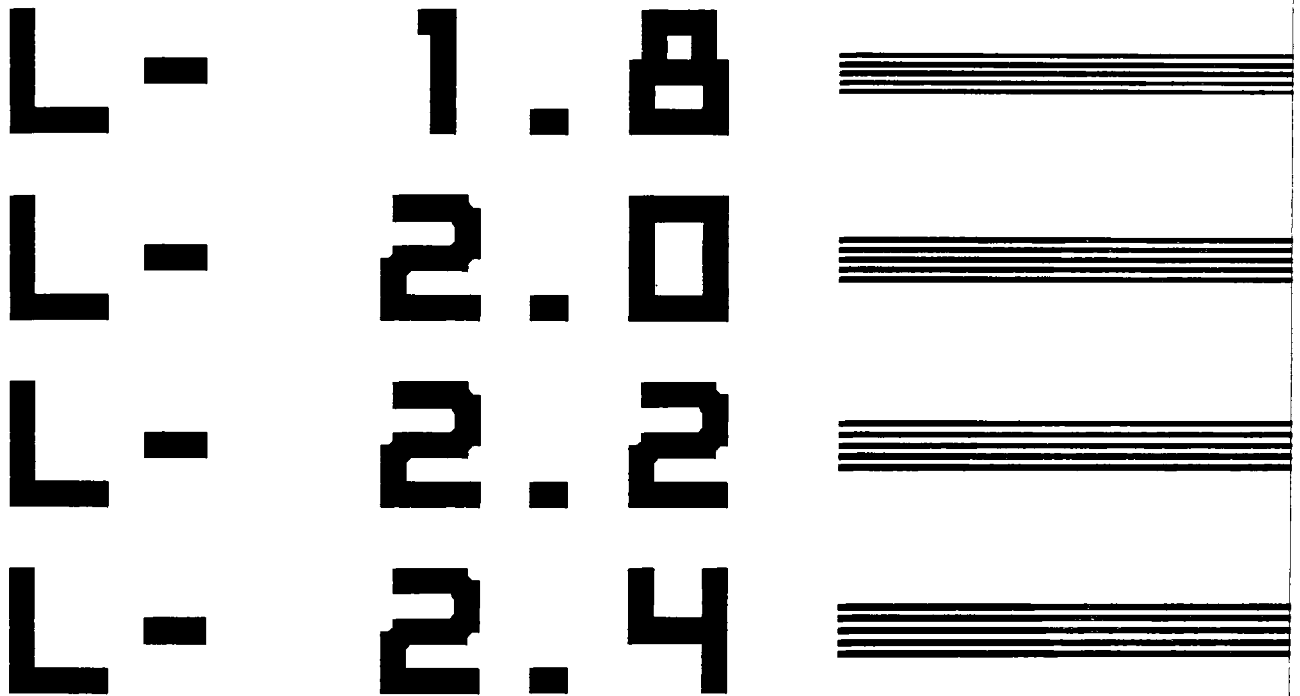

Figure A16: Lines/Spaces (1.8-2.4 microns)

Equal bars of lines and spaces are provided for dimensions 1.8, 2.0, 2.2 and 2.4 microns. The bars are approximately 1 millimeter long which eases the task of fracturing the wafer for edge profile analysis on a SEM.

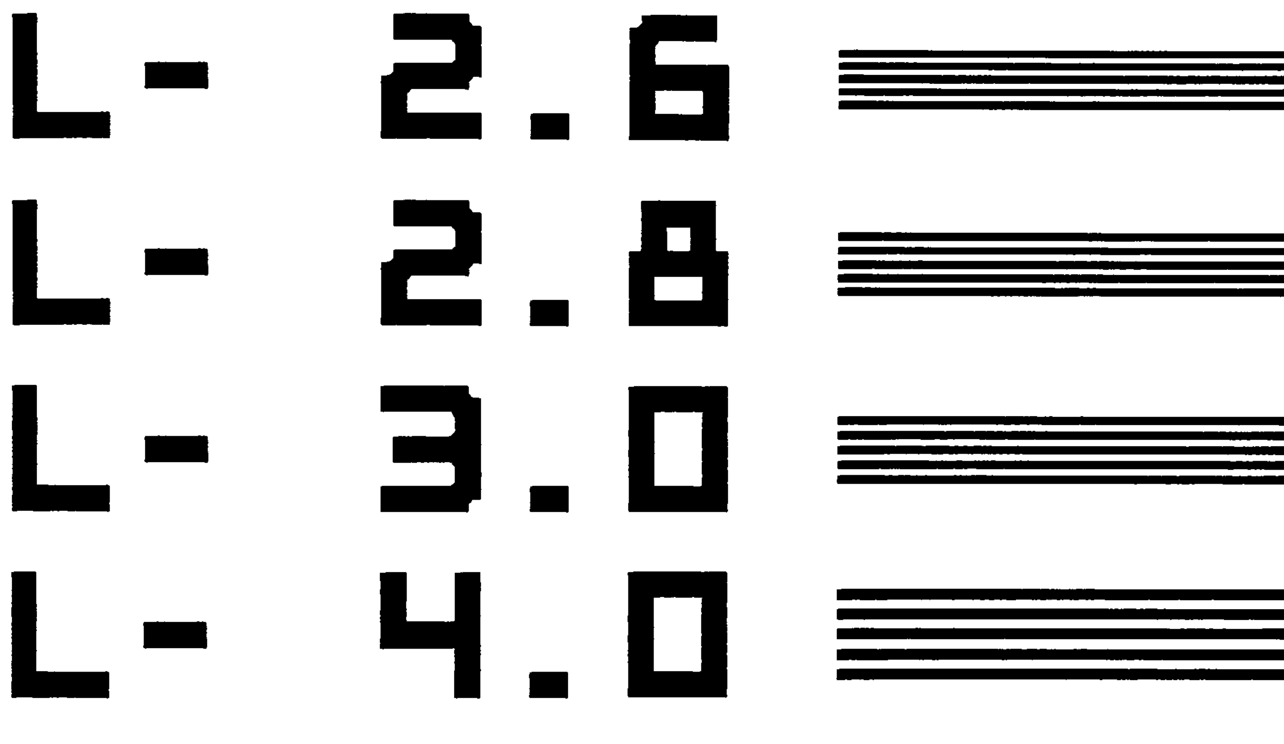

Figure A17: Lines/Spaces (2.6-4.0 microns)

Equal bars of lines and spaces are provided for dimensions 2.6, 2.8, 3.0 and 4.0 microns. The bars are approximately 1 millimeter long which eases the task of fracturing the wafer for edge profile analysis on a SEM.

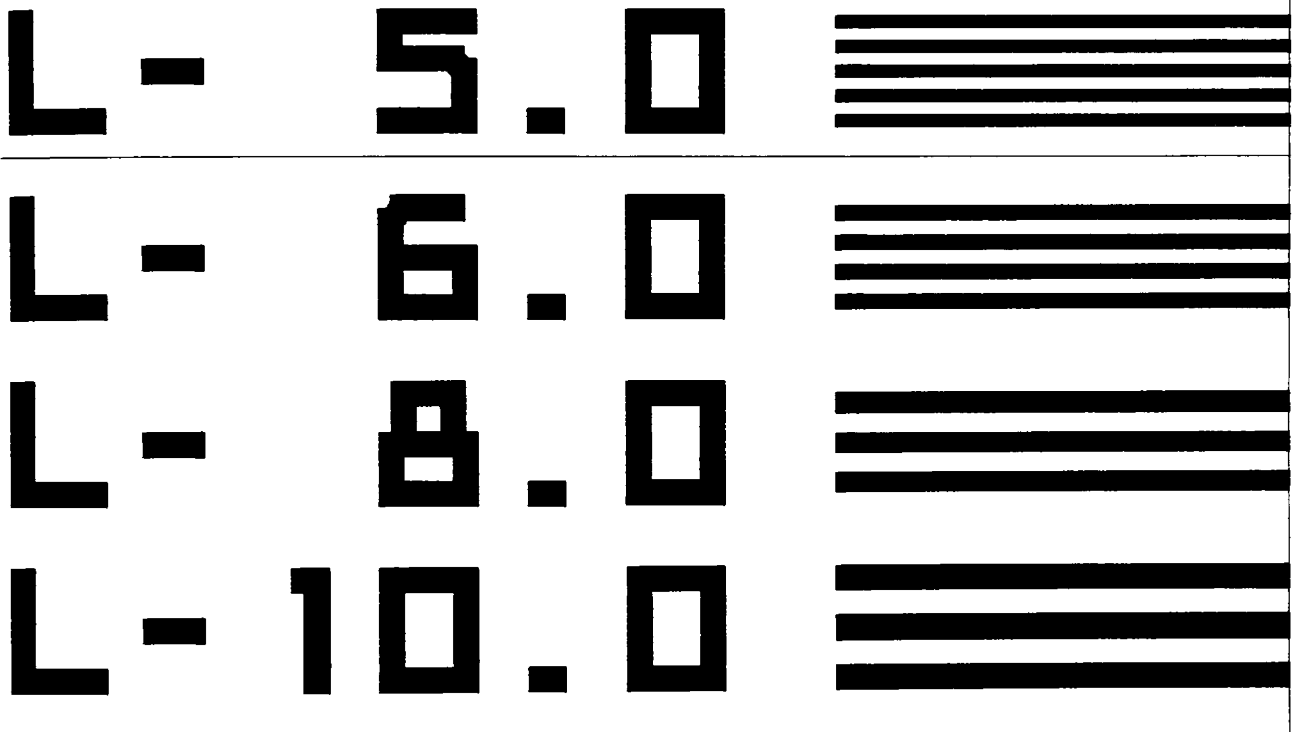

Figure A18: Lines/Spaces (5.0-10.0 microns)

Equal bars of lines and spaces are provided for dimensions 5.0, 6.0, 8.0 and 10.0 microns. The bars are approximately 1 millimeter long which eases the task of fracturing the wafer for edge profile analysis on a SEM.

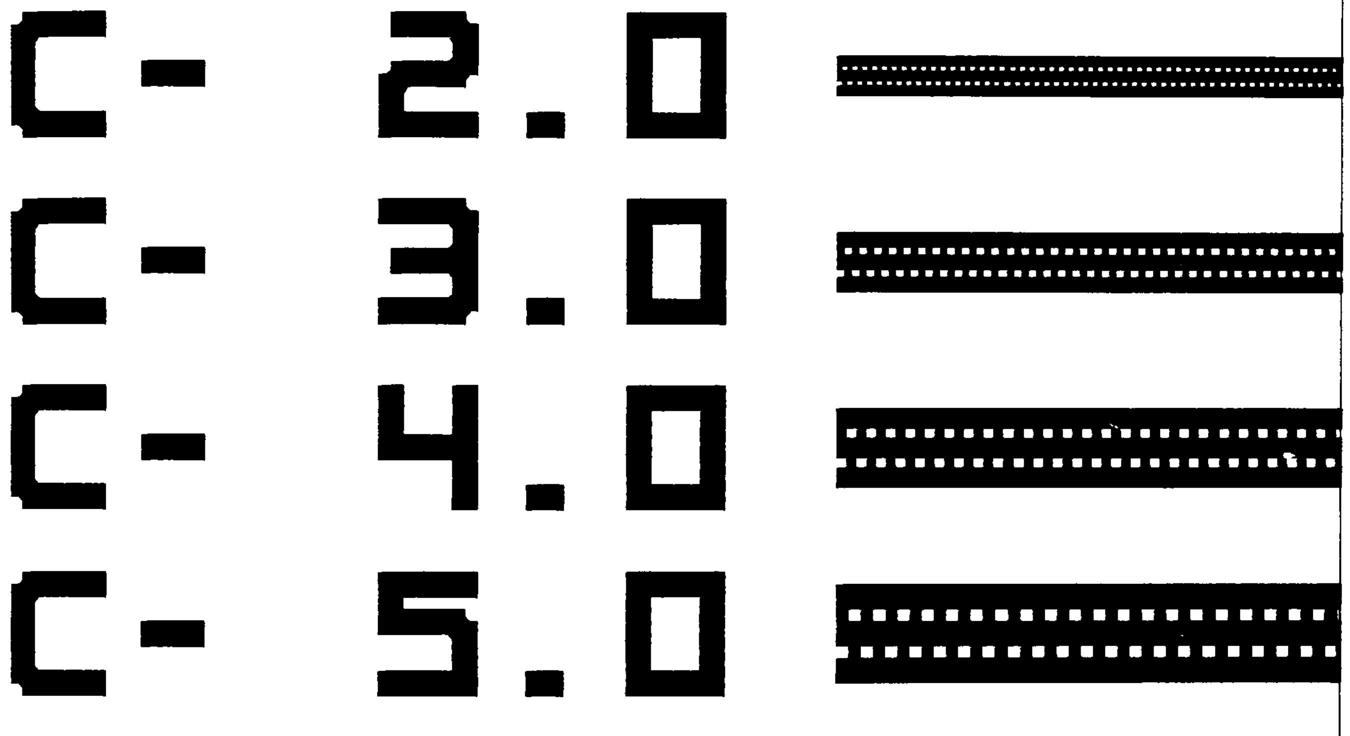

Figure A19: Contact Geometries

Square contact "cuts" are provided for dimensions of 2, 3, 4 and 5 microns to determine the ability of the exposure tool to open small spaces. Two rows are offset such that any cleave line for SEM evaluation will disect a contact cut.

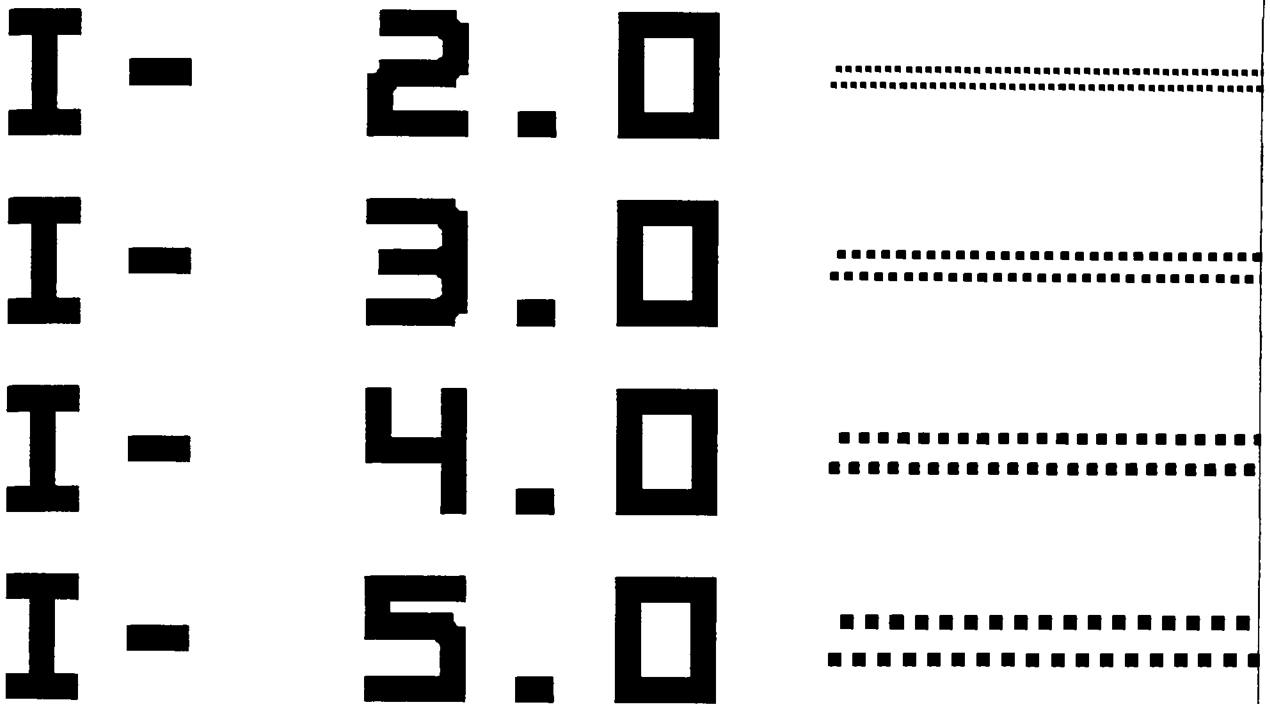

Figure A20: Island Geometries

Square geometries which will result in resist islands are presented of 2, 3, 4 and 5 microns. A comparison of the ability of the exposure tool to resolve the islands versus the contacts can be done.

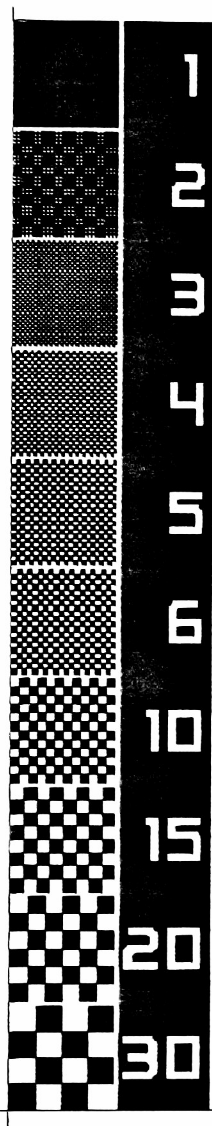

Figure A21: Checkerboard Patterns

Large checkerboards are included which have a range of dimensions from 1 to 30 microns. These provide a quick and easy method of determining a rough estimate of the exposure tool's resolution capability.

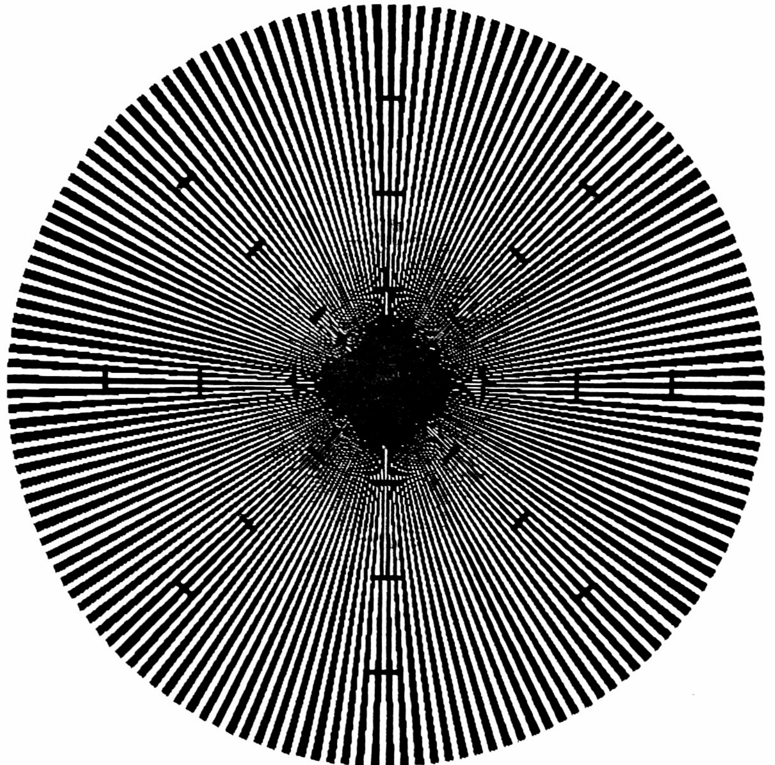

Figure A22: Clear Field Focus Star

This optical pattern of radial polygons has a range of resolution from 0.2 to 2.0 microns with indicators at every 0.5 microns. The focus star can be inspected to identify any astigmatism problems with an exposure tool which render resolution in one direction better than another as well as parallelism of the mask or reticle to the wafer.

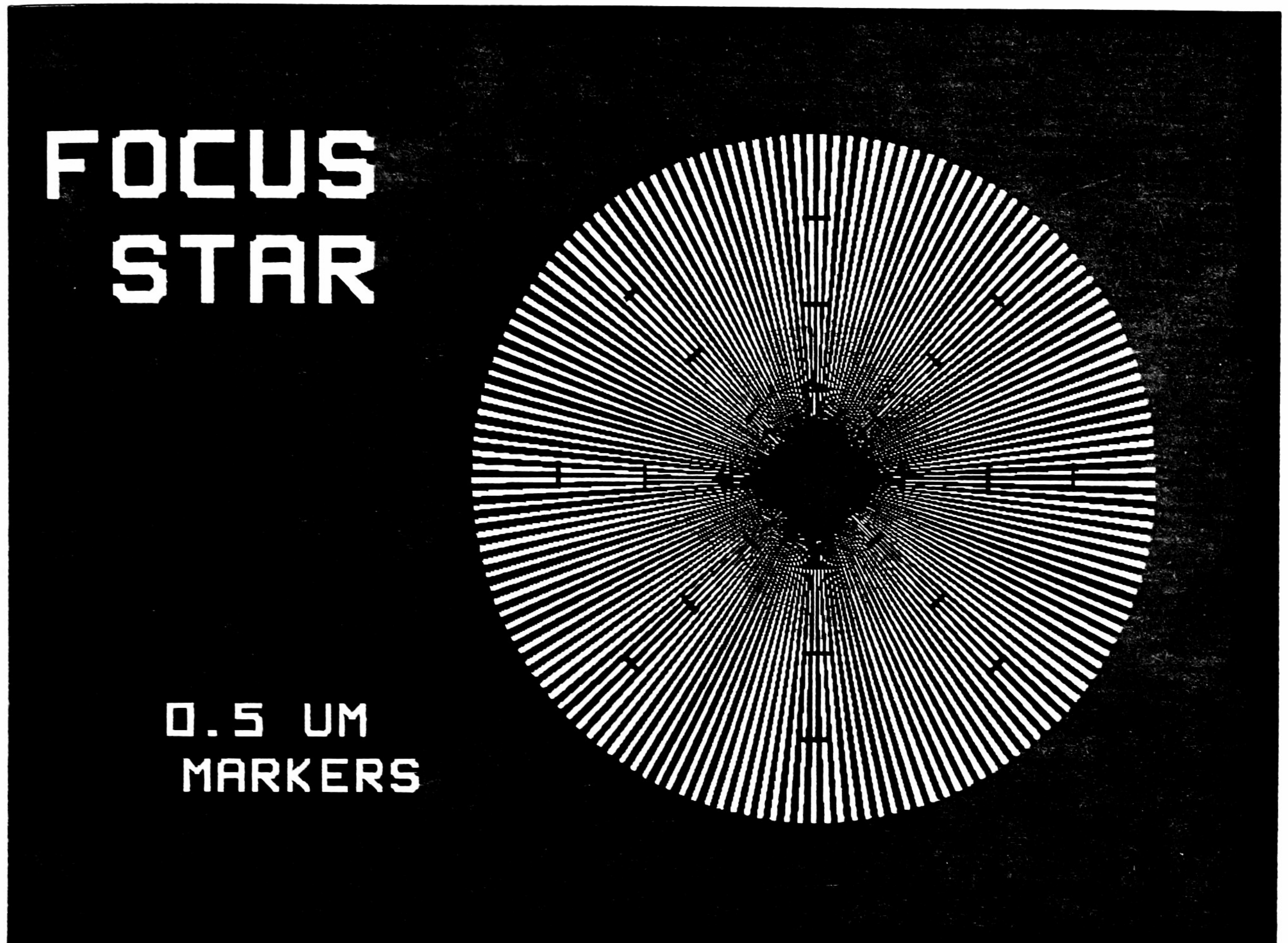

Figure A23: Dark Field Focus Star

This optical pattern of radial polygons has a range of resolution from 0.2 to 2.0 microns with indicators at every 0.5 microns. The focus star can be inspected to identify any astigmatism problems with an exposure tool which render resolution in one direction better than another as well as parallelism of the mask or reticle to the wafer.

45 DEGREE RESOLUTION CHARTS

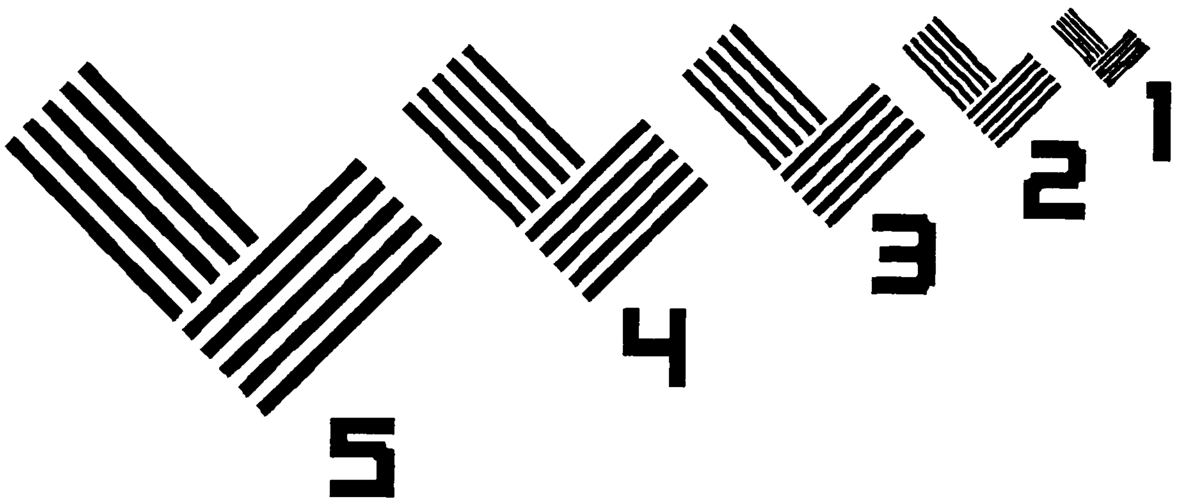

Figure A24: Clear Field 45 Degree Resolution Charts

Geometries of 1, 2, 3, 4 and 5 microns which are orthogonal and tilted 45 degrees with respect to the wafer flat. This optical pattern can be inspected to determine the exposure tool's resolution cabability for "off angle" features commonly used for metal routing in semiconductor devices.

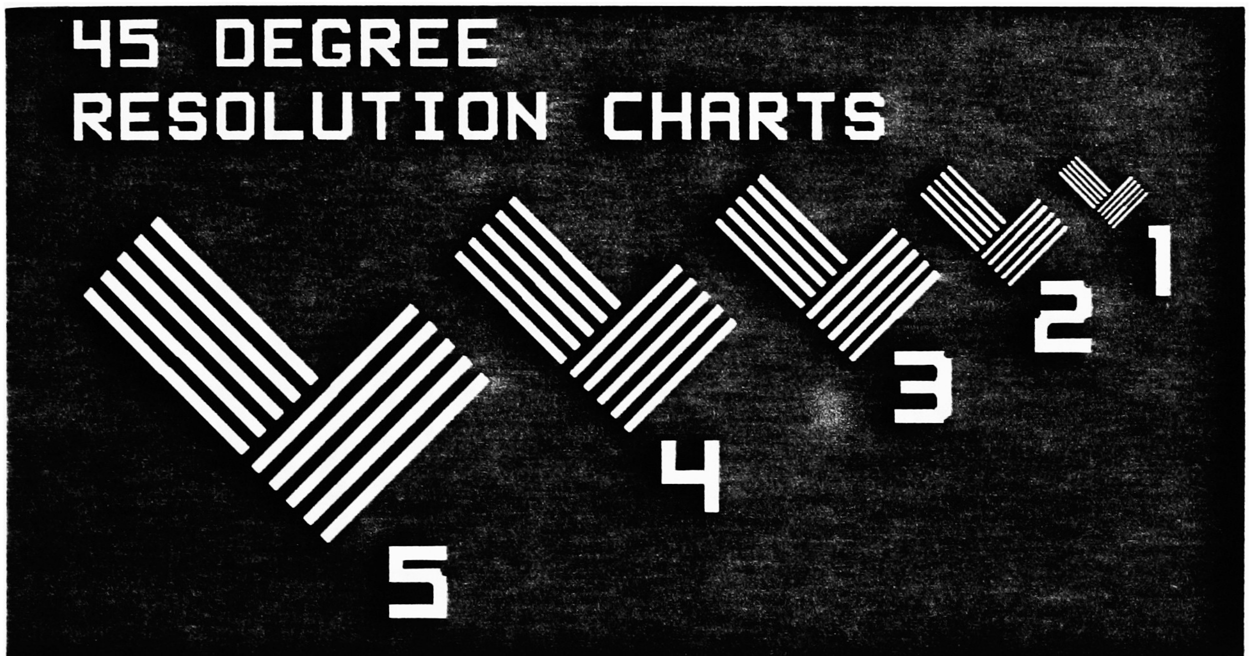

Figure A25: Dark Field 45 Degree Resolution Charts

The reverse tone features of the 45 Degree Resolution Chart. Comparison of the ability to clean spaces in an opaque field versus lines in a clear field can be accomplished.

1-5 UM
RESOLUTION CHART

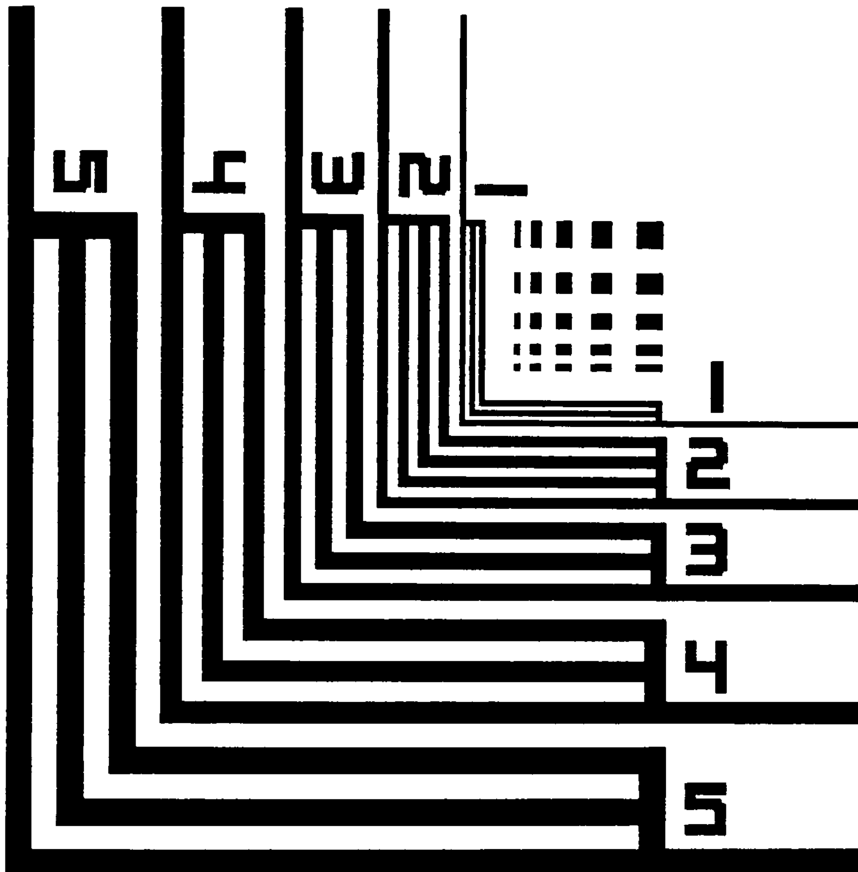

Figure A26: Clear Field Resolution Chart

A basic optical structure with equal lines and spaces of dimensions 1, 2, 3, 4 and 5 microns. This pattern allows for rapid evaluation of the exposure tool's resolution capability. A comparison of the critical dimension measurement of a line within a field of lines to one which is isolated can be performed by also reviewing the extended lines.

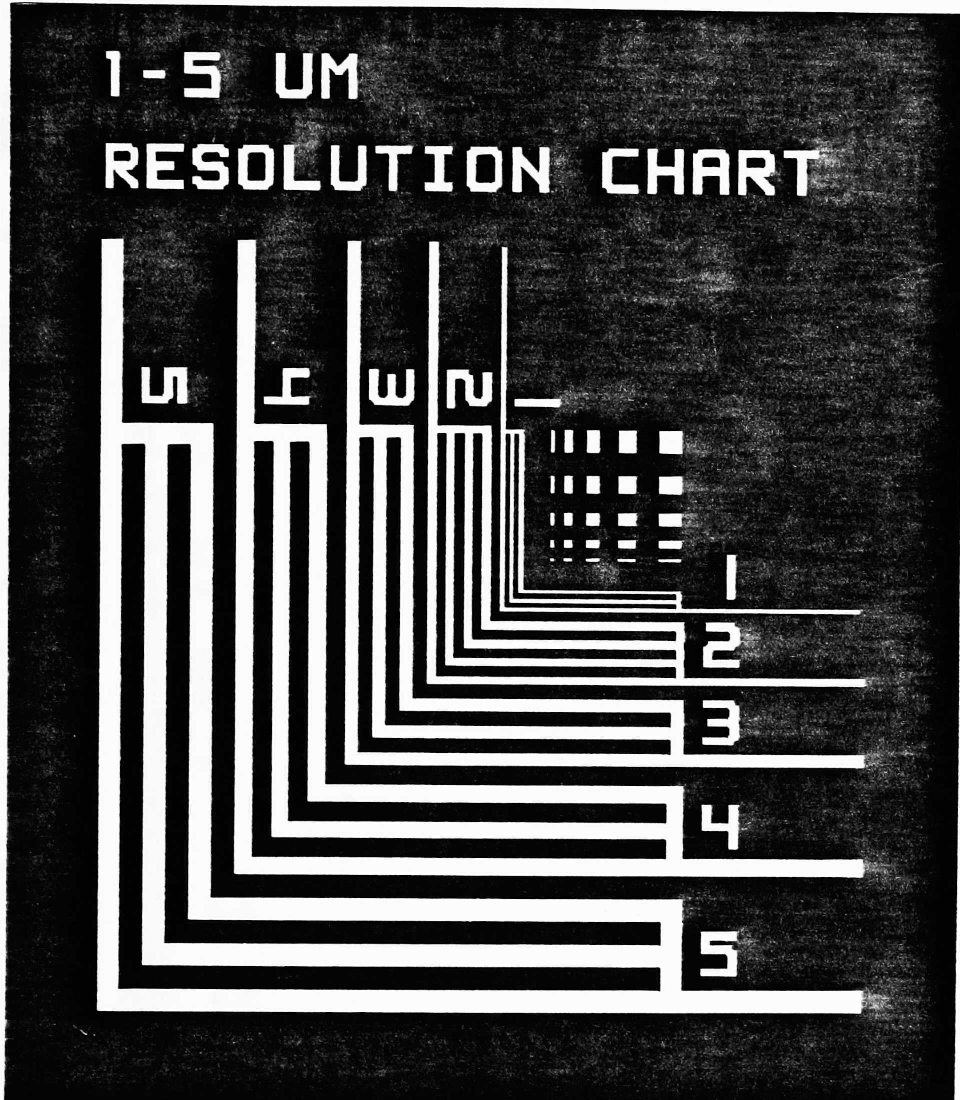

Figure A27: Dark Field Resolution Chart

A basic optical structure with equal lines and spaces of dimensions 1, 2, 3, 4 and 5 microns. This pattern allows for rapid evaluation of the exposure tool's resolution capability. A comparison of the critical dimension measurement of a space within a field of spaces to one which is isolated can be performed by also reviewing the extended spaces.

Figure A28: Clear Field Murray Daggers

Two sets of Murray Daggers are included for a quick resolution inspection. Fine geometries from 0.2 to 2.0 microns and coarse geometries from 1 to 10 microns are provided. By searching for the location of the finest geometry observed, the resolution can easily be determined.

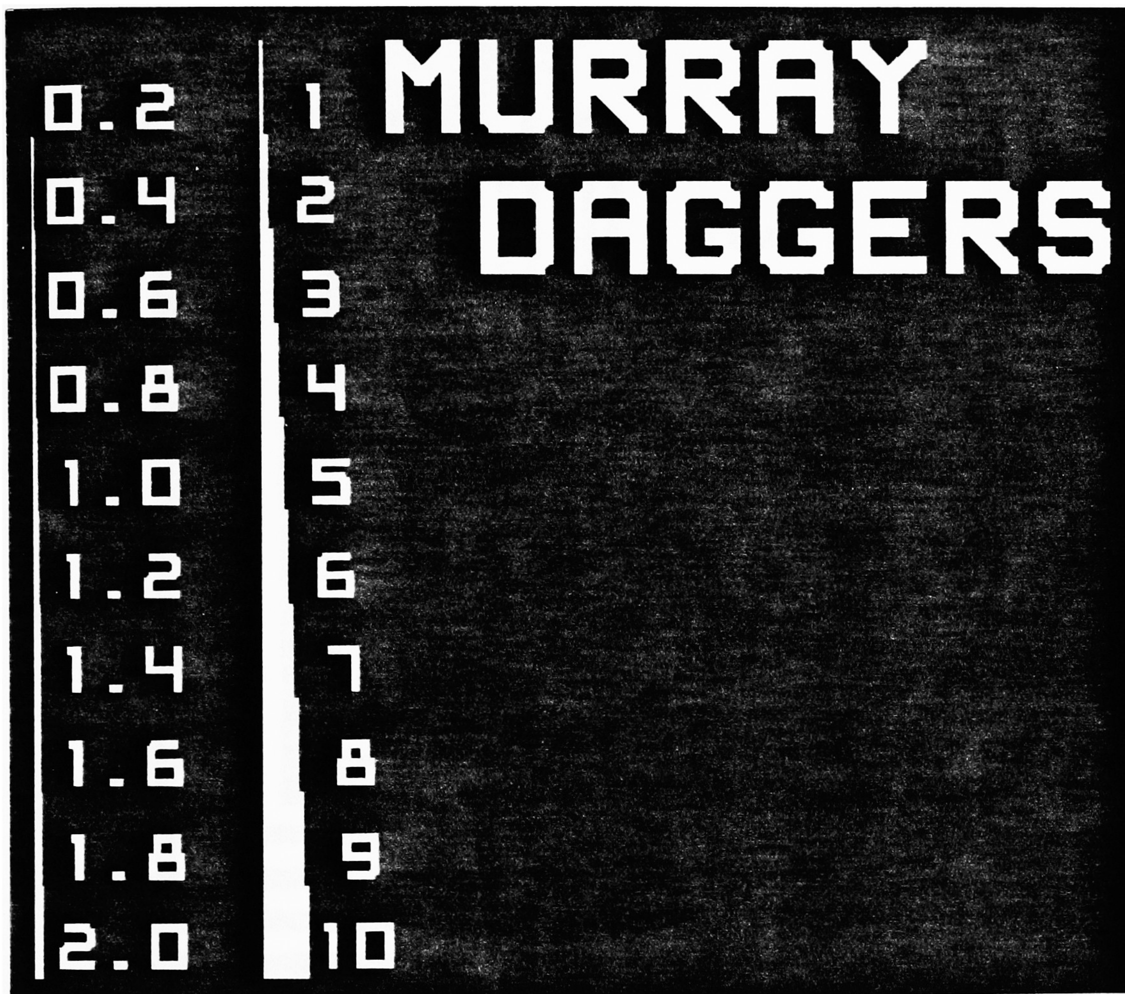

Figure A29: Dark Field Murray Daggers

Two sets of Murray Daggers are included for a quick resolution inspection. Fine geometries from 0.2 to 2.0 microns and coarse geometries from 1 to 10 microns are provided. By searching for the location of the finest geometry observed, the resolution can easily be determined.

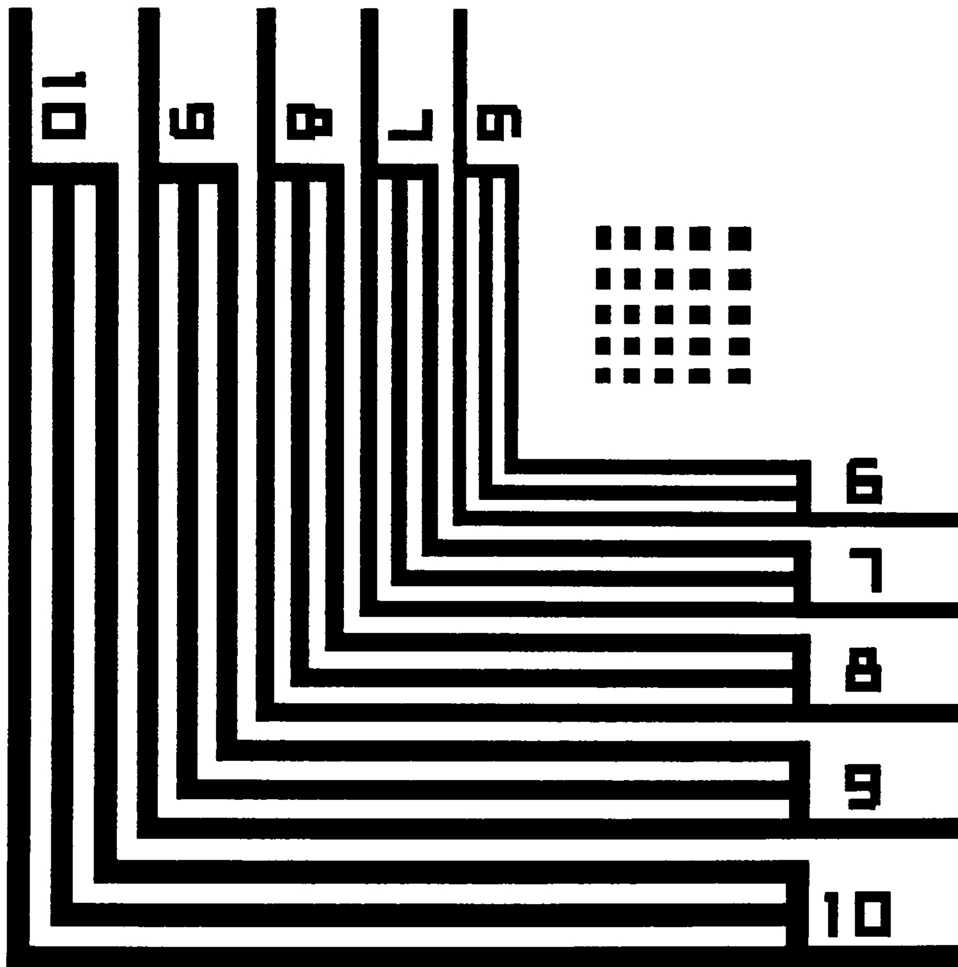

Figure A30: Clear Field Resolution Chart

A basic optical structure with equal lines and spaces of dimensions 6, 7, 8, 9 and 10 microns. This pattern allows for rapid evaluation of the exposure tool's resolution capability. A comparison of the critical dimension measurement of a line within a field of lines to one which is isolated can be performed by also reviewing the extended lines.

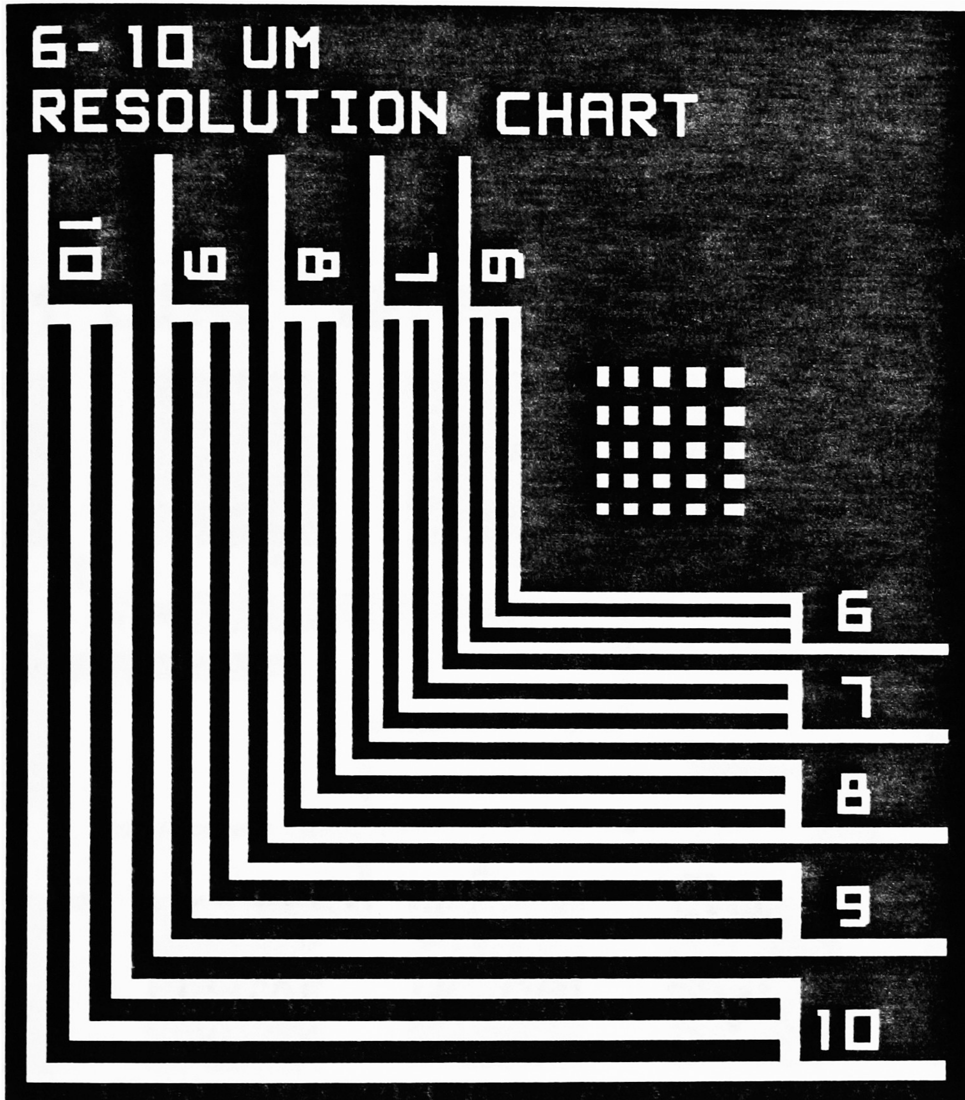

Figure A31: Dark Field Resolution Chart

A basic optical structure with equal lines and spaces of dimensions 6, 7, 8, 9 and 10 microns. This pattern allows for rapid evaluation of the exposure tool's resolution capability. A comparison of the critical dimension measurement of a space within a field of spaces to one which is isolated can be performed by also reviewing the extended spaces.

2 UM LINE 12PAD

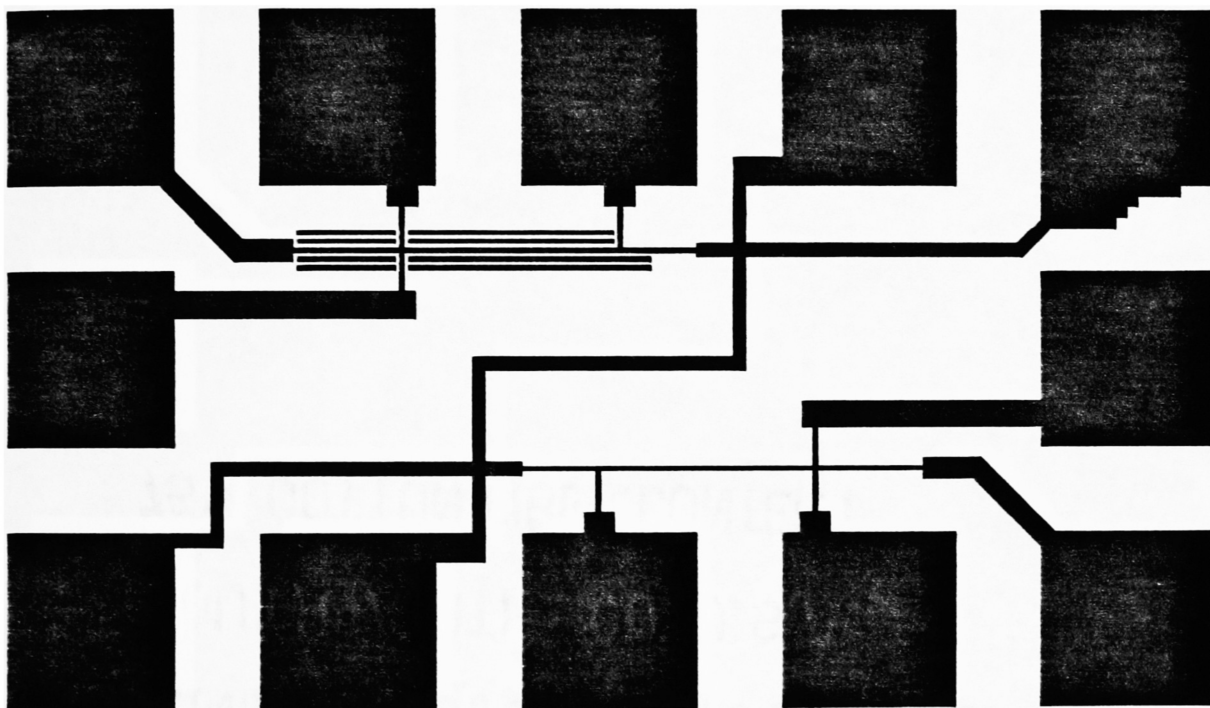

Figure A32: Electrical Linewidth Structure for 2 Micron Lines

This standard 12 pad test structure shares 2 micron features, one of which is within a field of other 2 micron lines and one which is alone. The method of electrical probing and theory is included in Appendix C. The results can be compared to similar features for optical patterns.

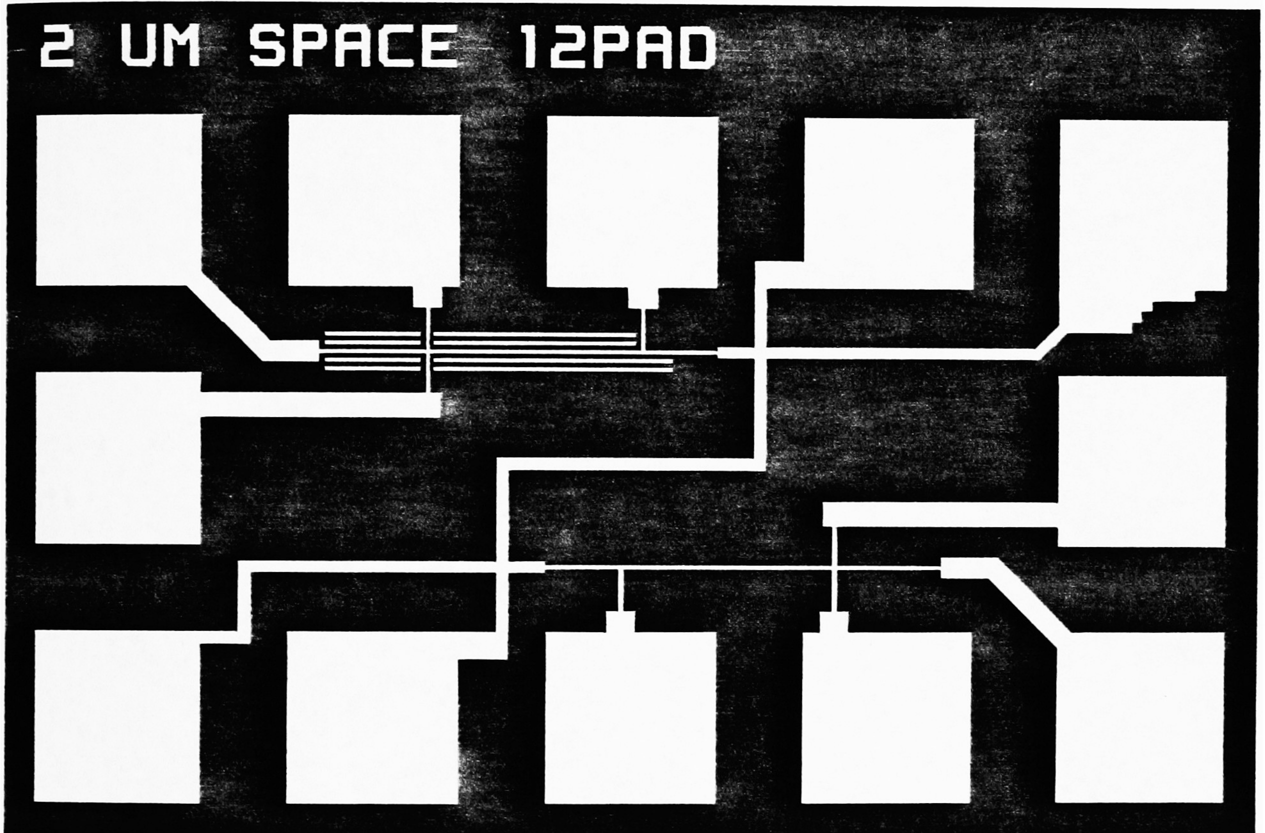

Figure A33: Electrical Linewidth Structure for 2 Micron Spaces

This standard 12 pad test structure shares 2 micron features, one of which is within a field of other 2 micron spaces and one which is alone. The method of electrical probing and theory is included in Appendix C. Comparison of the results to the clearfield structure can be done.

3 UM LINE 12PAD

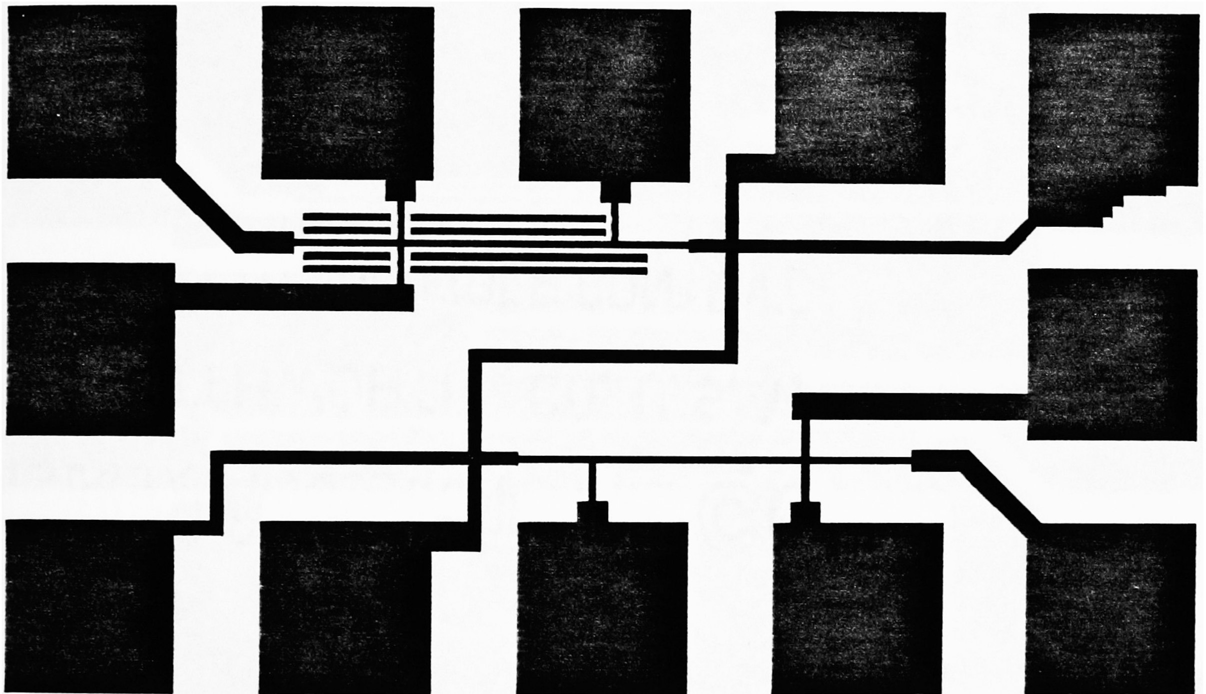

Figure A34: Electrical Linewidth Structure for 3 Micron Lines

This standard 12 pad test structure shares 3 micron features, one of which is within a field of other 3 micron lines and one which is alone. The method of electrical probing and theory is included in Appendix C. The results can be compared to similar features for optical patterns.

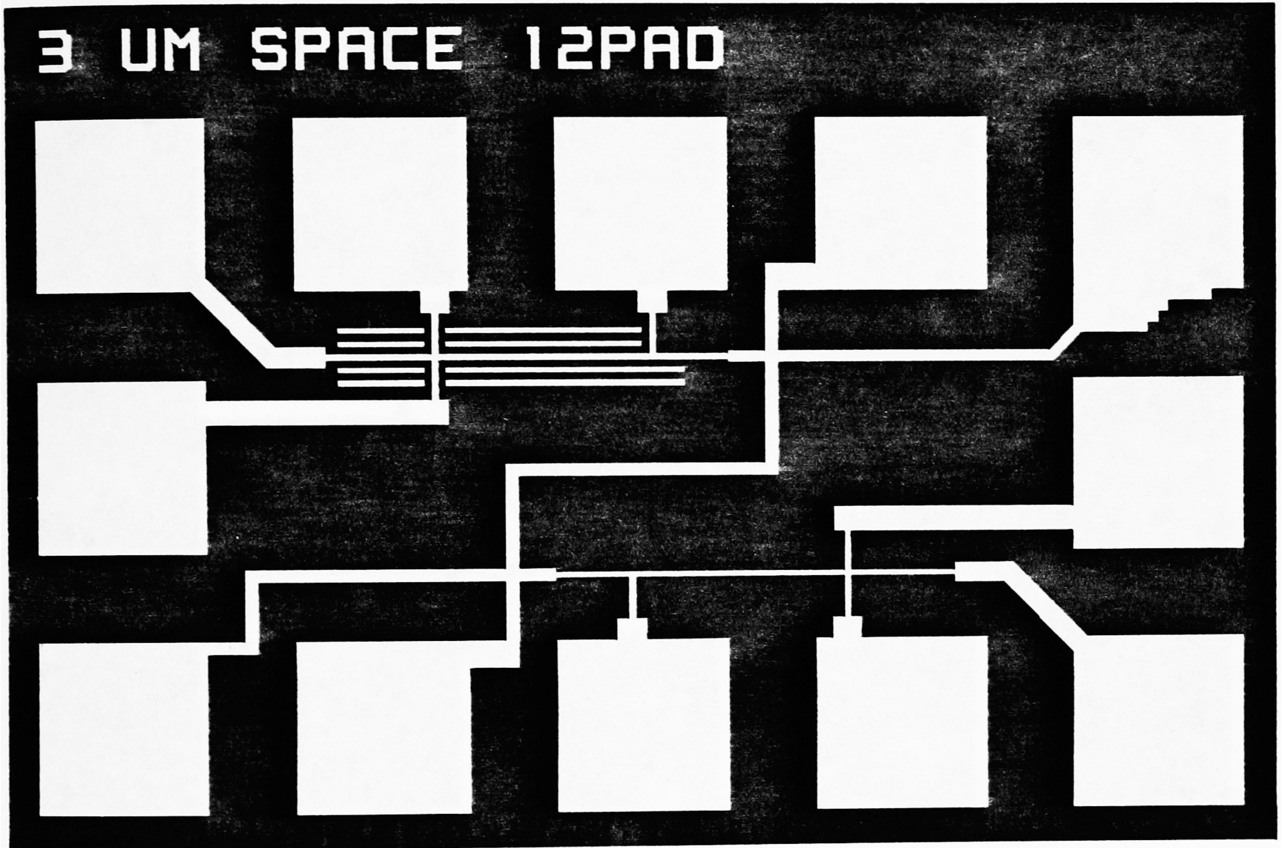

Figure A35: Electrical Linewidth Structure for 3 Micron Spaces

This standard 12 pad test structure shares 3 micron features, one of which is within a field of other 3 micron spaces and one which is alone. The method for electrical probing and theory is included in Appendix C. Comparison of the results to the clearfield structure can be done.

5 UM LINE 12PAD

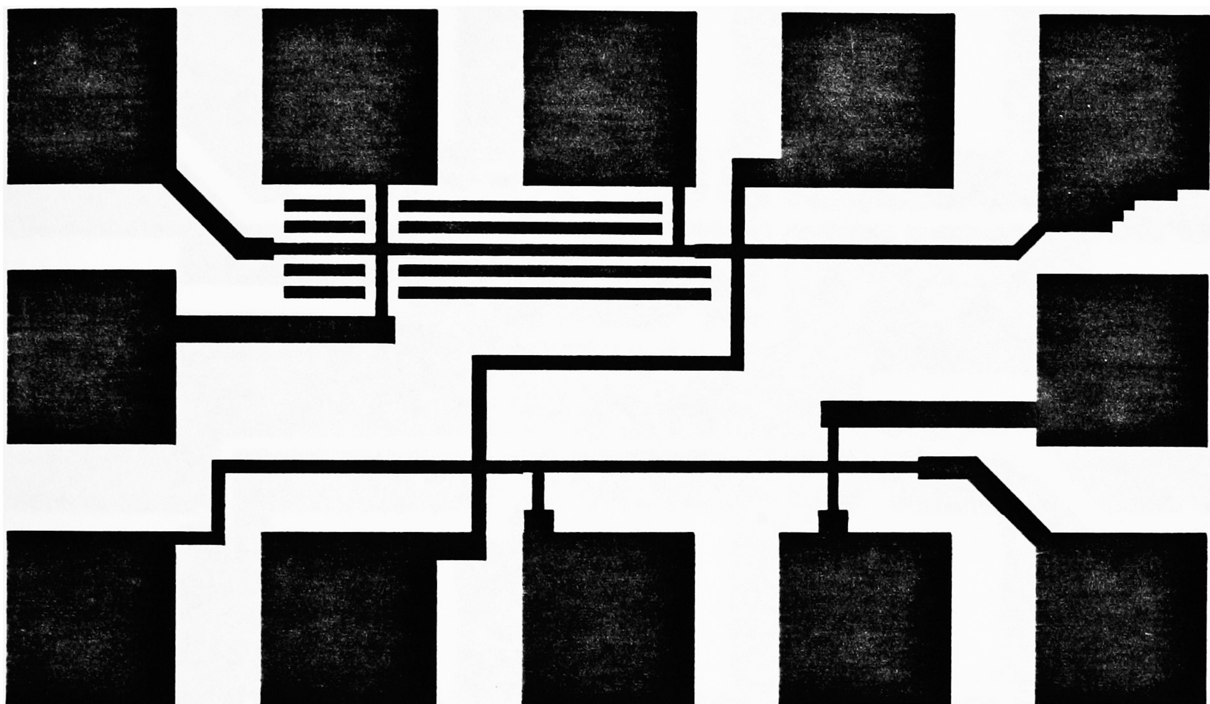

Figure A36: Electrical Linewidth Structure for 5 Micron Lines

This standard 12 pad test structure shares 5 micron features, one of which is within a field of other 5 micron lines and one which is alone. The method of electrical probing and theory is included in Appendix C. The results can be compared to similar features for optical patterns.

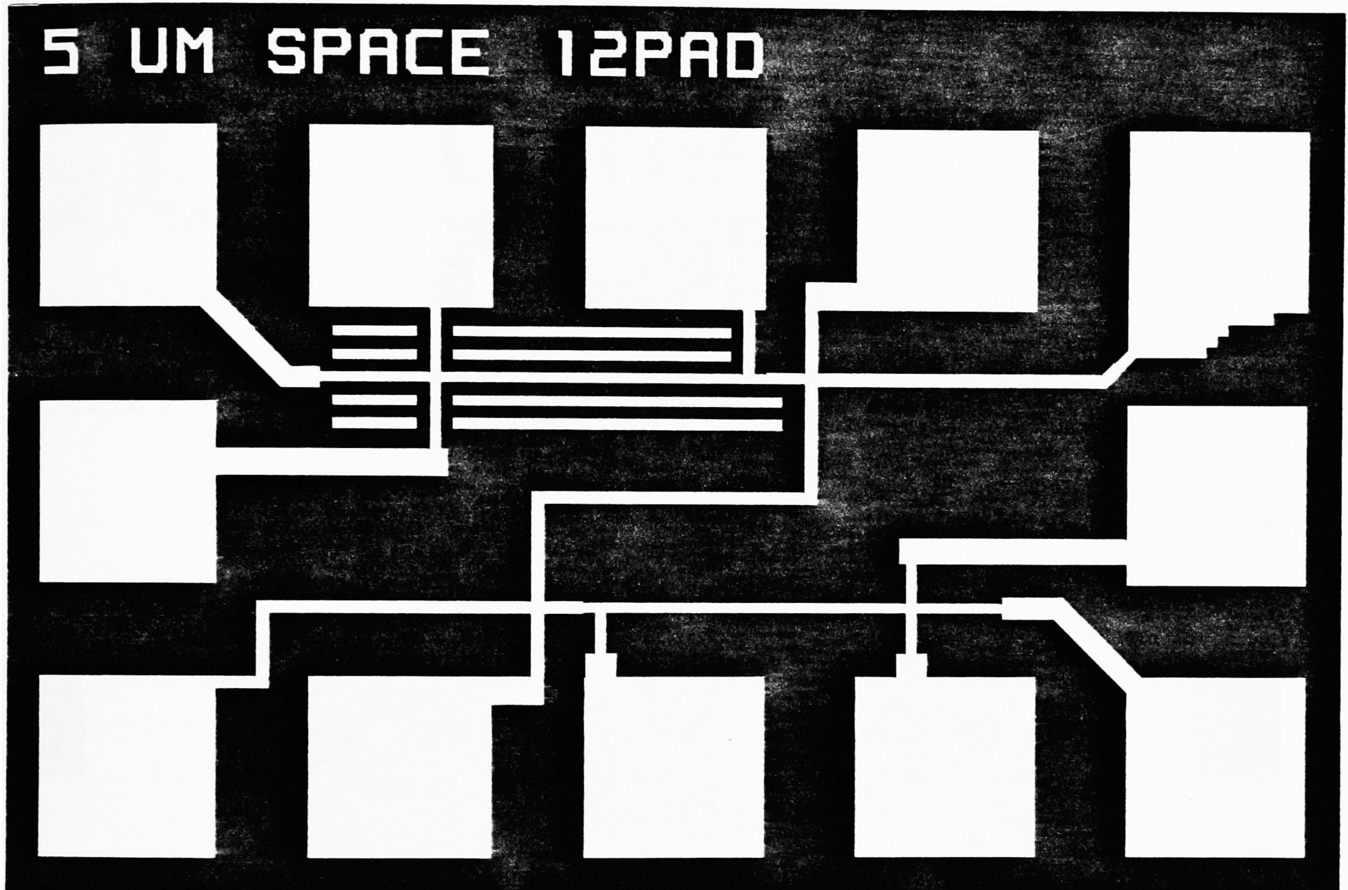

Figure A37: Electrical Linewidth Structure for 5 Micron Spaces

This standard 12 pad test structure shares 5 micron features, one of which is within a field of other 5 micron spaces and one which is alone. The method of electrical probing and theory is included in Appendix C. Comparison of the results to the clearfield structure can be done.

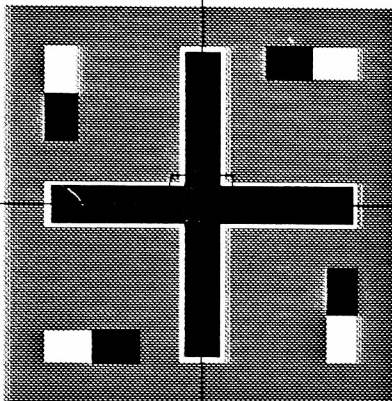

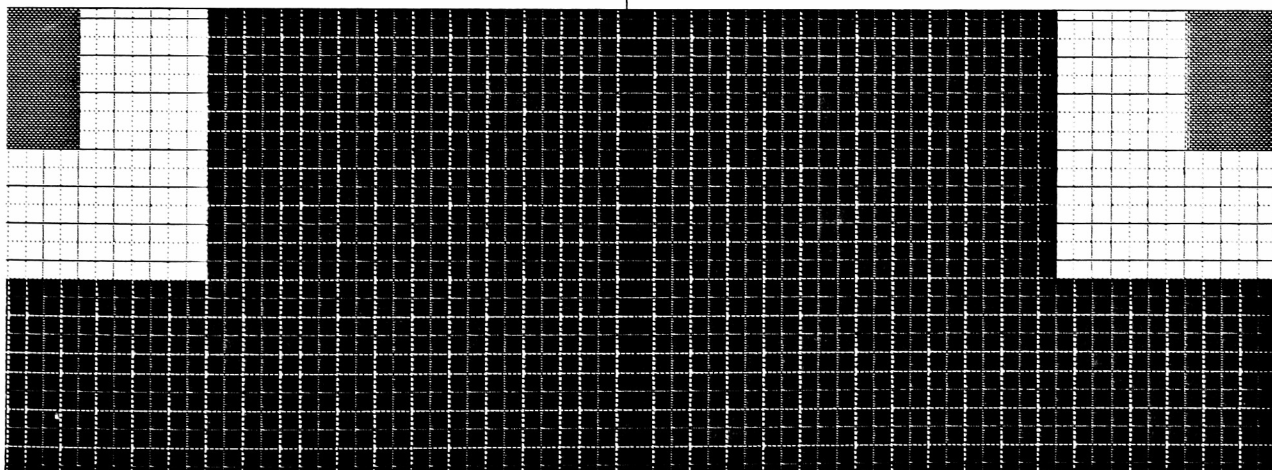

Figure A38: Manual Alignment Cross

This target will be used for all manual alignments after the offset has been performed for bi-level experiments.

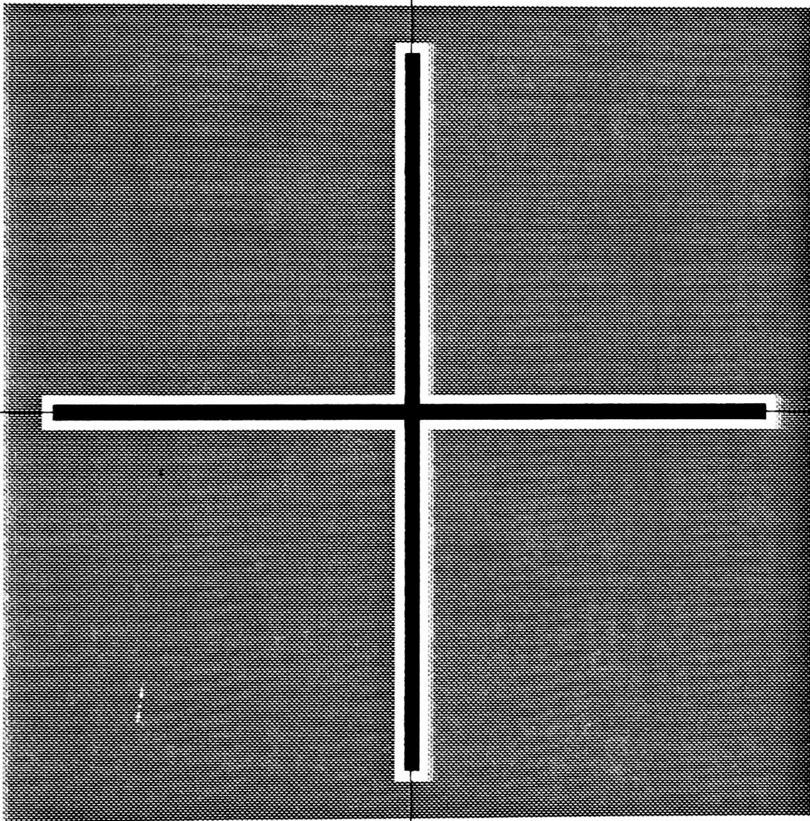

Figure A39: GCA Alignment Cross

This is the target existing on standard GCA Wafer Stepper Test Masks.

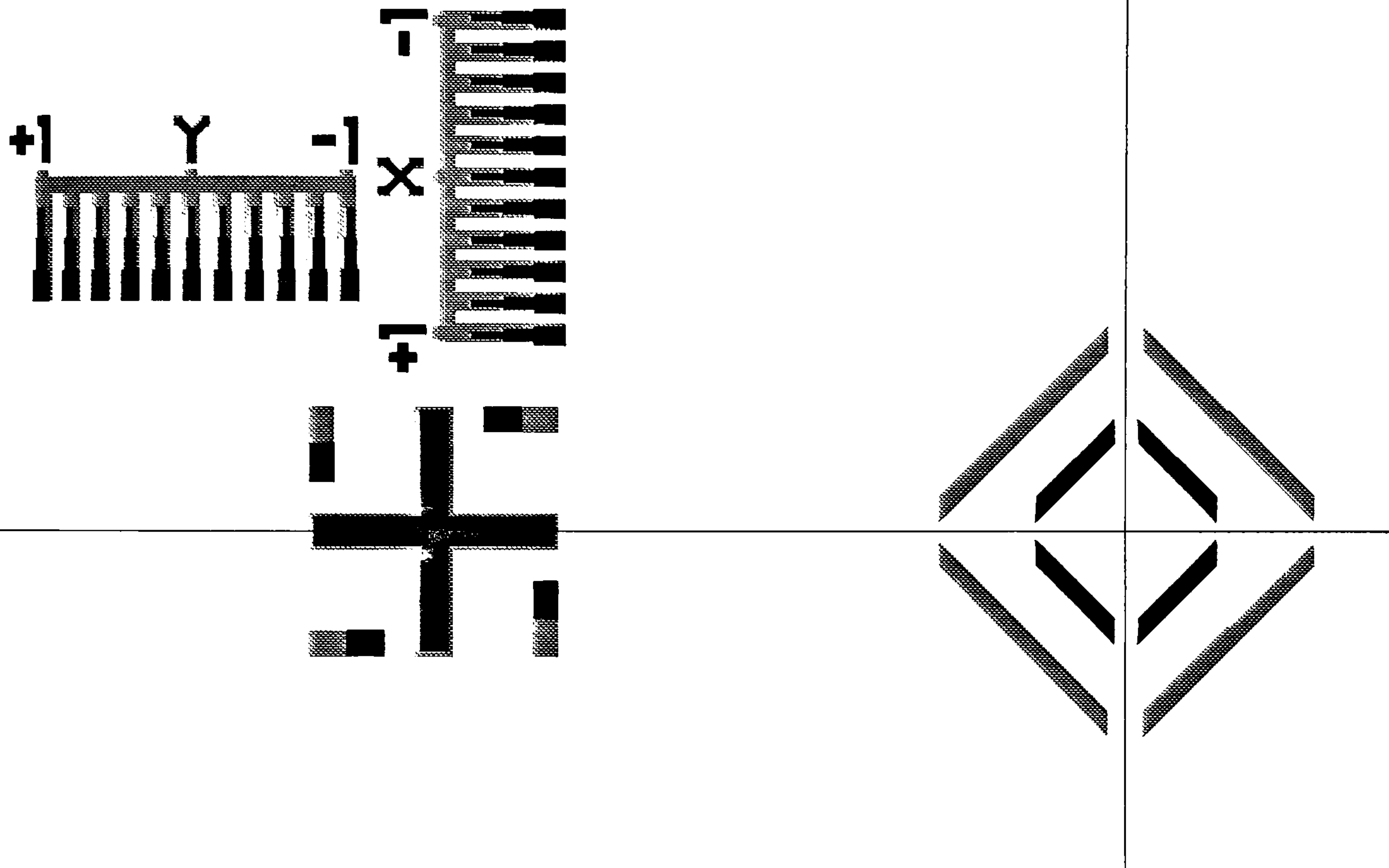

Figure A40: Perkin-Elmer 200/300 Series AFA CF-CF Target

This Automatic Fine Alignment target is designed with both clearfield first and second levels. The structure also includes the standard manual cross and optical verniers. This target is to be used with Perkin-Elmer 200/300 series scanners which are equipped with Automatic Fine Alignment systems.

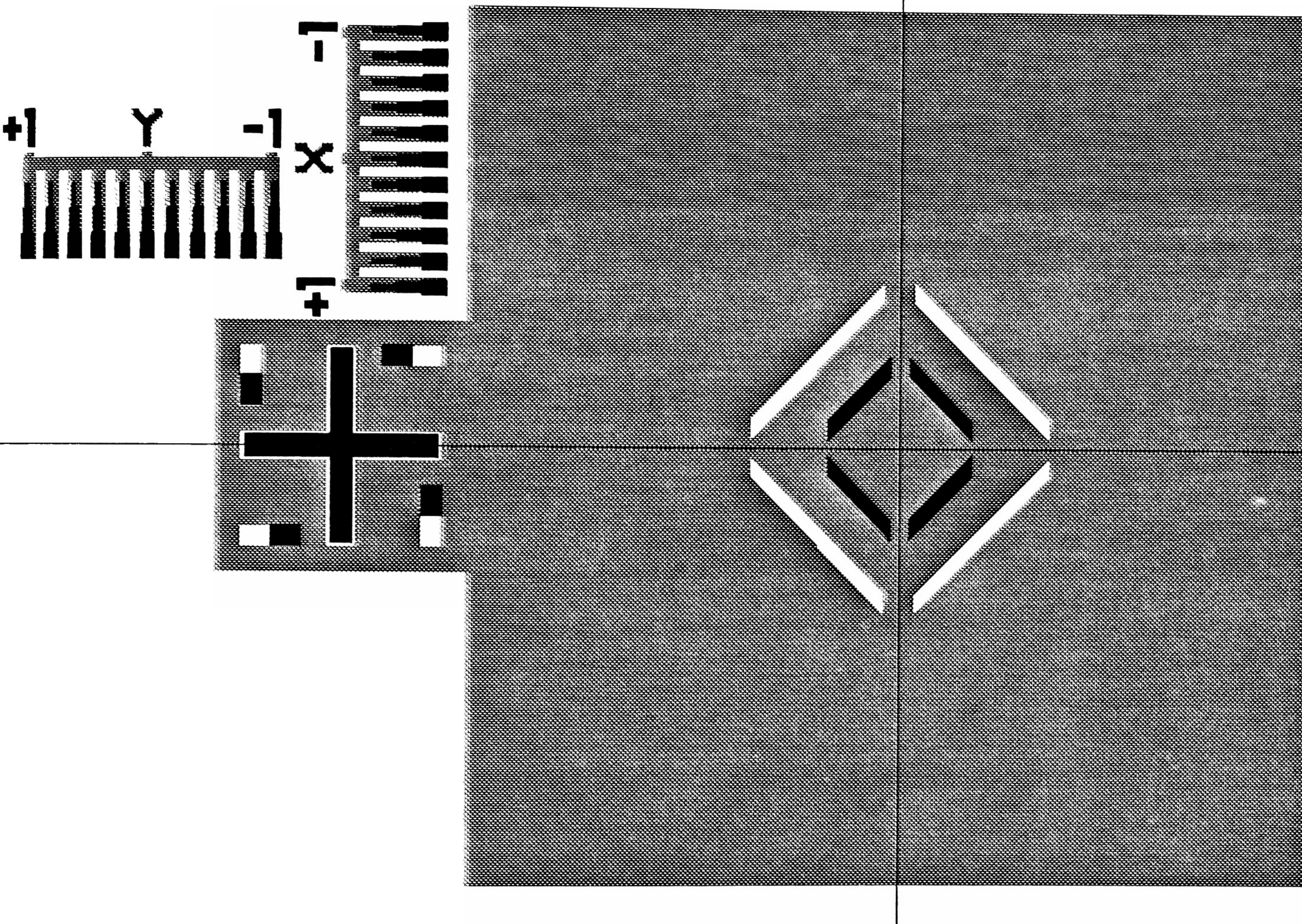

Figure A41: Perkin-Elmer 200/300 Series AFA CF-DF Target

This Automatic Fine Alignment target is designed with darkfield first level and clearfield second level. The structure also includes the standard manual cross and optical verniers. This target is to be used with Perkin-Elmer 200/300 series scanners which are equipped with Automatic Fine Alignment systems.

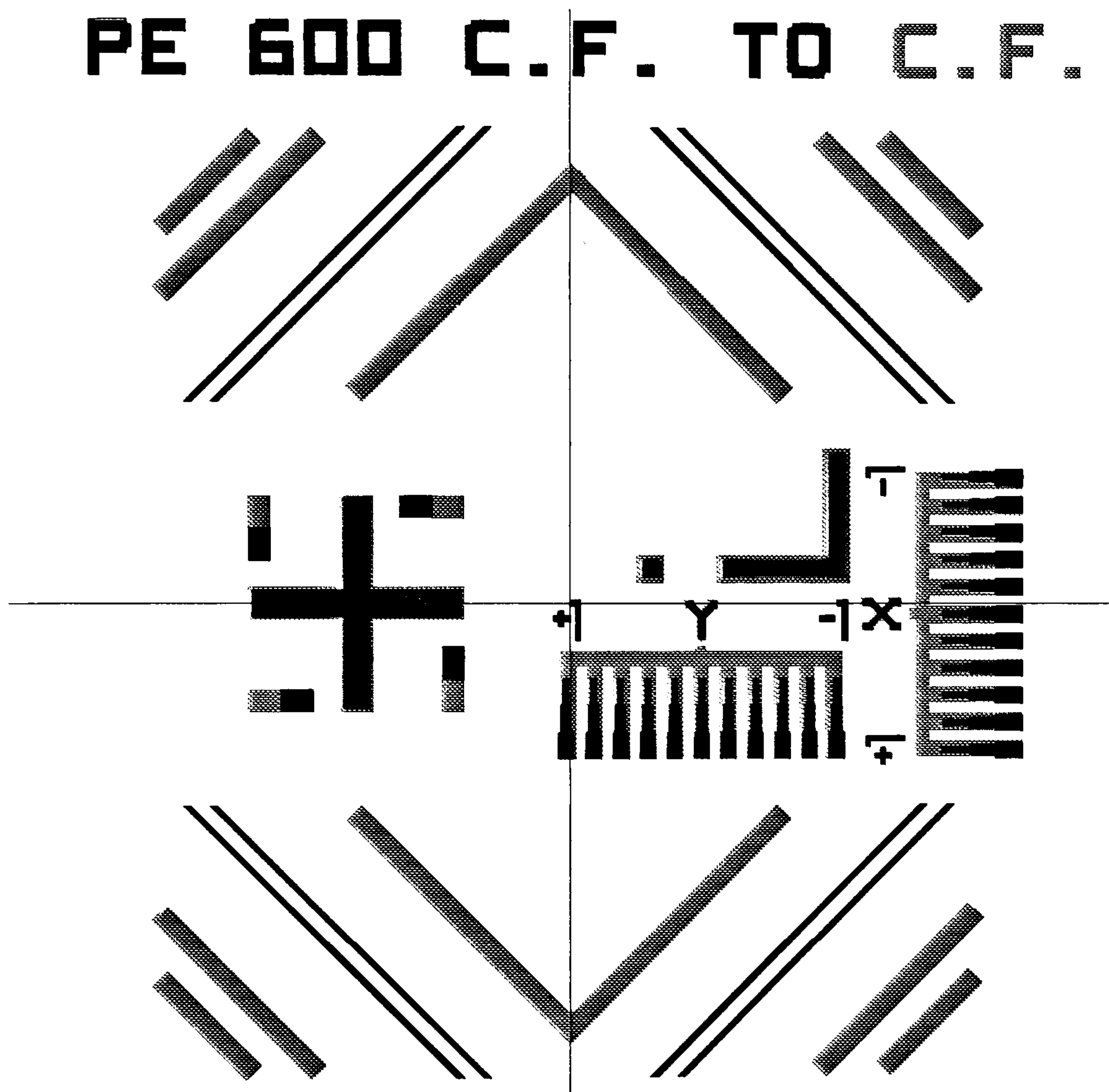

Figure A42: Perkin-Elmer 500/600 Series AFA CF-CF Target

This Automatic Fine Alignment target is designed with both clearfield first and second levels. The structure also includes the standard manual cross and optical verniers. This target is to be used with Perkin-Elmer 500/600 scanners.

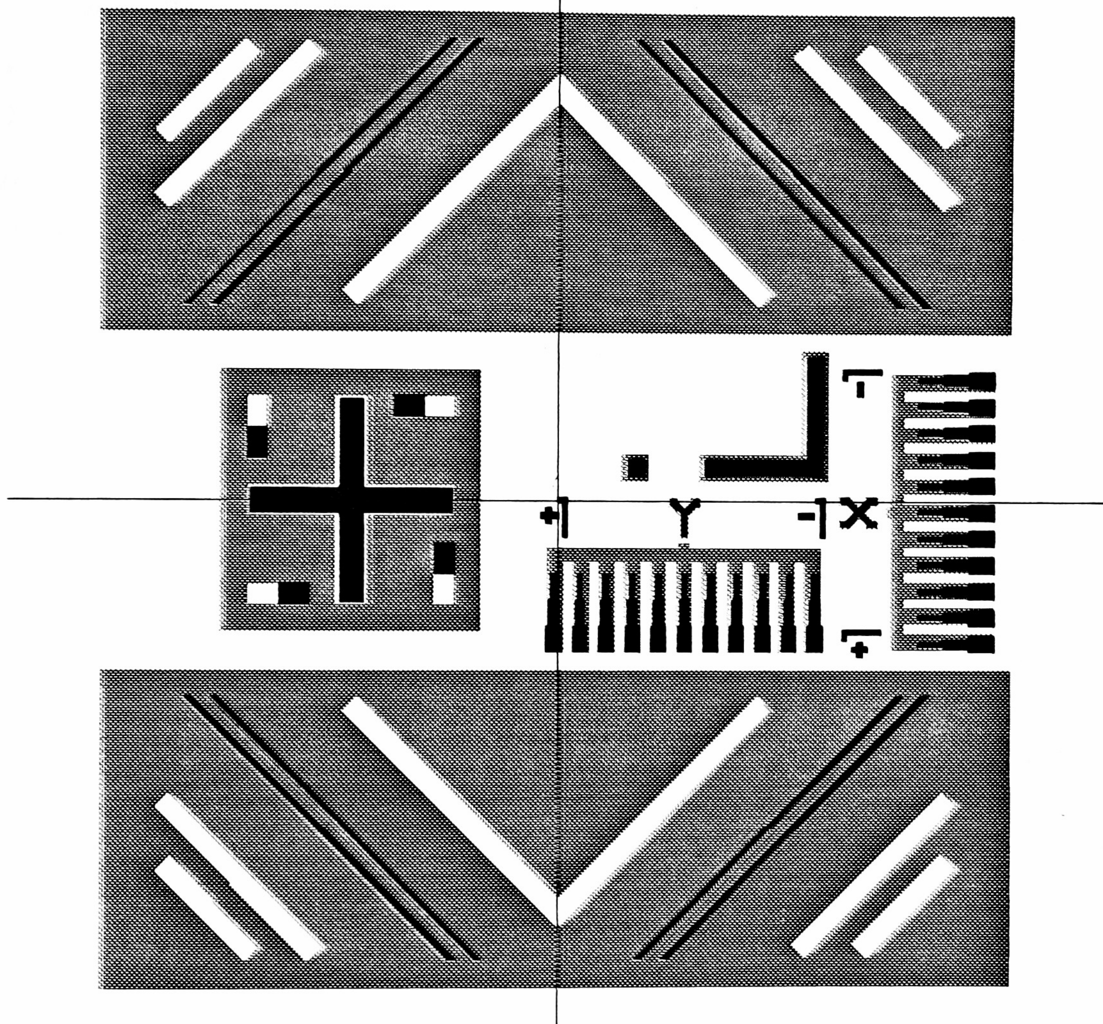

Figure A43: Perkin-Elmer 500/600 Series AFA CF-DF Target

This Automatic Fine Alignment target is designed with darkfield first level and clearfield second level. The structure also includes the standard manual cross and optical verniers. This target is to be used with Perkin-Elmer 500/600 scanners.

OPTICAL VERNIERS
1 UM RANGE
0.2 UM RESOLUTION

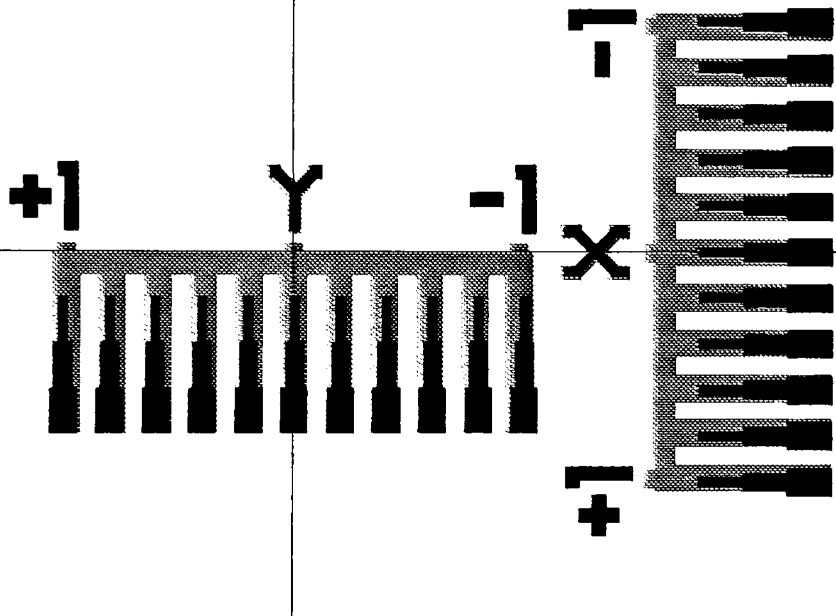

Figure A44: Optical Verniers (+/- 1 micron range)

This structure provides a means of optically determining misregistration of one layer with respect to another. The maximum range is +/- 1 micron with resolution of 0.2 microns. The axes are labled according to the convention used during viewing a wafer during alignment in a Perkin-Elmer 200/300 series scanner. For a detailed discussion on interpreting verniers, refer to Appendix B.

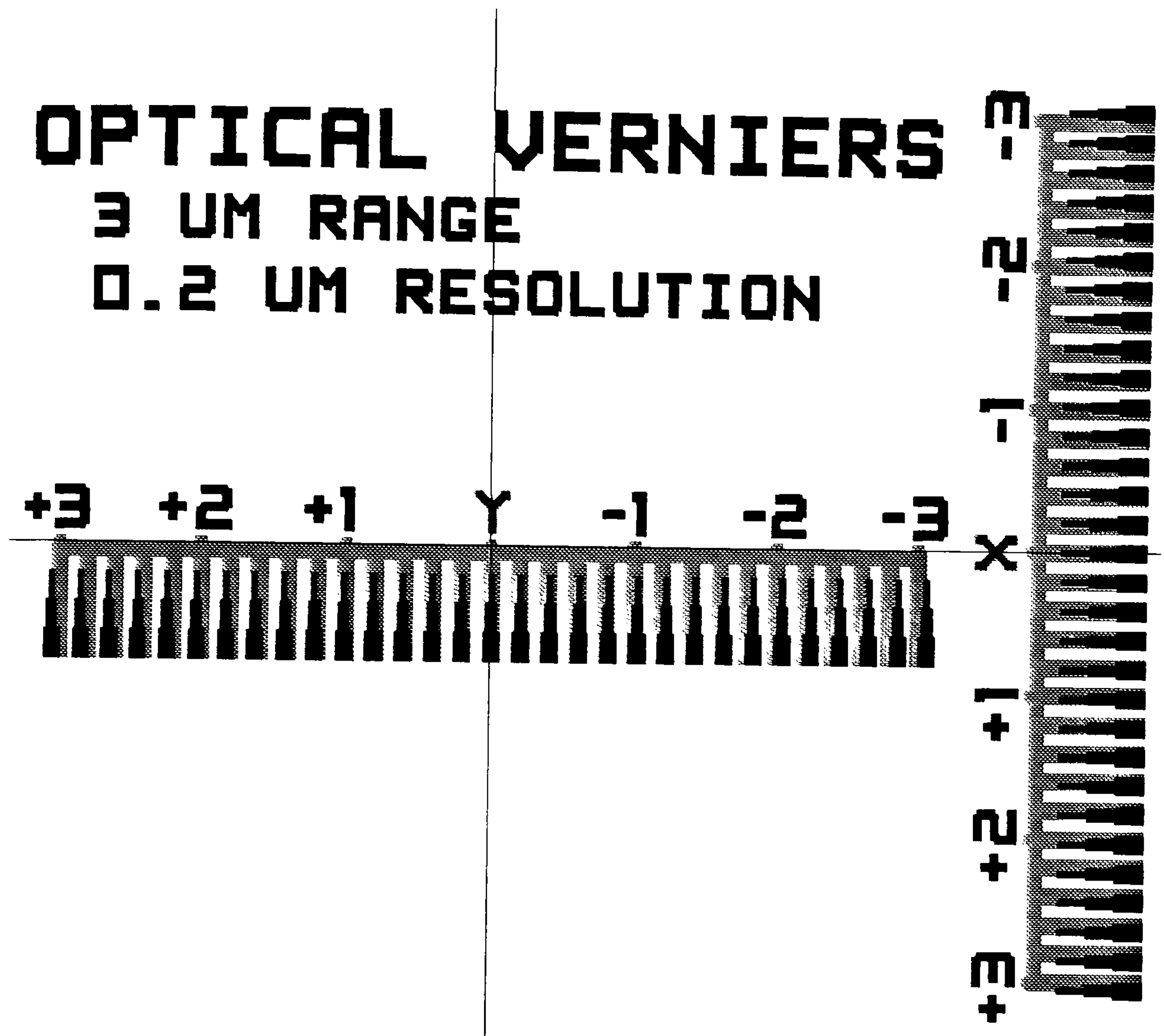

Figure A45: Optical Verniers (+/- 3 micron range)

This structure provides a means of optically determining misregistration of one layer with respect to another. The maximum range is +/- 3 micron with resolution of 0.2 microns. The axes are labled according to the convention used during viewing a wafer during alignment in a Perkin-Elmer 200/300 series scanner. For a detailed discussion on interpreting verniers, refer to Appendix B.

ALIGN 12PAD C.F. TO C.F.

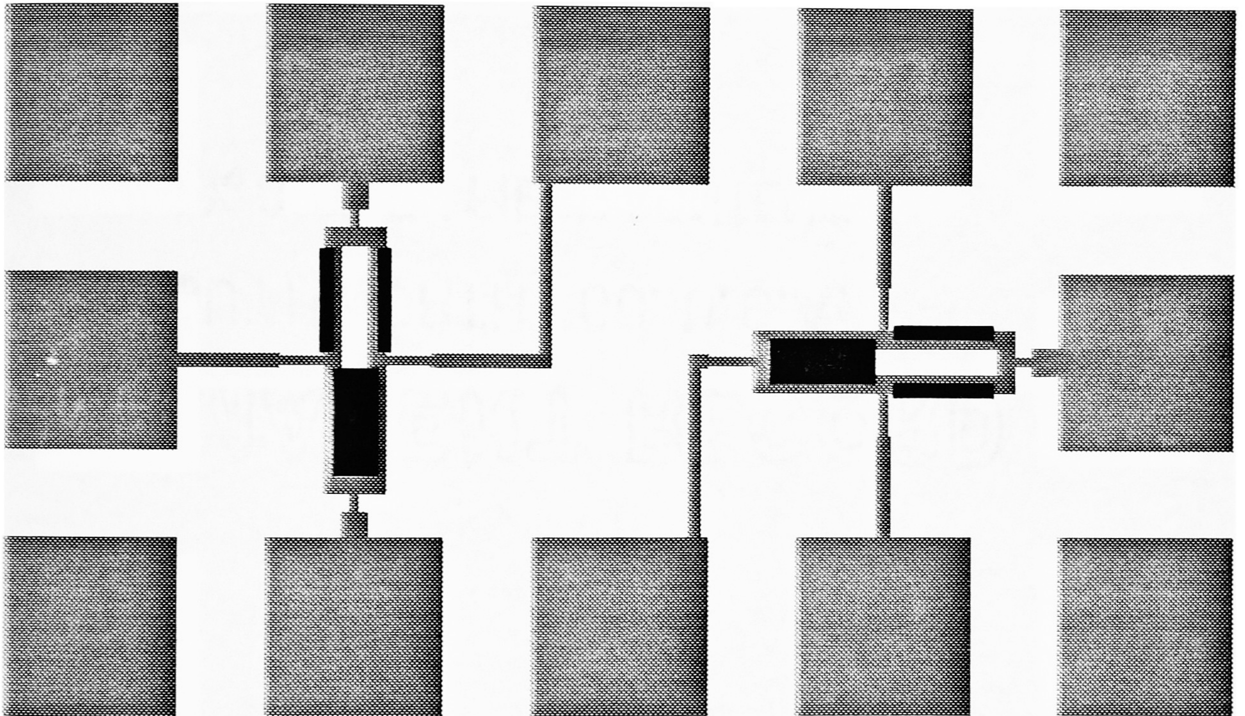

Figure A46: Electrical Alignment Test Structure (CF-CF)

This is a Wheatstone Bridge structure which can be used as an indicator of mis-registration of the two clearfield patterns of which it is made. For theory and probing requirements, refer to Appendix D.

ALIGN 12PAD C.F. TO D.F.

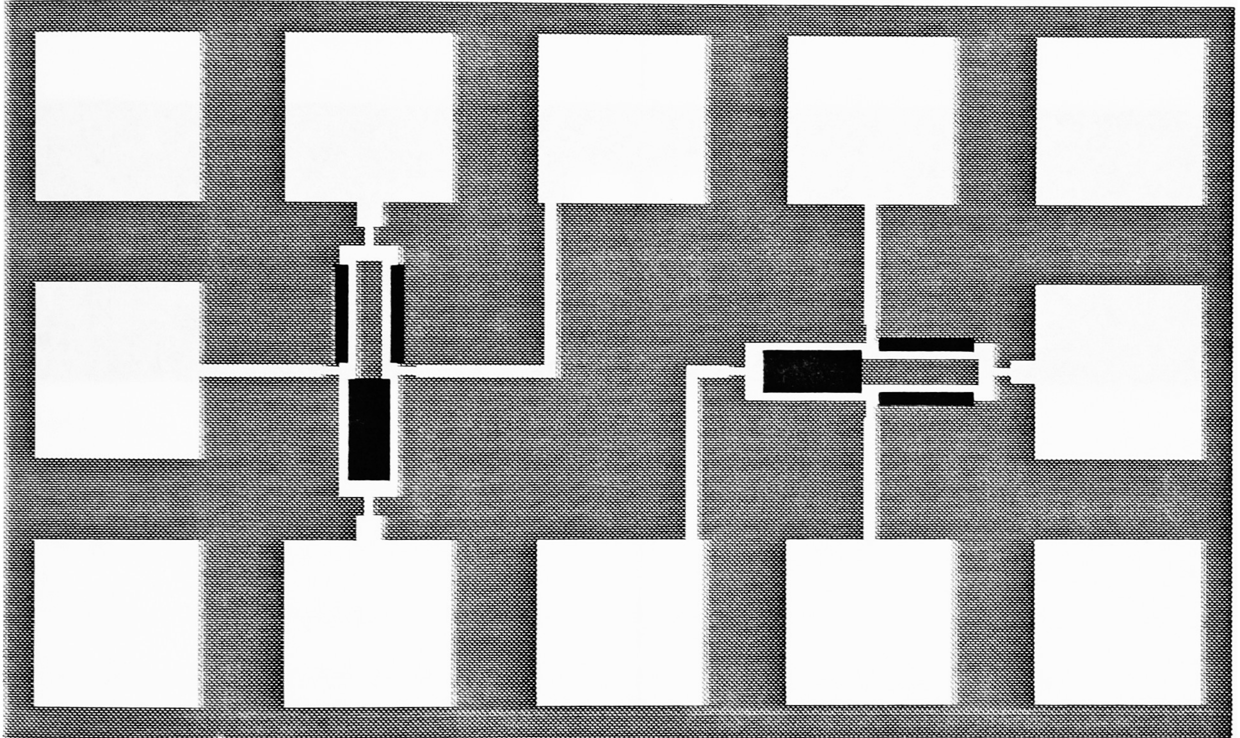

Figure A47: Electrical Alignment Test Structure (CF-DF)

This is a Wheatstone Bridge structure which can be used as an indicator of mis-registration of a clearfield second level to a darkfield first level. For theory and probing requirements refer to Appendix D.

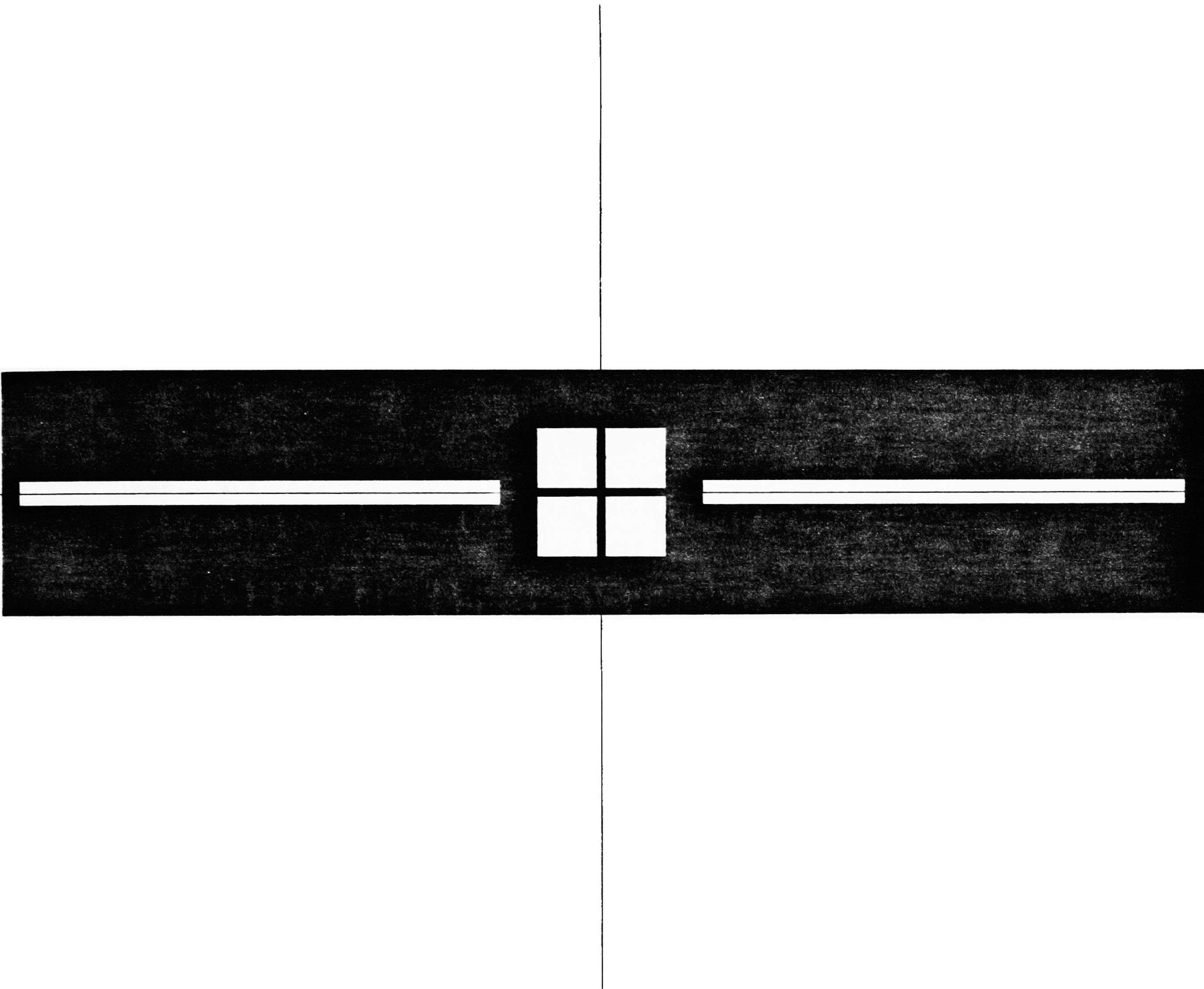

Figure A48: GCA Street Target

This is the standard structure provided on GCA reticles for field to field stepping. It exists only on the 10X reticle in the streets on each side of the die.

APPENDIX F: CHARACTERIZATION REPORT

A performance characterization of a Perkin-Elmer Micralign 241 Scanner was performed using the procedures outlined in section IV. This encompassed a number of exposures on various substrate materials. After subsequent processing, the wafers were evaluated optically and electrically as necessary. The results of these tests are reported in this appendix. Also, listed below are the materials and equipment used during the experiments.

Materials:

- Photoresist: KTI-820, 1.2 microns thick.
- Developer: KTI-934 MIF.
- Phosphorus Source: POCl3.

Equipment:

- Photoresist/Bake and Develop/Bake Tracks: Eaton, Model LSI 45/60.
- Exposure Tool: Perkin-Elmer, Micralign 241 Scanner.
- Optical Inspection: Leitz, Ergolux Microscope.
- Optical Linewidth measurement: Leitz, C.D. Ergolux Microscope.
- Polysilicon Deposition: BTU/ACS, LPCVD System.
- Thermal Oxide / Phosphorus Diffusion: BTU, Atmospheric Diffusion.
- Plasma Oxide Etcher: Tegal, Model 903 Plasma Etcher.
- Plasma Polysilicon Etcher: Tegal, Model 701 Plasma Etcher.
- Photoresist Stripper: Tegal, Model 415 Plasma Etcher.
- Electrical Probe Station: Rucker & Kolls, Model 680A Wafer Prober.
- Mask Repair: Florod Corp., Model LMT Laser Zapper.

Critical dimension uniformity was evaluated for a 2 micron line within a field of other 2 micron lines and is displayed in the map of Figure A49.

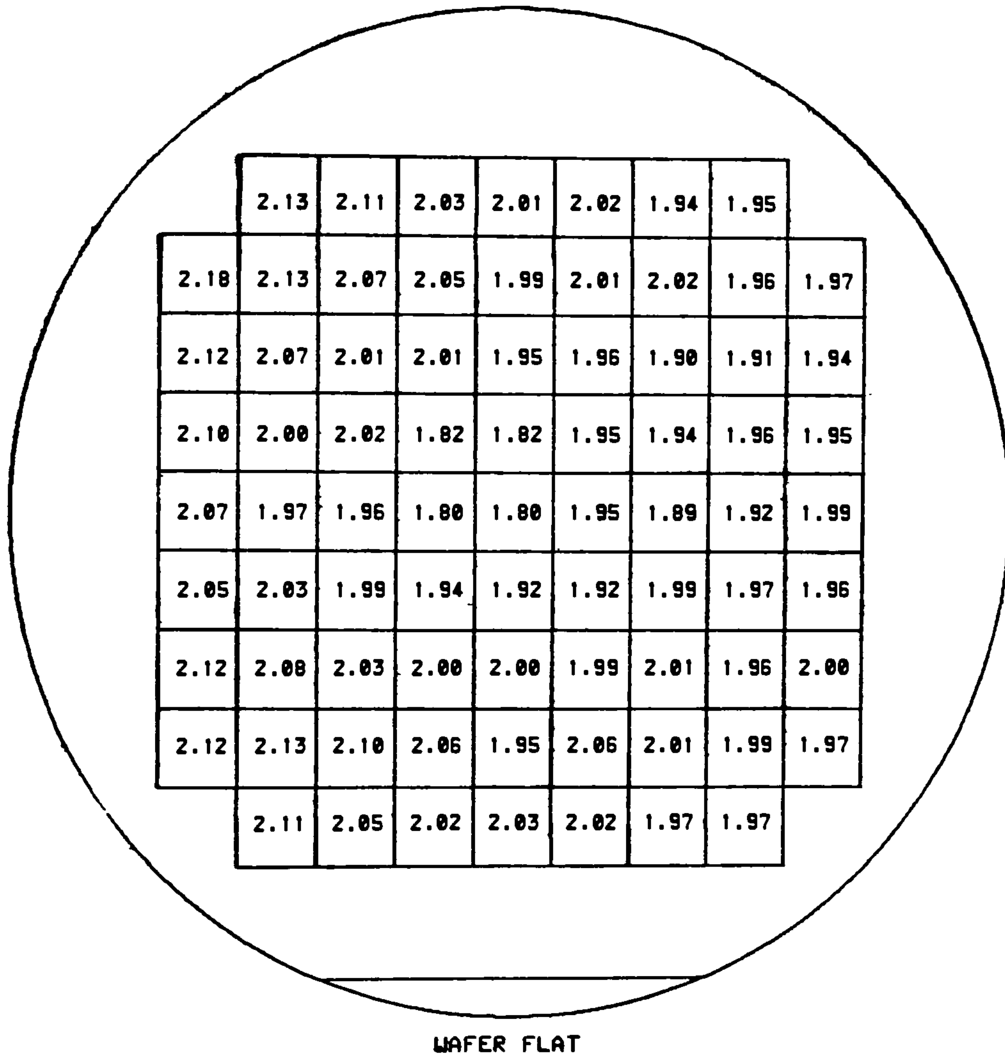

Figure A49: C.D. Uniformity Map (Line Within a Field of Lines).

Critical dimension uniformity was evaluated for a 2 micron line within a field of other 2 micron lines and is displayed in the histogram of Figure A50.

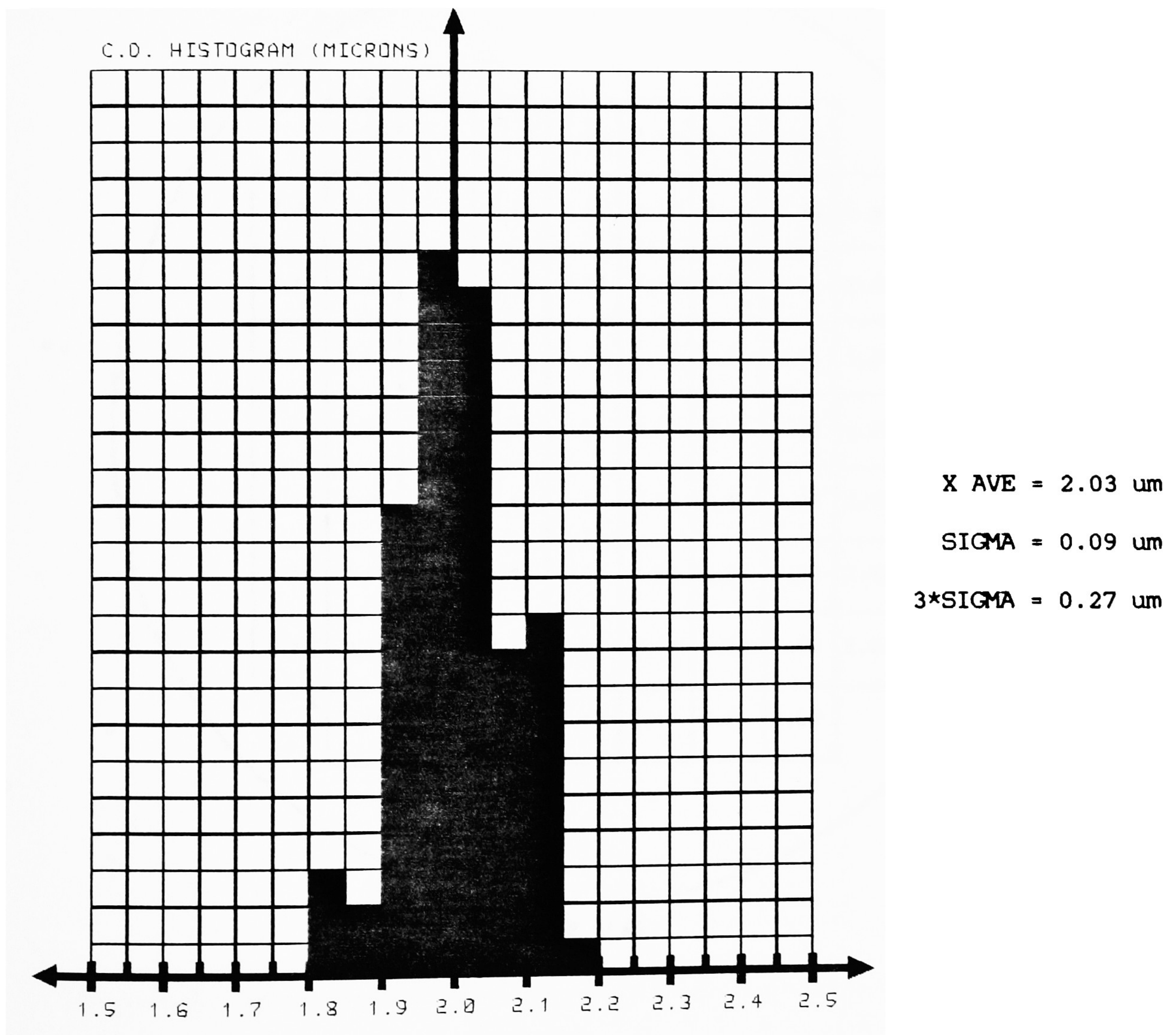

Figure A50: C.D. Histogram (Line Within a Field of Lines).

For comparison, critical dimension uniformity was also studied for 2 micron lines which were isolated. The data is presented in Figure A51 below and the comparison is depicted in Figure 19.

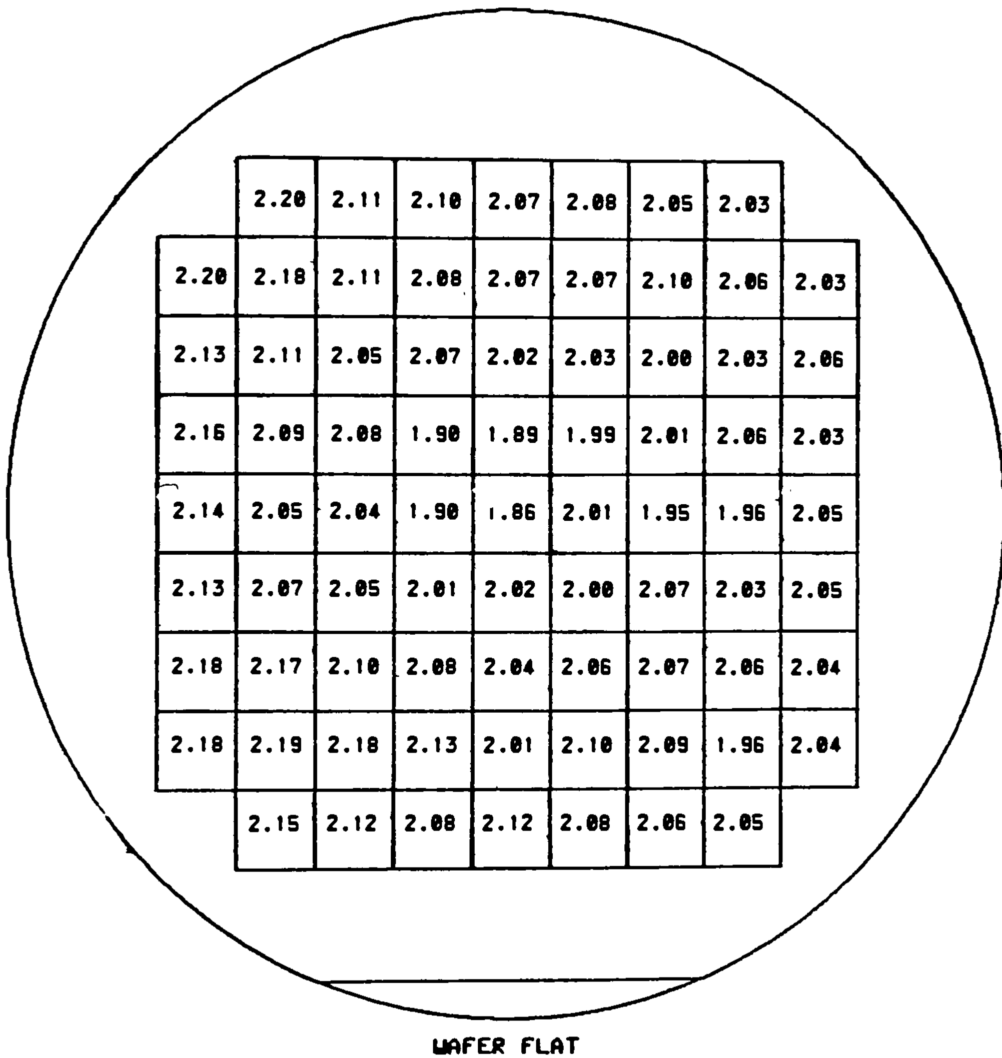

Figure A51: C.D. Uniformity Map (Isolated Line).

For comparison, critical dimension uniformity was also studied for 2 micron lines which were isolated. The data is presented in Figure A52 below and the comparison is depicted in Figure 19.

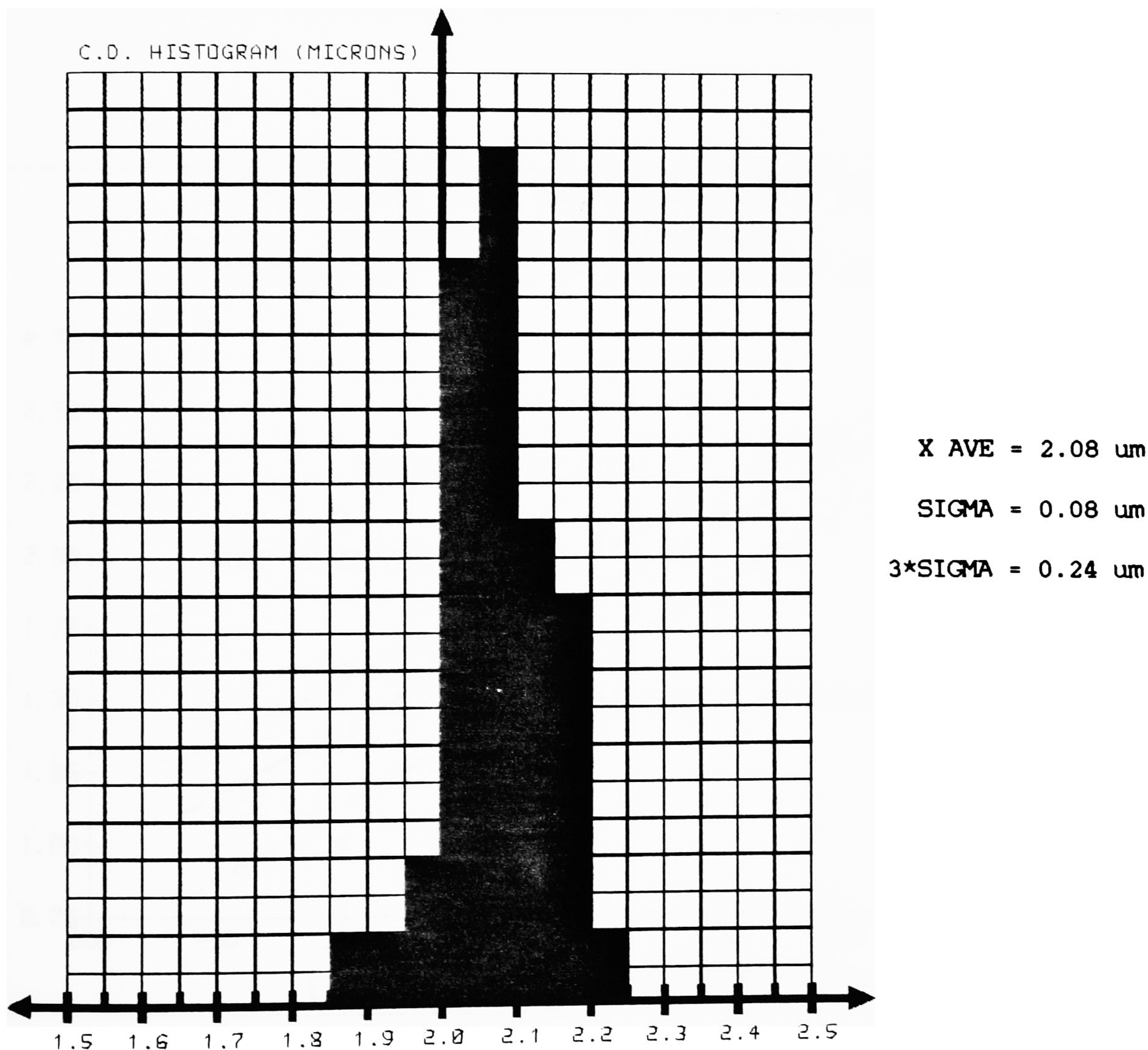

Figure A52: C.D. Histogram (Isolated Line).

A comparison between electrical and optical linewidth evaluations is presented below for a nominal 2 micron feature on wafers from an exposure series. It is reminded that the exposure setting on a Perkin-Elmer scanner is directly related to the carriage speed and inversely proportional to actual exposure dose. Therefore the linewidth increases with increasing exposure settings. Figures 20 and 21 address the differences observed for the data below.

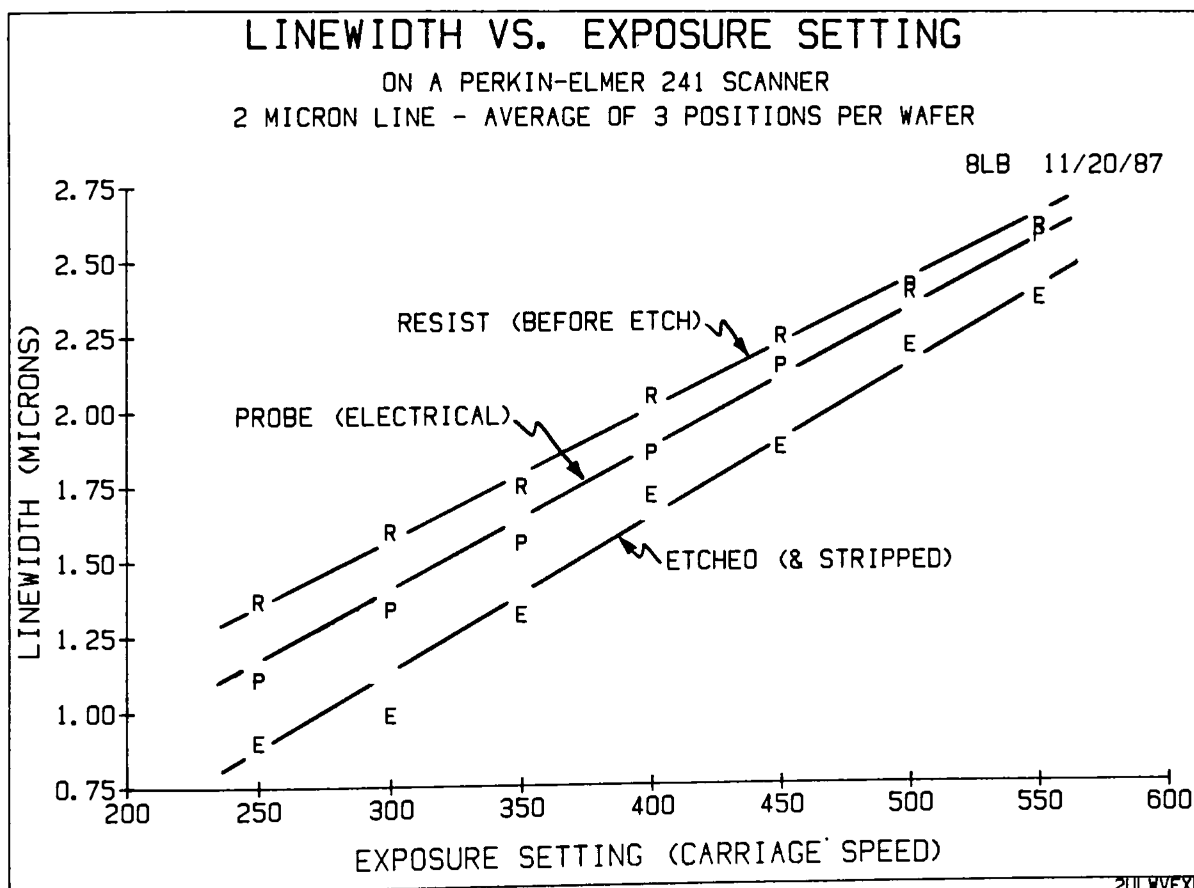

Figure A53: Linewidth vs. Exposure (2 Micron Line).

A comparison between electrical and optical linewidth evaluations is presented below for a nominal 3 micron feature on wafers from an exposure series. It is reminded that the exposure setting on a Perkin-Elmer scanner is directly related to the carriage speed and inversely proportional to actual exposure dose. Therefore the linewidth increases with increasing exposure settings. Figures 20 and 21 address the differences observed for the data below.

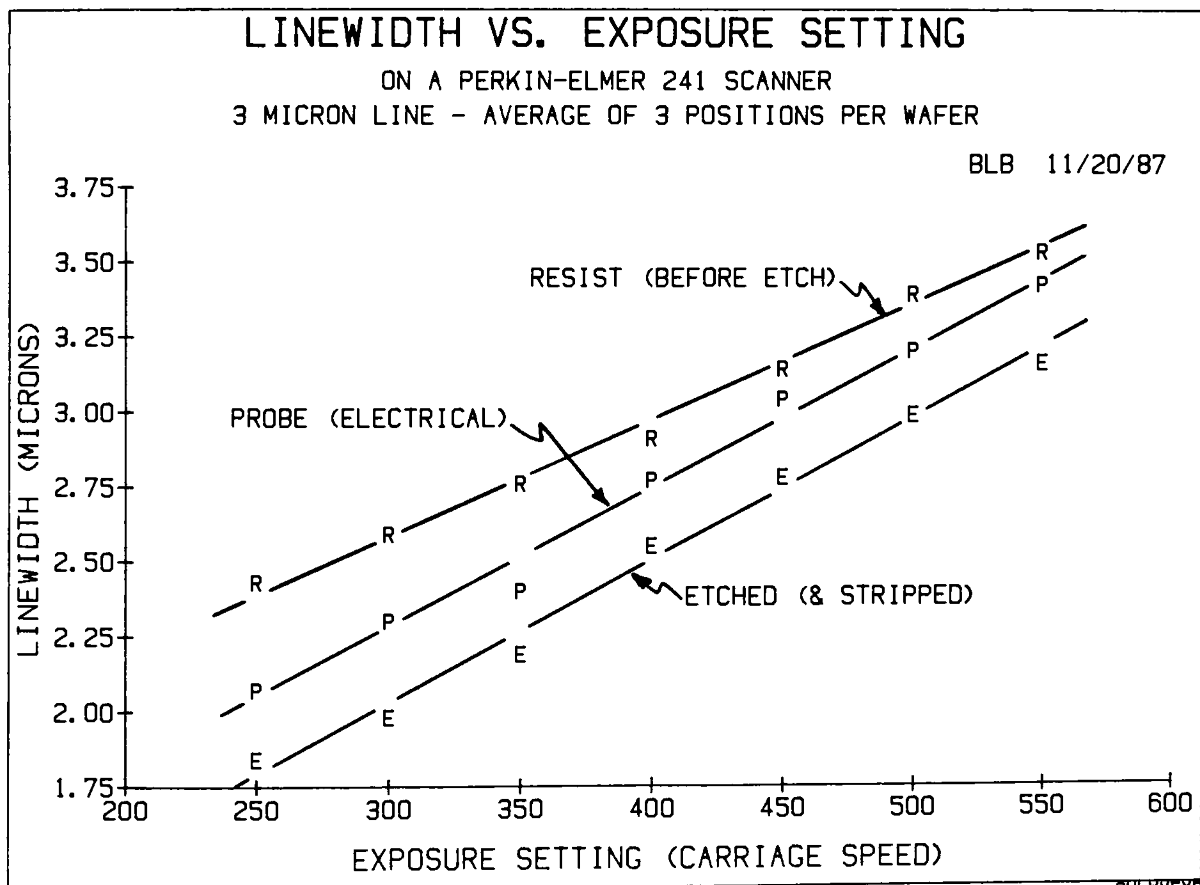

Figure A54: Linewidth vs. Exposure (3 Micron Line).

A comparison between electrical and optical linewidth evaluations is presented below for a nominal 5 micron feature on wafers from an exposure series. It is reminded that the exposure setting on a Perkin-Elmer scanner is directly related to the carriage speed and inversely proportional to actual exposure dose. Therefore the linewidth increases with increasing exposure settings. Figures 20 and 21 address the differences observed for the data below.

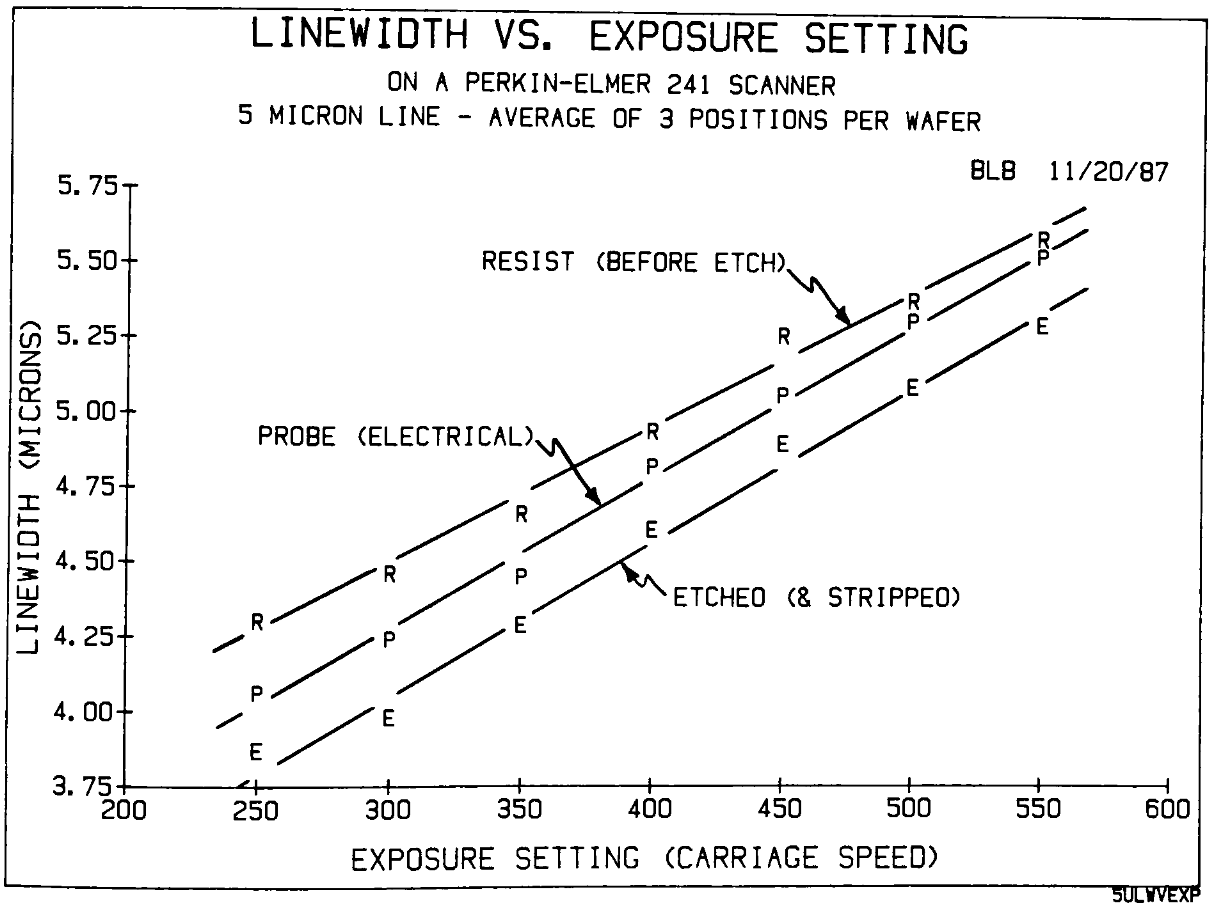

Figure A55: Linewidth vs. Exposure (5 Micron Line).

An exposure series was performed to determine the dependence of spacewidth on exposure setting (see Figure A56). Again, the exposure setting on a Perkin-Elmer scanner is directly related to the carriage speed and therefore inversely proportional to the actual exposure dose. In the case of a space, the width decreases as the exposure setting increases. The slight curve observed below is most likely due to the nonlinearity of the carriage drive system at the low end of the exposure setting scale.

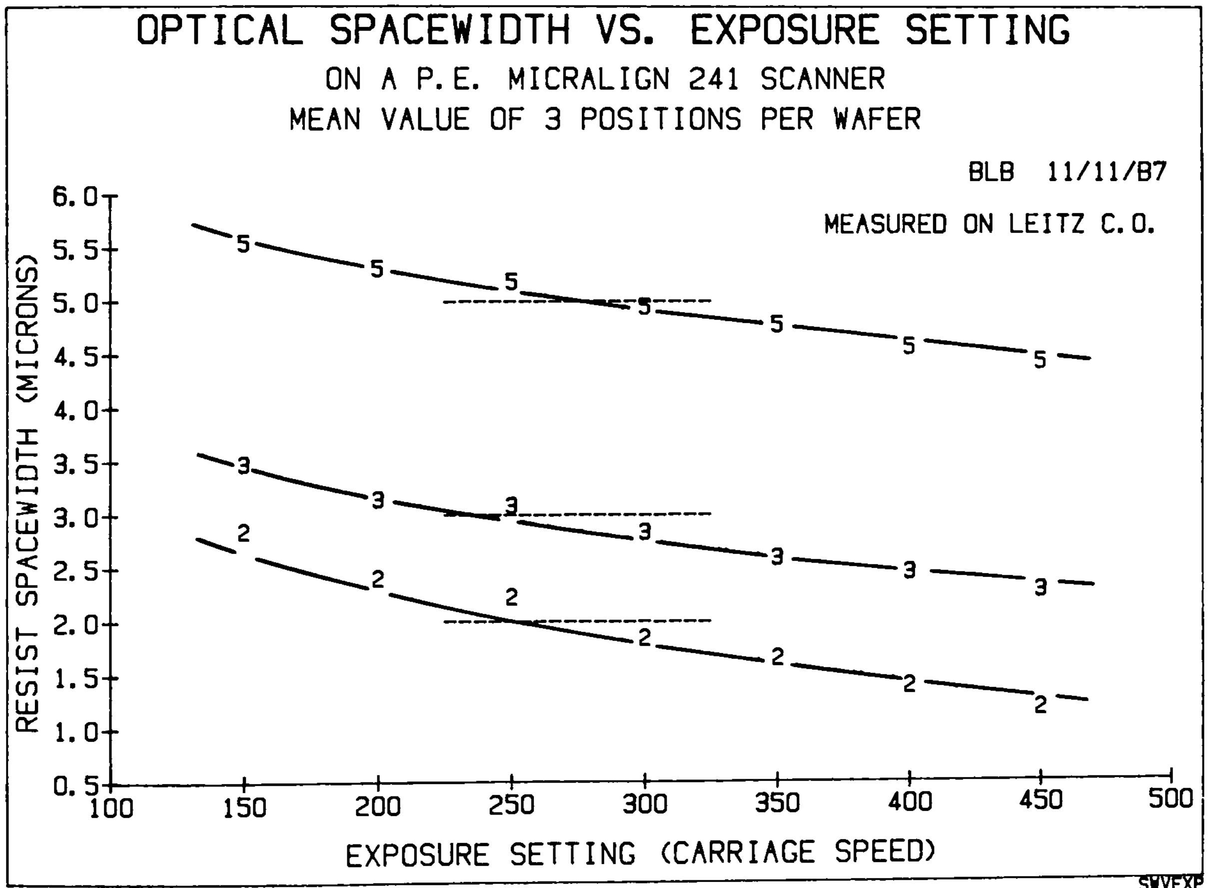

Figure A56: Optical Spacewidth vs. Exposure Setting.

APPENDIX F: CHARACTERIZATION REPORT

The resolution capabilities were investigated for both the Perkin-Elmer scanner as well as an ASET stepper and are reviewed in Figure A57 below. The SEM analysis of these features is included in Appendix G for a wafer exposed on the P.E. scanner.

- ALL DIMENSIONS ARE GIVEN IN MICRONS -

FEATURE	PERKIN-ELMER SCANNER		ASET STEPPER	
	CLEARFIELD	DARKFIELD	CLEARFIELD	DARKFIELD
LINE/SPACE ELEMENTS	1.4 is ok, 1.2 is bad		0.8 is ok, 0.6 is bad	
CONTACTS	3 um is ok, 2 um is ??		Clean down to 2 um.	
ISLANDS	3 um is ok, 2 um is ??		Clean down to 2 um.	
CHECKERBOARDS	Any under 5 um are bad		Any under 3 um are bad	
FOCUS STAR	< 1.8 bad	< 1.8 bad	< 0.8 bad	< 0.9 bad
45 DEGREE RESOLUTION	< 2.0 bad	< 2.0 bad	1.0 is ok	1.0 is ok
1-5 UM RES. CHART	< 2.0 bad	< 2.0 bad	1.0 is ok	1.0 is ok
MURRAY DAGGER	< 1.4 ???	< 1.6 ???	< 0.8 ???	< 0.8 ???
6-10 UM RES. CHART	all ok	all ok	all ok	all ok

Figure A57: Resolution Capabilities.

Alignment data for ten wafers at five positions is provided in Figure A58 in the form of a histogram. In this case, the wafers were manually aligned to fairly faint targets. Its likely that the results would be better if automatic alignment was employed. The average distortion values were calculated and are given below.

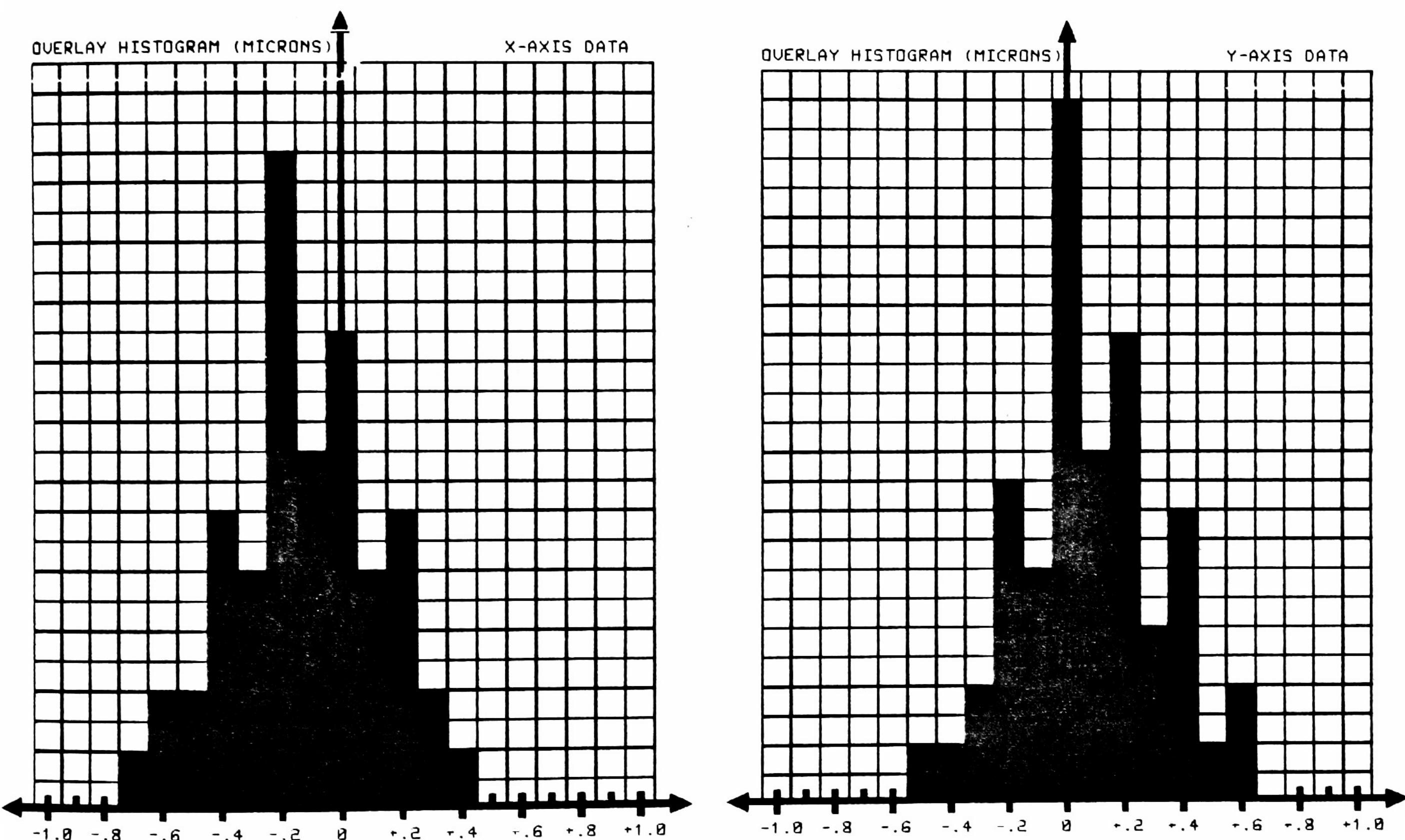

X AVE = −0.13 um	X MAG = +.125 um	Y AVE = +0.05 um
X SIGMA = 0.25 um	Y MAG = +.180 um	Y SIGMA = 0.23 um
3*X SIGMA = 0.75 um	THETA SKEW = +.090 um	3*Y SIGMA = 0.69 um

Figure A58: Alignment Histogram.

The numerical wafer map below includes the actual optical vernier readings for a wafer which was normally aligned. The associated vector map for this wafer is included as Figure 22. The values indicated on top are for X misalignment and on bottom are for Y misalignment.

| dX |
| dY |

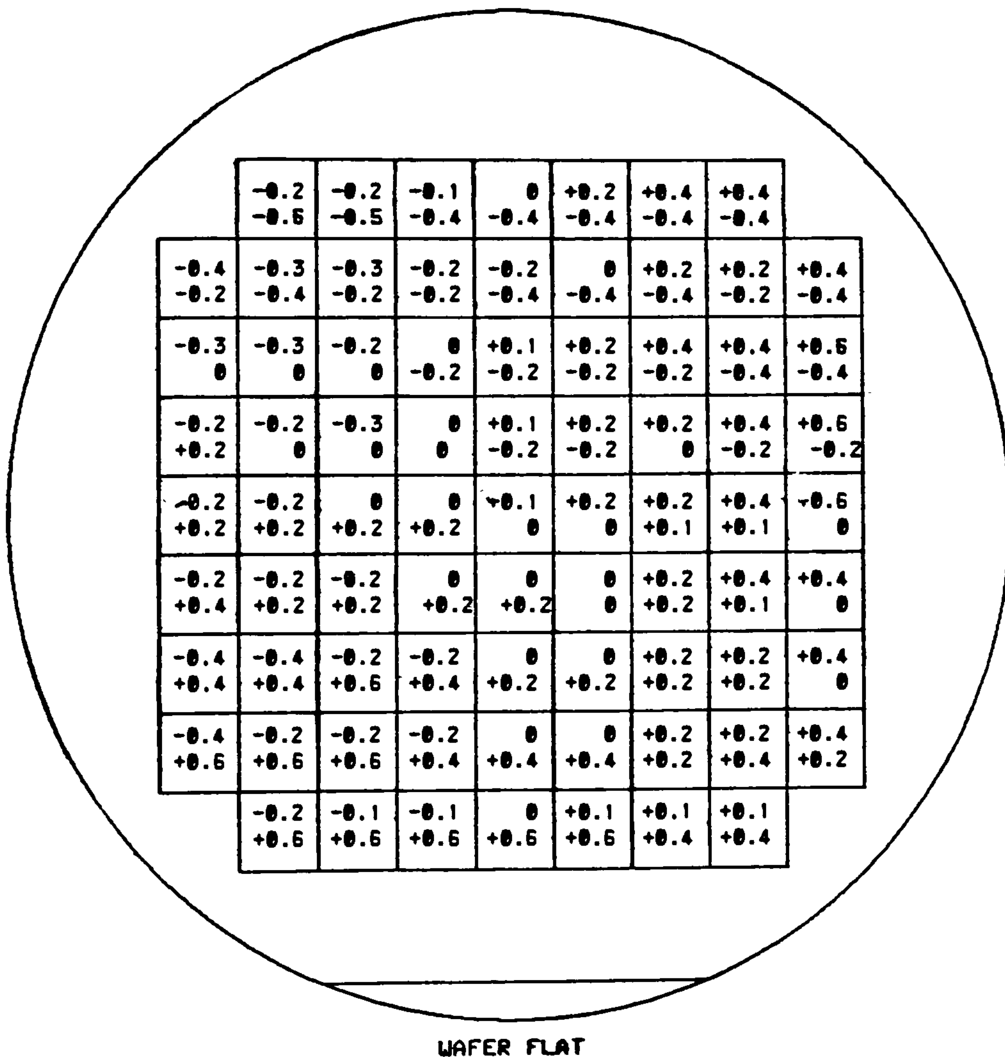

Figure A59: Overlay Wafer Map (Acceptable Alignment).

The numerical wafer map below includes the actual optical vernier readings for a wafer which was aligned with an induced translational error. The vector map for this wafer is included as Figure 23. The values indicated on top are for X misalignment and on bottom are for Y misalignment.

| dX |
| dY |

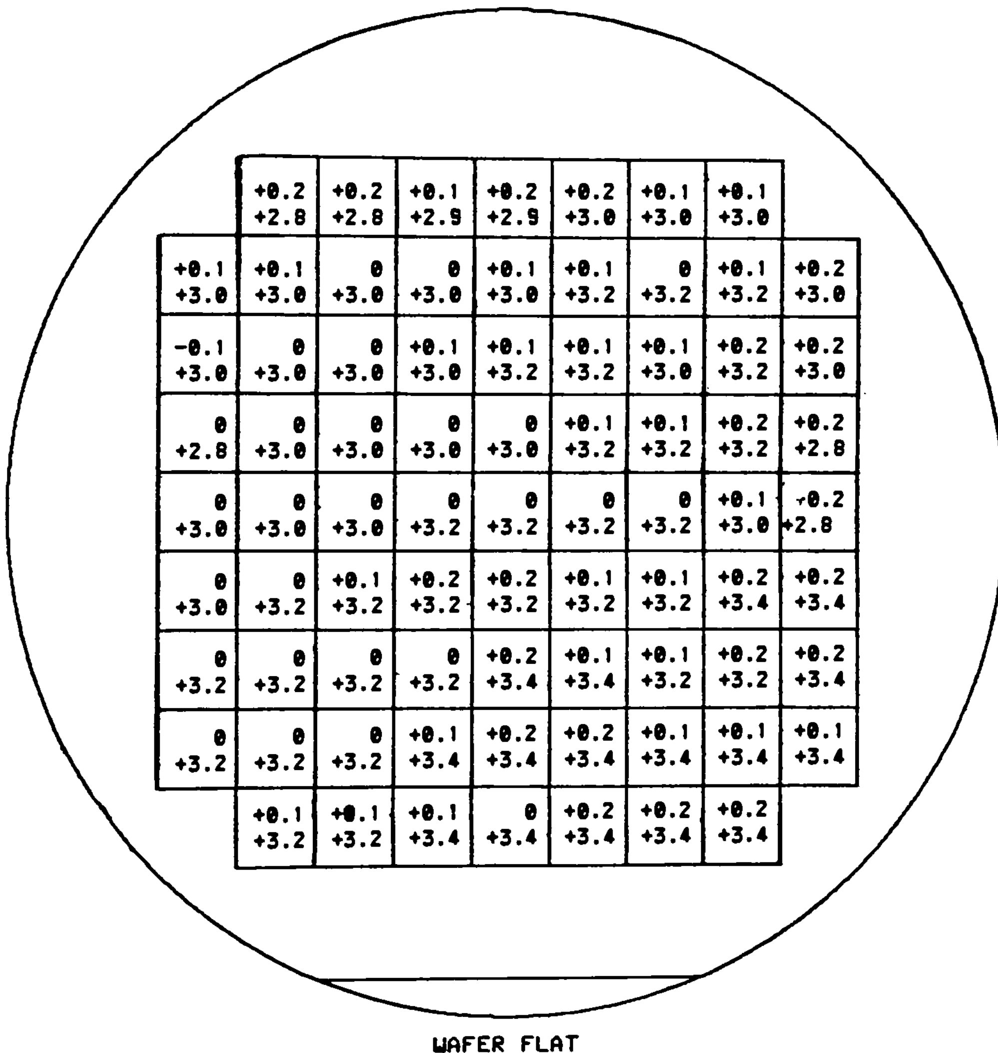

Figure A60: Overlay Wafer Map (Translational Error).

The numerical wafer map below includes the actual optical vernier readings for a wafer which had large rotational error. The vector map for this wafer is included as Figure 24. The values indicated on top are for X misalignment and on bottom are for Y misalignment.

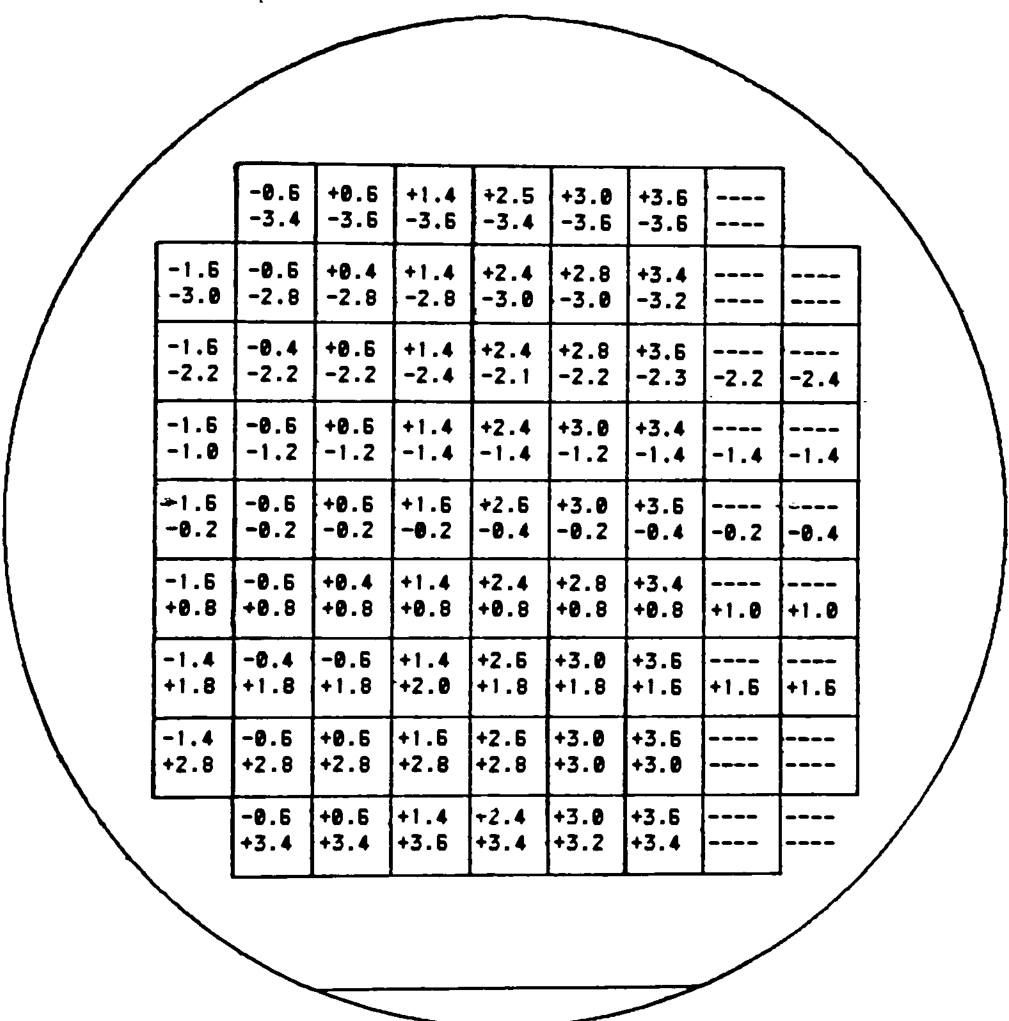

	-0.6 / -3.4	+0.6 / -3.6	+1.4 / -3.6	+2.5 / -3.4	+3.0 / -3.6	+3.6 / -3.6	---- / ----	
-1.6 / -3.0	-0.6 / -2.8	+0.4 / -2.8	+1.4 / -2.8	+2.4 / -3.0	+2.8 / -3.0	+3.4 / -3.2	---- / ----	---- / ----
-1.6 / -2.2	-0.4 / -2.2	+0.6 / -2.2	+1.4 / -2.4	+2.4 / -2.1	+2.8 / -2.2	+3.6 / -2.3	---- / -2.2	---- / -2.4
-1.6 / -1.0	-0.6 / -1.2	+0.6 / -1.2	+1.4 / -1.4	+2.4 / -1.4	+3.0 / -1.2	+3.4 / -1.4	---- / -1.4	---- / -1.4
-1.6 / -0.2	-0.6 / -0.2	+0.6 / -0.2	+1.6 / -0.2	+2.6 / -0.4	+3.0 / -0.2	+3.6 / -0.4	---- / -0.2	---- / -0.4
-1.6 / +0.8	-0.6 / +0.8	+0.4 / +0.8	+1.4 / +0.8	+2.4 / +0.8	+2.8 / +0.8	+3.4 / +0.8	---- / +1.0	---- / +1.0
-1.4 / +1.8	-0.4 / +1.8	-0.6 / +1.8	+1.4 / +2.0	+2.6 / +1.8	+3.0 / +1.8	+3.6 / +1.6	---- / +1.6	---- / +1.6
-1.4 / +2.8	-0.6 / +2.8	+0.6 / +2.8	+1.6 / +2.8	+2.6 / +2.8	+3.0 / +3.0	+3.6 / +3.0	---- / ----	---- / ----
	-0.6 / +3.4	+0.6 / +3.4	+1.4 / +3.6	+2.4 / +3.4	+3.0 / +3.2	+3.6 / +3.4	---- / ----	---- / ----

Figure A61: Overlay Wafer Map (Rotational Error).

The numerical wafer map below includes the actual optical vernier readings for a wafer which had large rotational error. The plot comparing this data to the electrical test structure results is included as Figure 25. The values indicated are for X misalignment only.

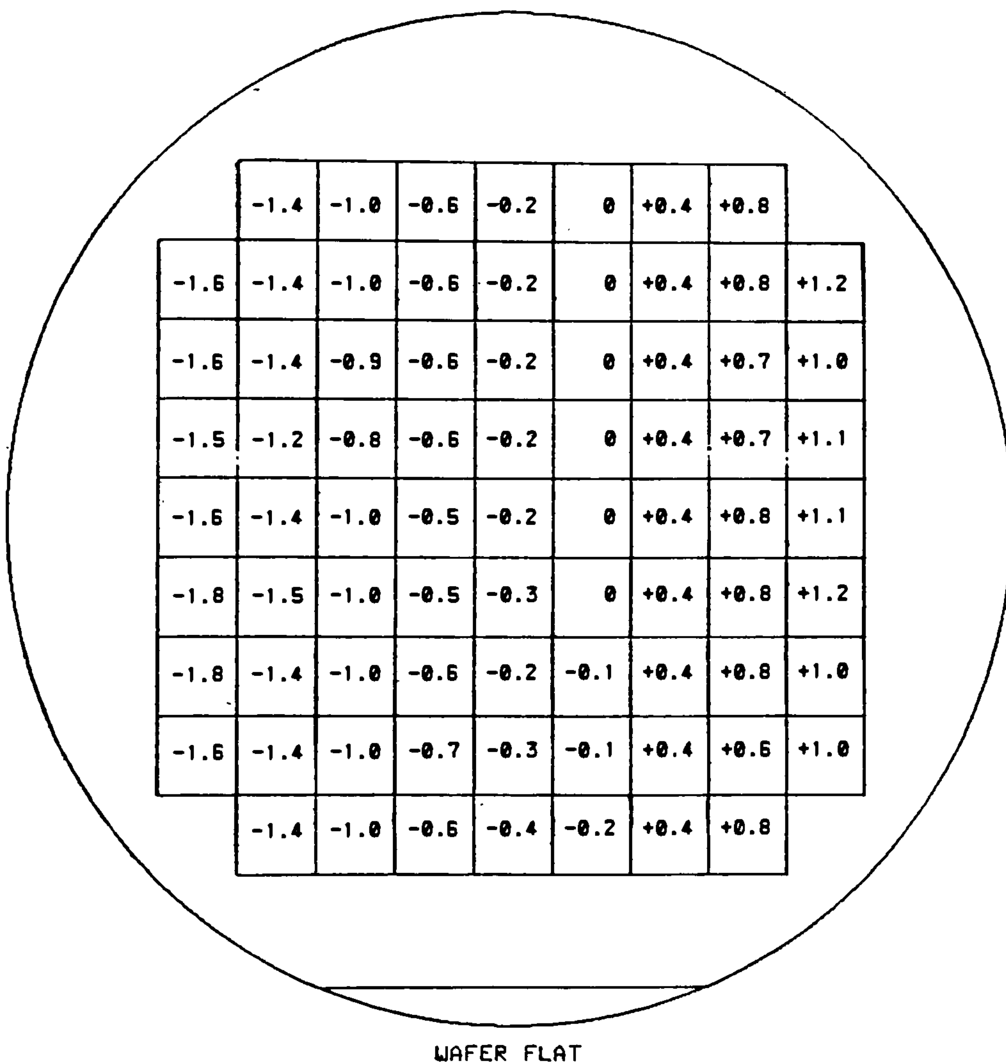

	-1.4	-1.0	-0.6	-0.2	0	+0.4	+0.8	
-1.6	-1.4	-1.0	-0.6	-0.2	0	+0.4	+0.8	+1.2
-1.6	-1.4	-0.9	-0.6	-0.2	0	+0.4	+0.7	+1.0
-1.5	-1.2	-0.8	-0.6	-0.2	0	+0.4	+0.7	+1.1
-1.6	-1.4	-1.0	-0.5	-0.2	0	+0.4	+0.8	+1.1
-1.8	-1.5	-1.0	-0.5	-0.3	0	+0.4	+0.8	+1.2
-1.8	-1.4	-1.0	-0.6	-0.2	-0.1	+0.4	+0.8	+1.0
-1.6	-1.4	-1.0	-0.7	-0.3	-0.1	+0.4	+0.6	+1.0
	-1.4	-1.0	-0.6	-0.4	-0.2	+0.4	+0.8	

Figure A62: Optical Alignment Evaluation.

The numerical wafer map below includes the electrical test structure results for a wafer which had large rotational error. The plot comparing this data to optical vernier results is included as Figure 25. The values indicated are for X misalignment only.

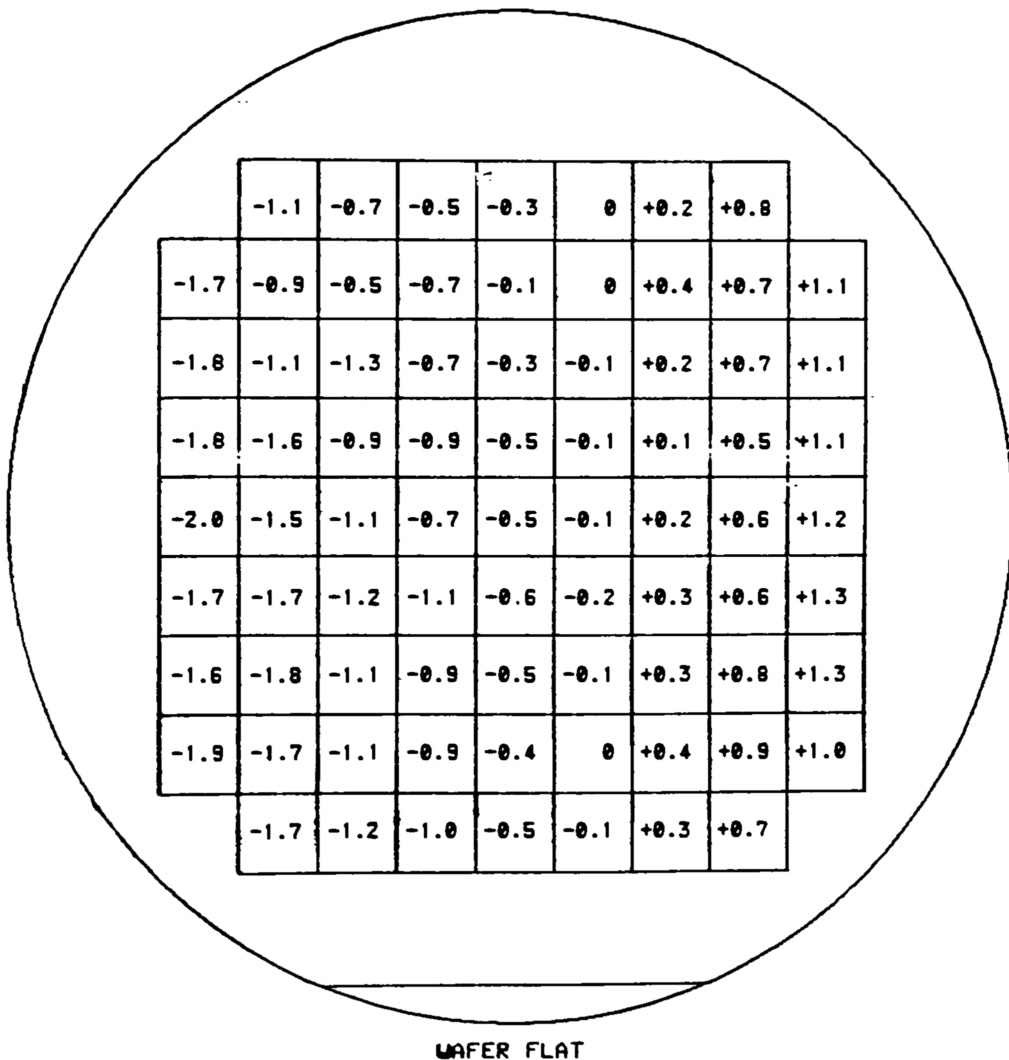

	-1.1	-0.7	-0.5	-0.3	0	+0.2	+0.8	
-1.7	-0.9	-0.5	-0.7	-0.1	0	+0.4	+0.7	+1.1
-1.8	-1.1	-1.3	-0.7	-0.3	-0.1	+0.2	+0.7	+1.1
-1.8	-1.6	-0.9	-0.9	-0.5	-0.1	+0.1	+0.5	+1.1
-2.0	-1.5	-1.1	-0.7	-0.5	-0.1	+0.2	+0.6	+1.2
-1.7	-1.7	-1.2	-1.1	-0.6	-0.2	+0.3	+0.6	+1.3
-1.6	-1.8	-1.1	-0.9	-0.5	-0.1	+0.3	+0.8	+1.3
-1.9	-1.7	-1.1	-0.9	-0.4	0	+0.4	+0.9	+1.0
	-1.7	-1.2	-1.0	-0.5	-0.1	+0.3	+0.7	

Figure A63: Electrical Alignment Evaluation.

APPENDIX G: SEM MICROGRAPHS

A test mask for exposure tool characterization could be measured by its ability to qualitatively evaluate the image transferred from a mask to a wafer. This can be accomplished with optical microscopy but is certainly best done with Scanning Electron Microscopy (SEM). The following pages illustrate the types of analysis which can be performed with the existing patterns on ETM-1.

The micrographs were taken on a Cambridge S100 SEM from wafers which did not receive any special preparation. Better results would be expected if the samples were gold coated and evaluated on a SEM with higher magnification and resolution. Captions are provided at the top of each micrograph for clarity.

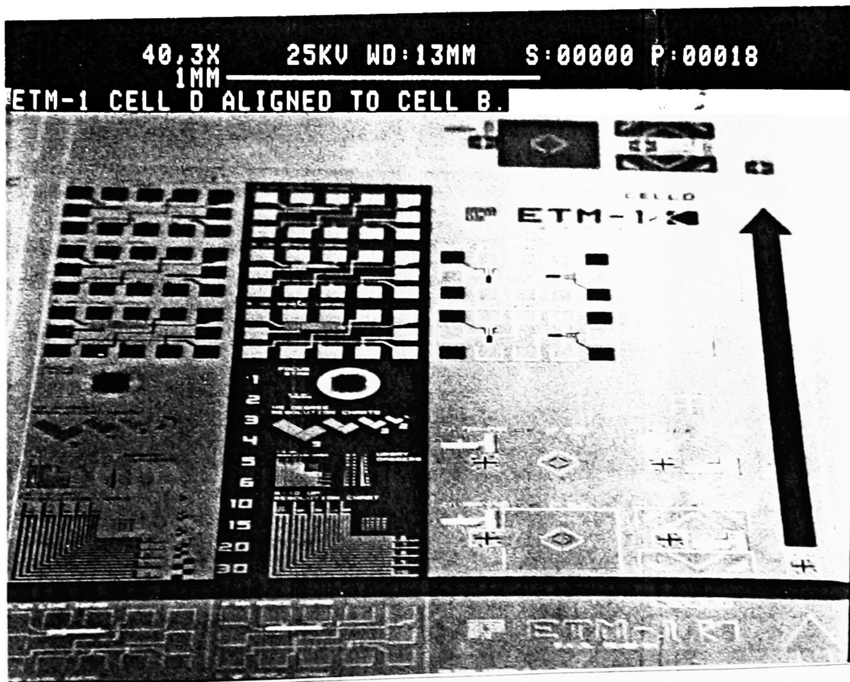

Figure A64: ETM-1 Cell D Aligned to Cell A.

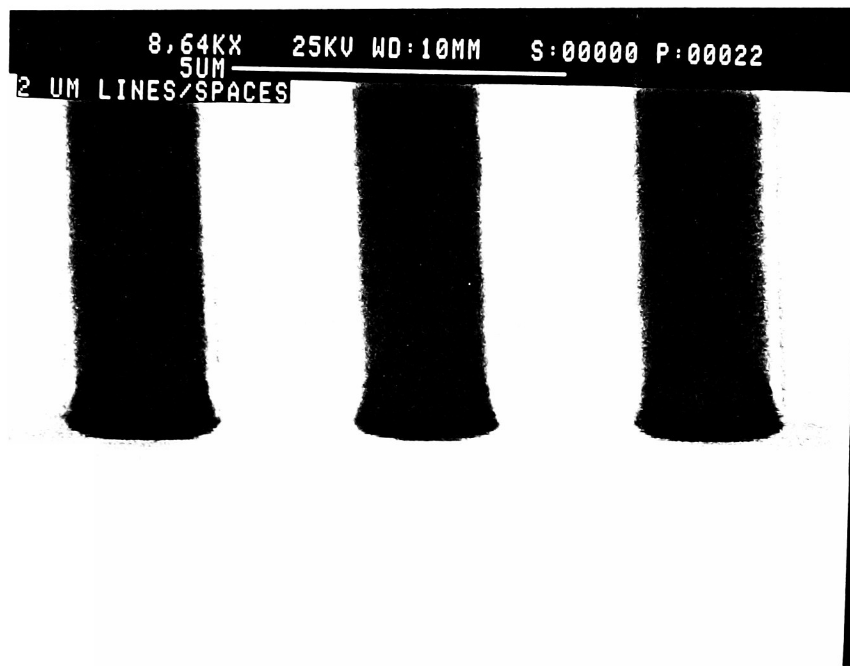

Figure A65: Line/Space Elements.

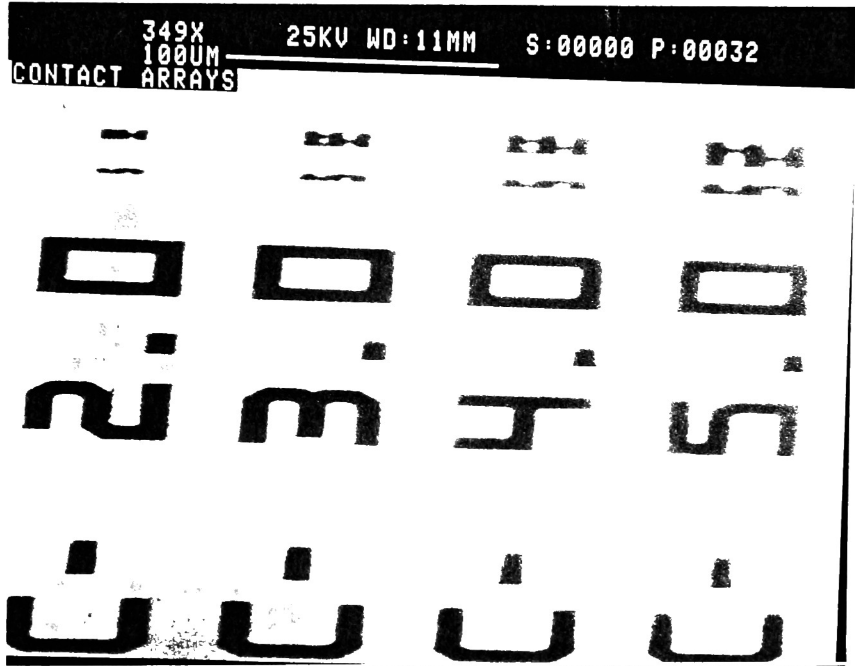

Figure A66: Contact Array.

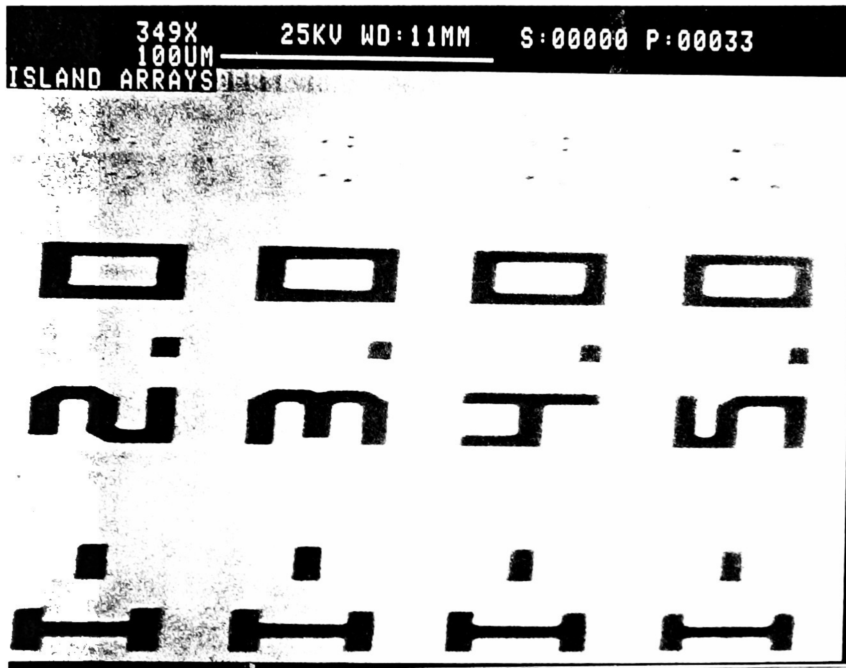

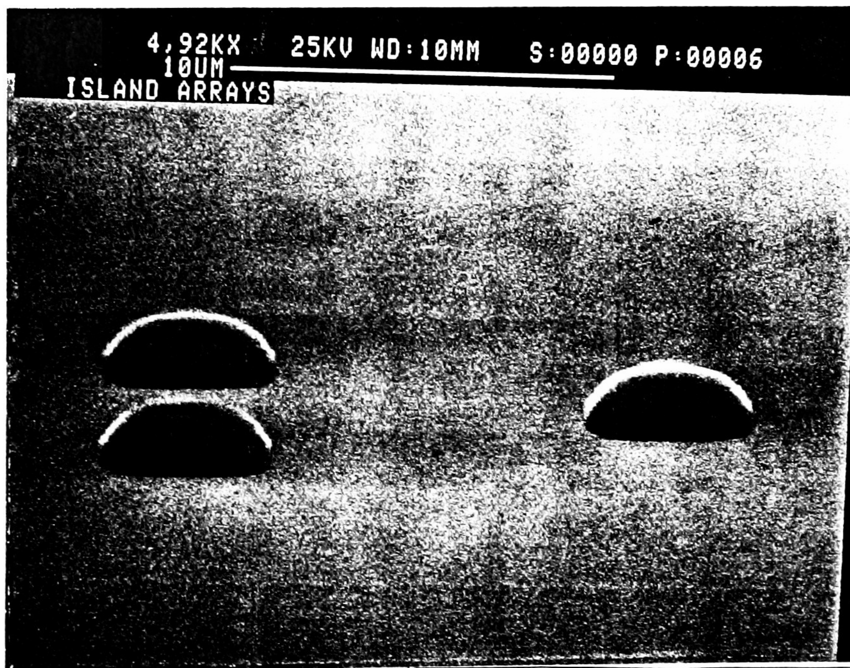

Figure A67: Island Array.

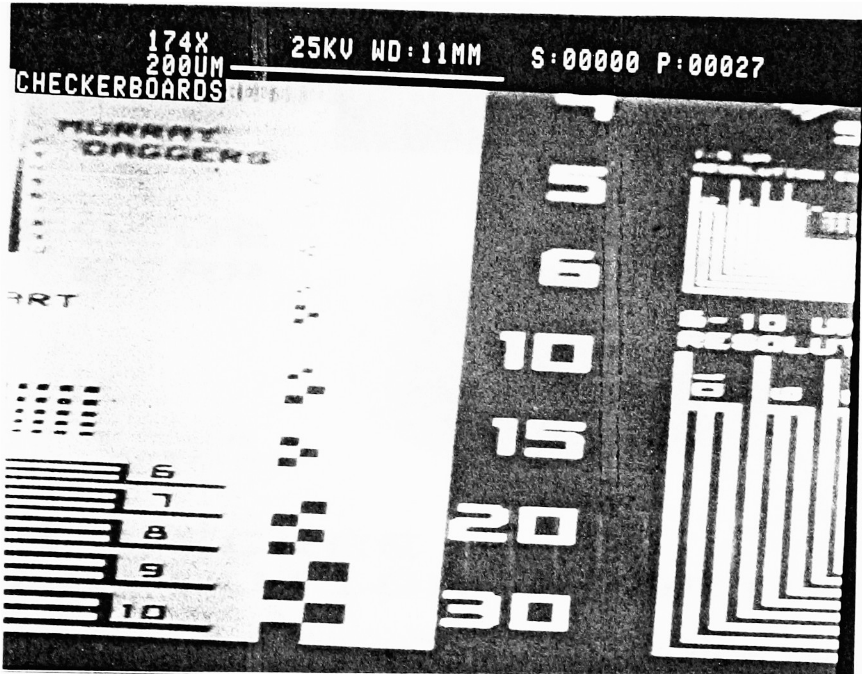

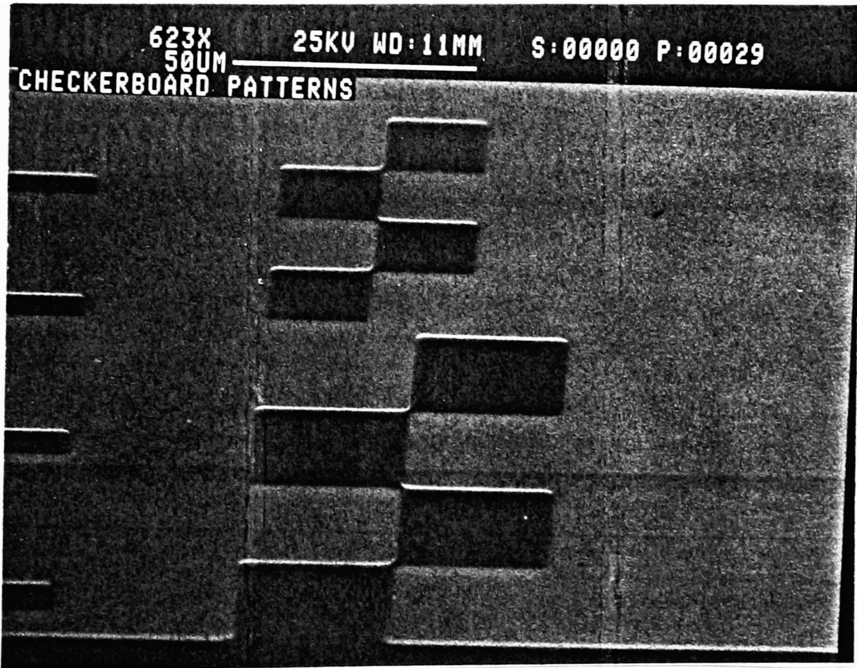

Figure A68: Checkerboard Array.

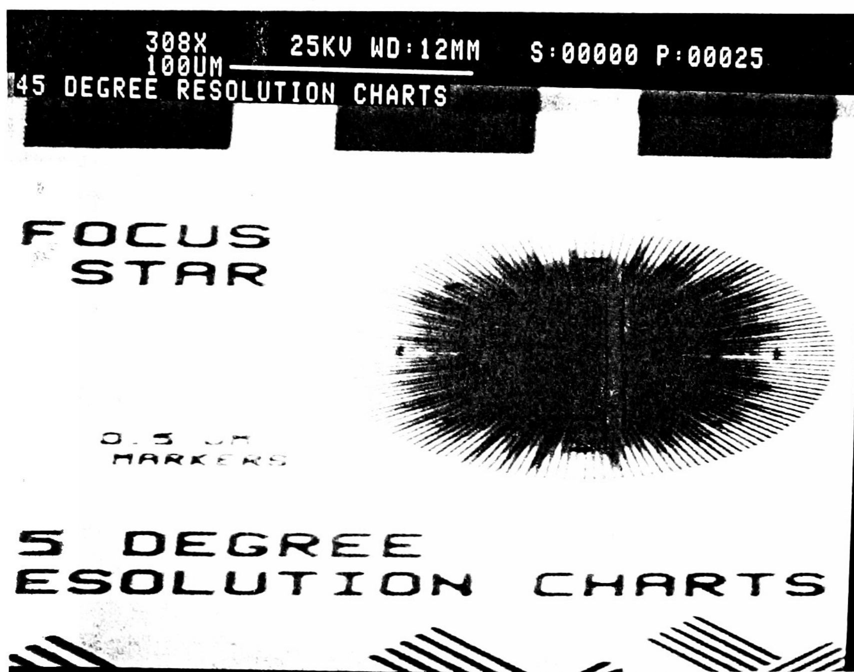

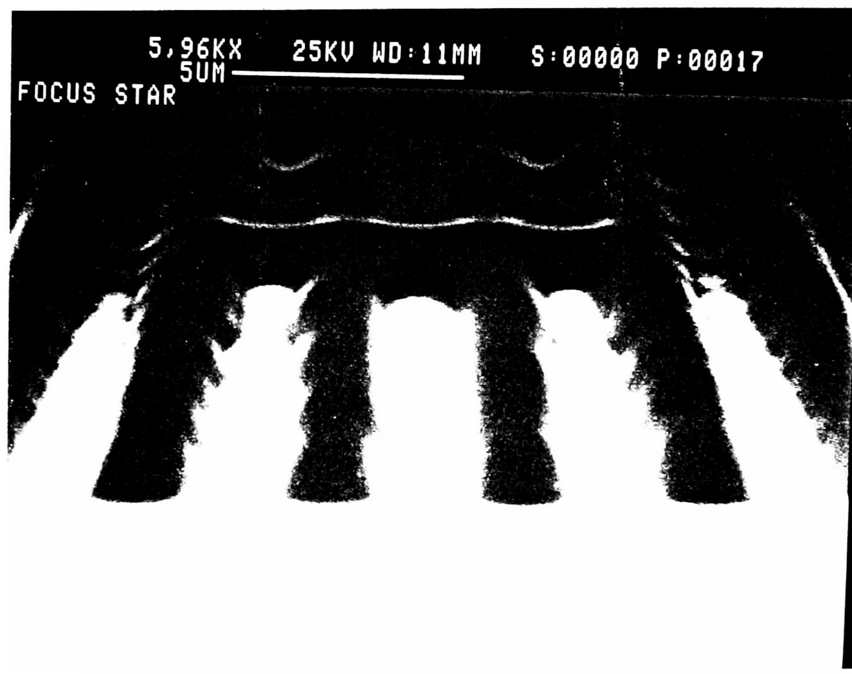

Figure A69: Focus Star.

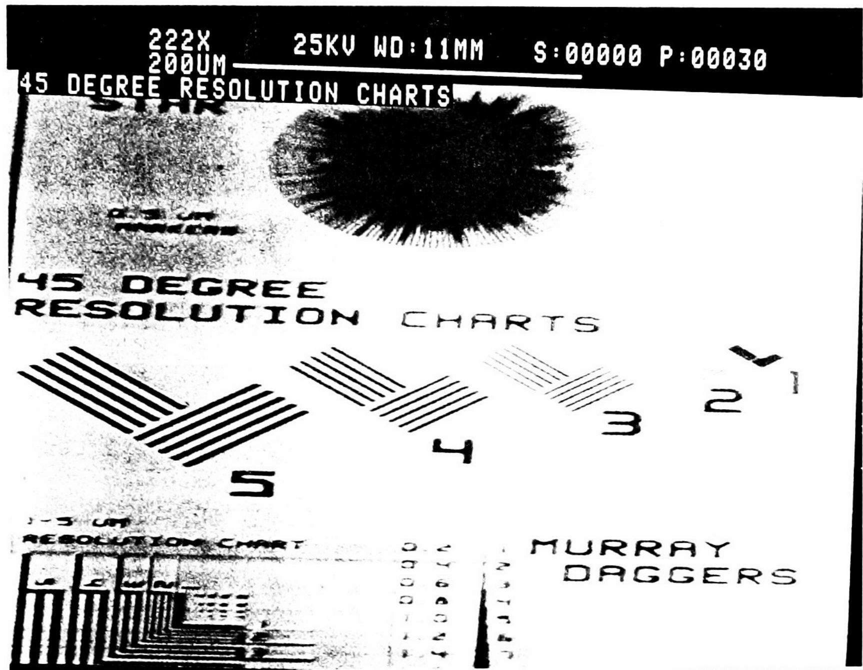

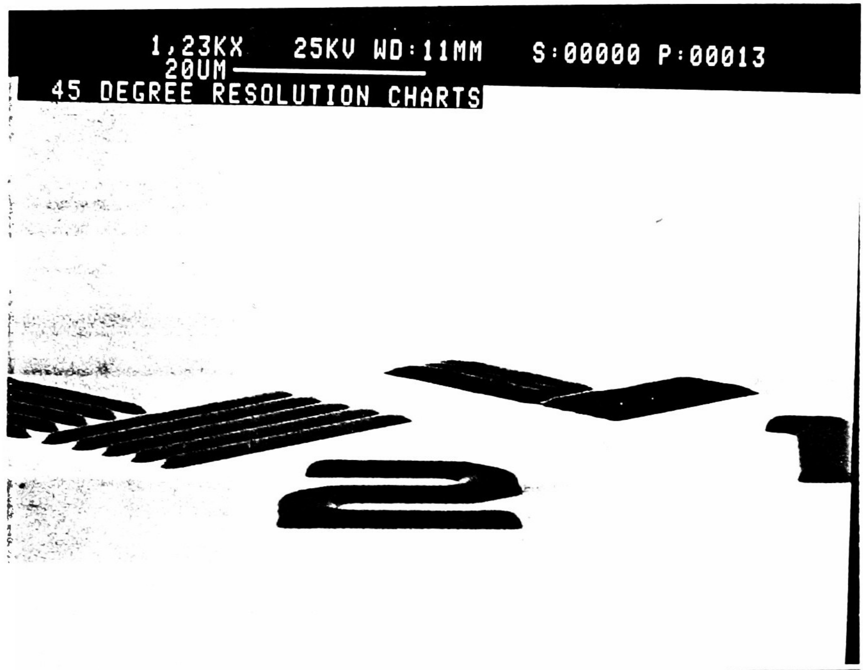

Figure A70: 45 Degree Resolution Charts.

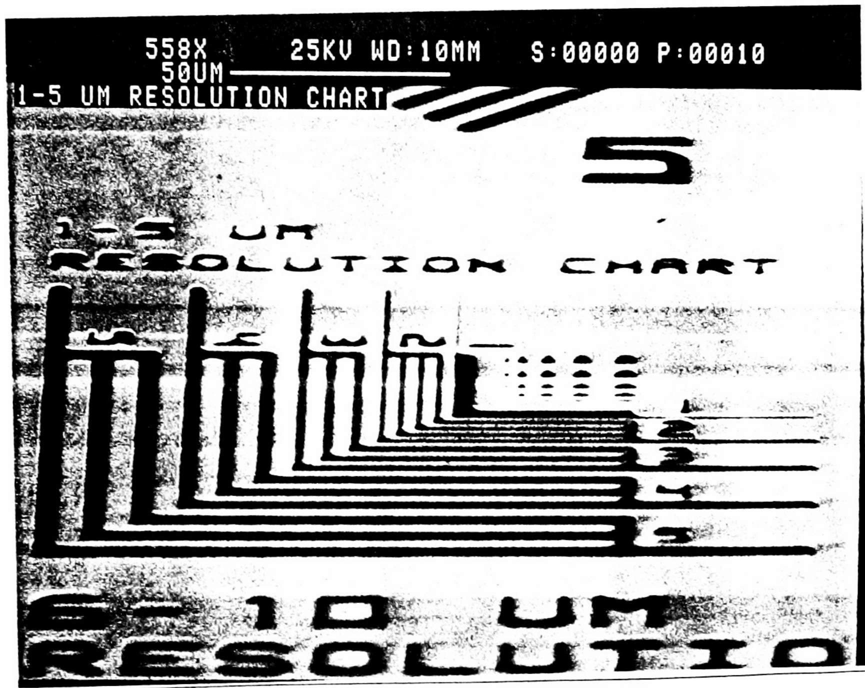

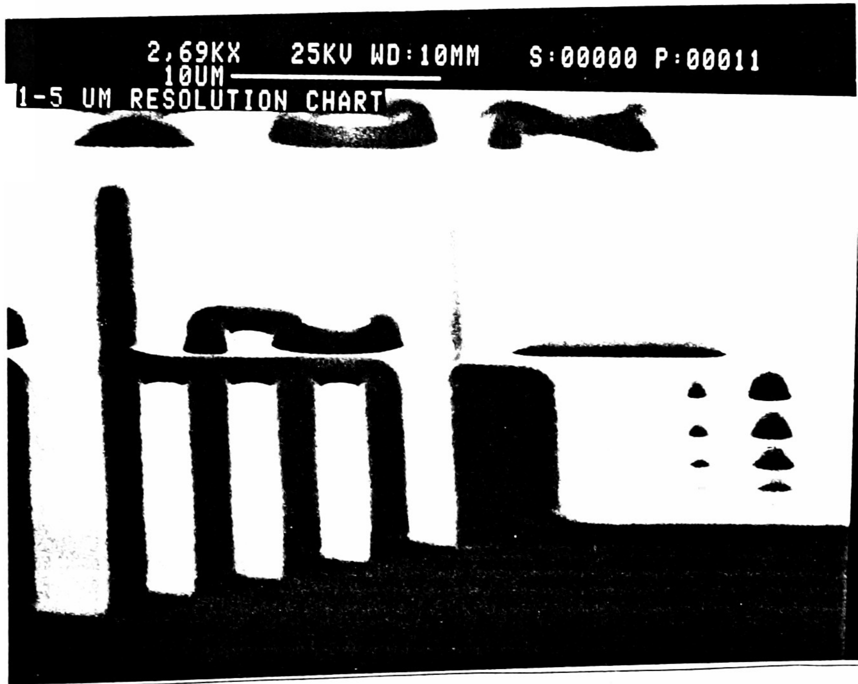

Figure A71: 1-5 Micron Resolution Chart.

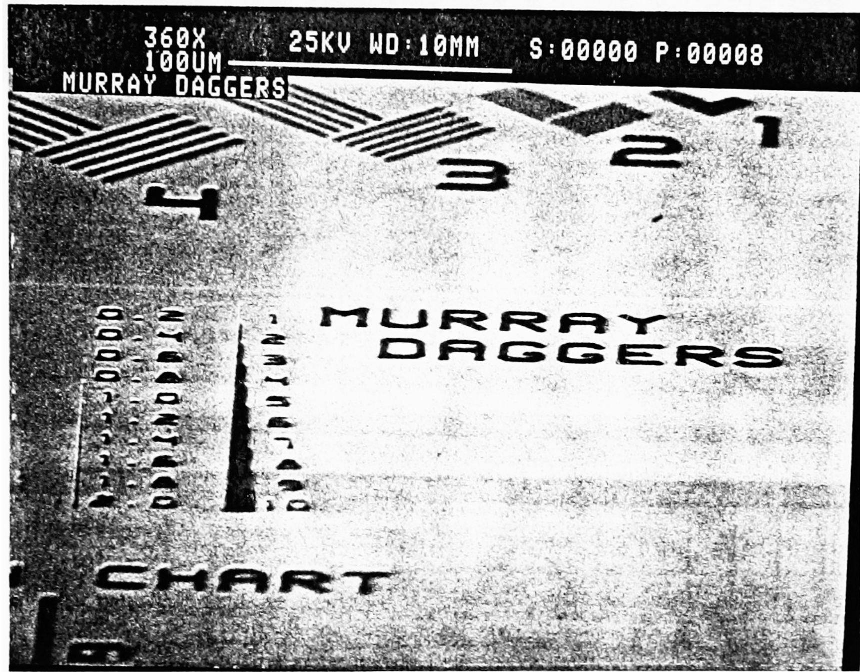

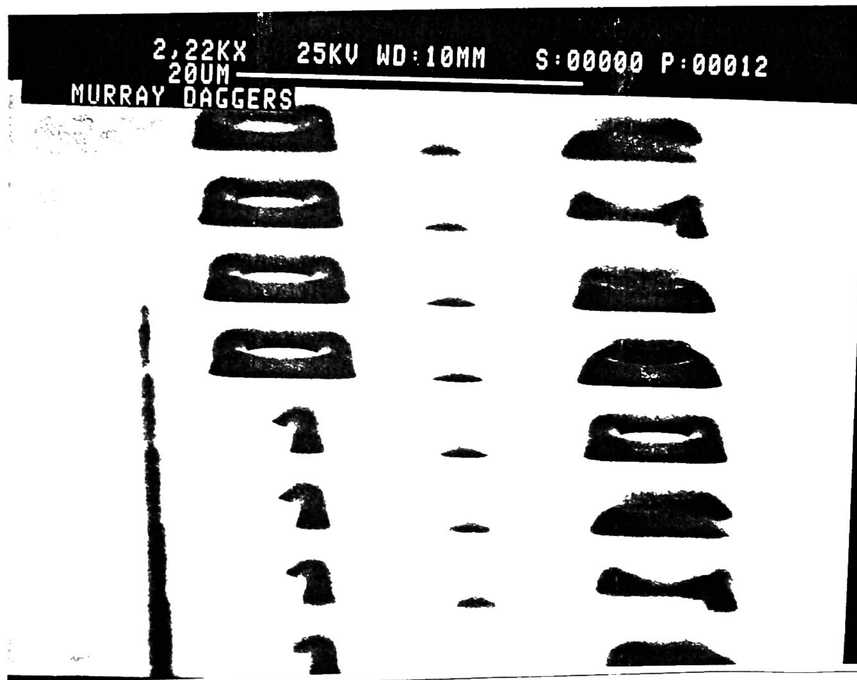

Figure A72: Murray Daggers.

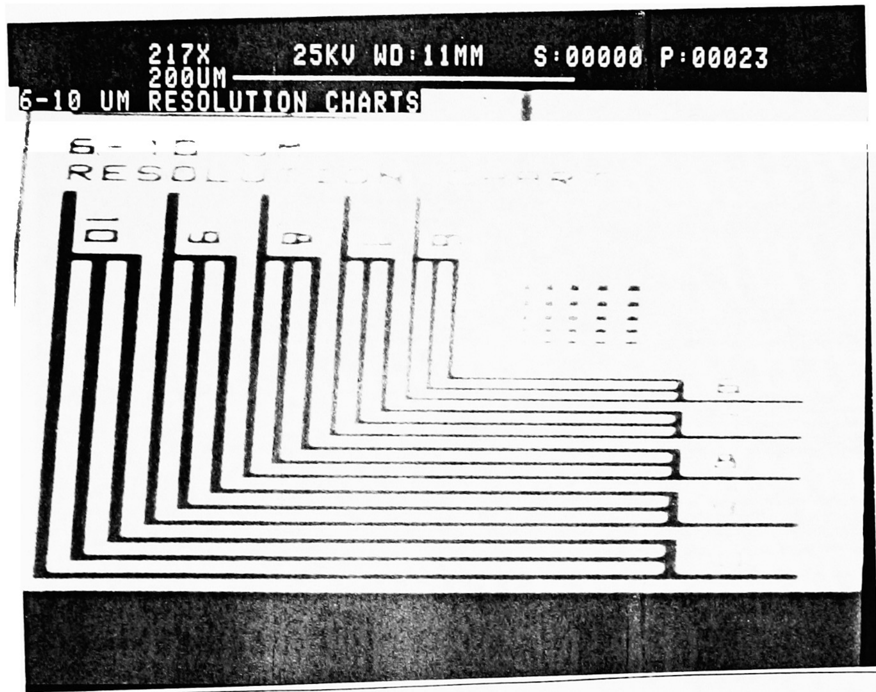

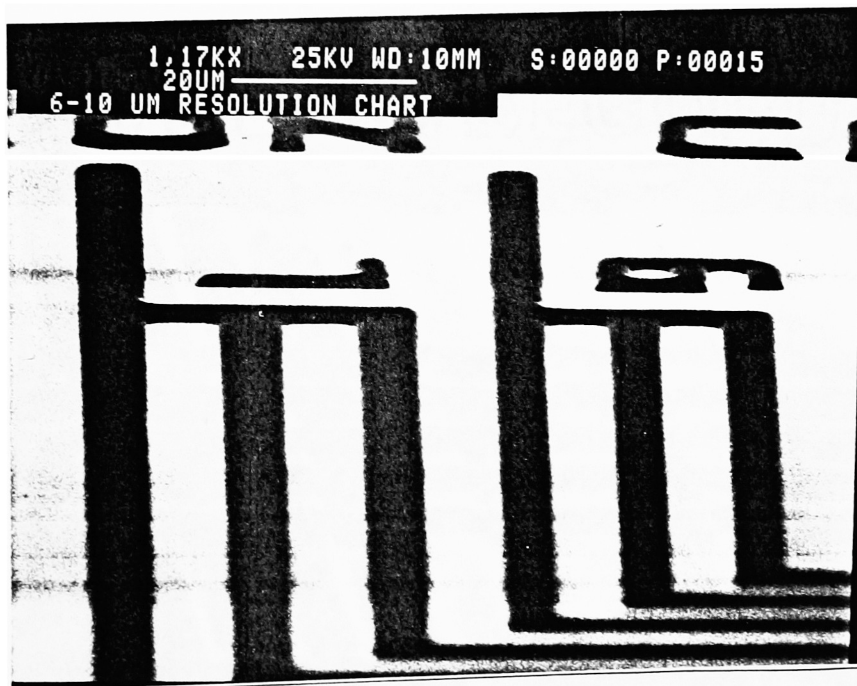

Figure A73: 6-10 Micron Resolution Chart.

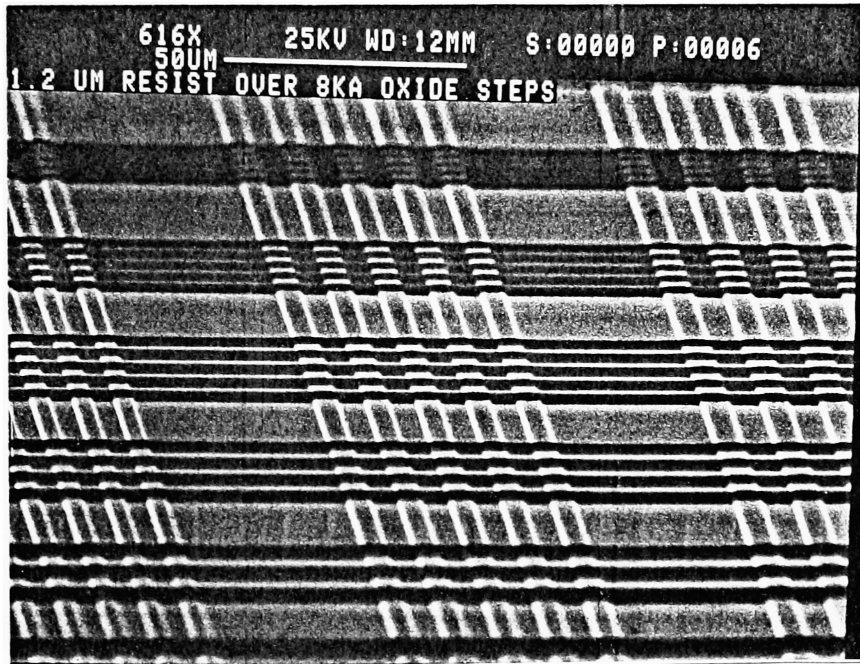

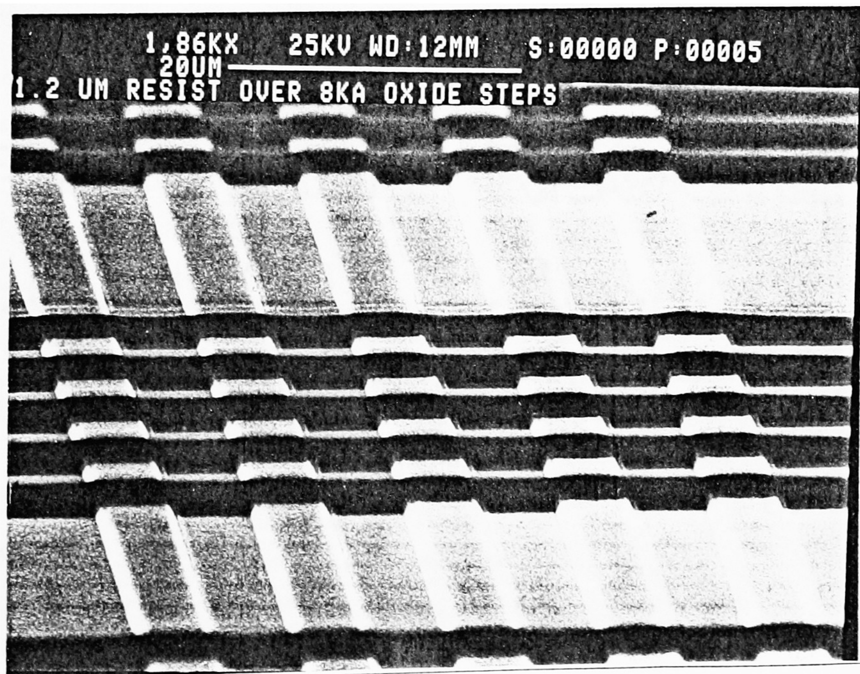

Figure A74: Resist Imaging Over Topography.

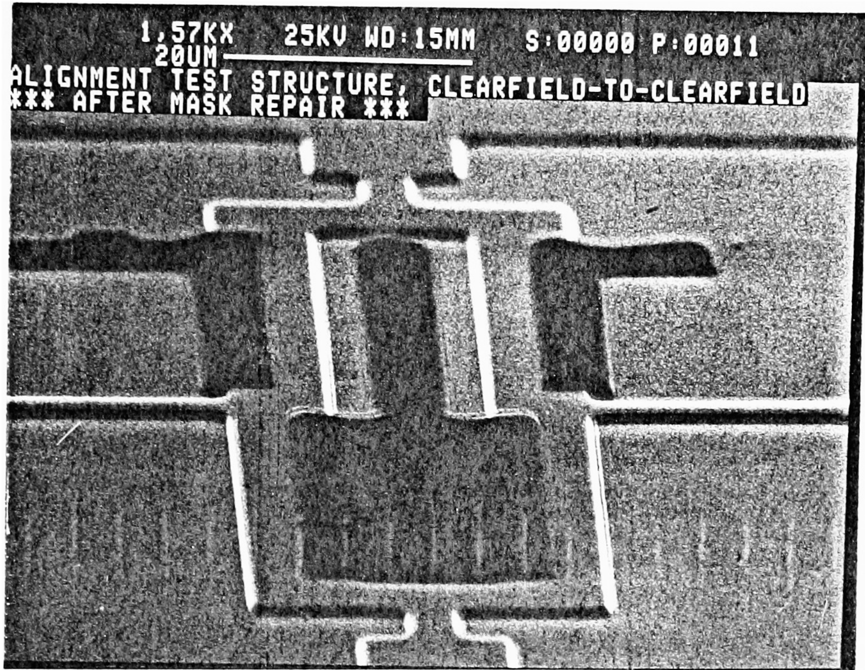

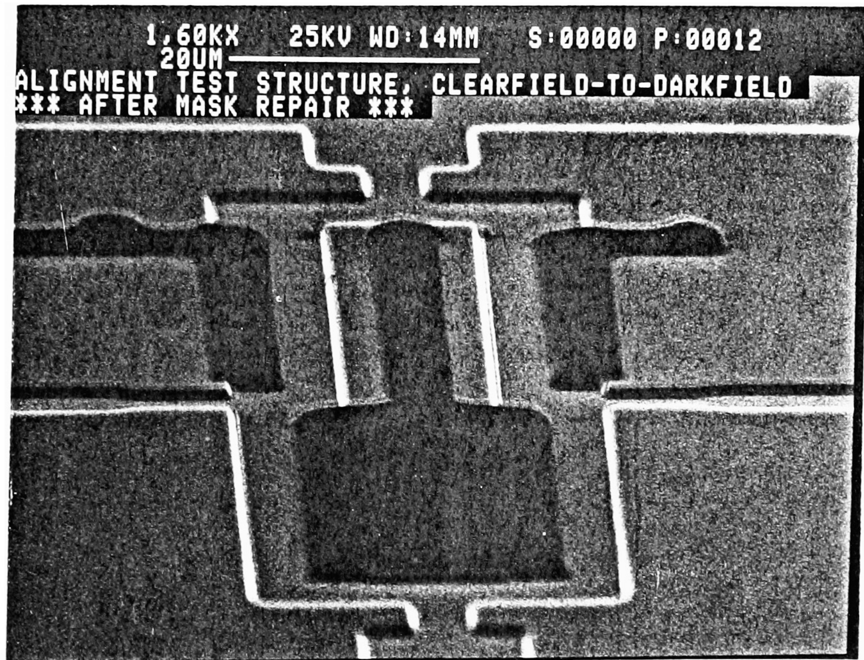

Figure A75: Electrical Alignment Structures.